IMPI's 56TH ANNUAL MICROWAVE POWER SYMPOSIUM (IMPI 56)

2022 PROCEEDINGS

June 14-16, 2022

The DeSoto Hotel
Savannah, Georgia, USA

ISSN 1070-0129

Presented by the
INTERNATIONAL MICROWAVE POWER INSTITUTE
PO Box 1140, Mechanicsville, VA 23111
Email: info@impi.org
WWW.IMPI.ORG

Welcome to the 56th IMPI Symposium

Each year, IMPI brings together researchers from across the globe to share the latest findings in microwave and RF heating theories and applications, and this year we have an outstanding array of researchers in attendance. If you are not yet a member of IMPI, we strongly encourage you to consider joining onsite. IMPI membership connects you to microwave and RF academia, researchers, developers and practitioners across the globe. Talk to an IMPI member today to learn more about the value of joining our outstanding organization!

Thank you for joining us. We hope you learn from the technical presentations, interact with your colleagues, and enjoy the atmosphere of the Symposium. And do take the opportunity to visit the many interesting sites in and around Savannah, Georgia.

Special thanks to the IMPI 56 Technical Program Committee for their dedication to this Symposium:

Chairs
Vadim Yakovlev, Worcester Polytechnic Institute, USA, Chair
Candice Ellison, National Energy Technology Laboratory, USA, Vice-Chair

Organizers of Special Sessions
Raymond Boxman, Tel Aviv University, Israel
Ulrich Erle, Nestle R&D, USA
Marzena Olszewska-Placha, QWED, Poland
Marilena Radoiu, Microwave Technologies Consulting, France

Members
Eleanor Binner, University of Nottingham, UK
Graham Brodie, University of Melbourne, Australia
John F. Gerling, Gerling Consulting, Inc., USA
Satoshi Horikoshi, Sophia University, Japan
B. Reeja Jayan, Carnegie Mellon University, USA
Yang Jiao, Shanghai Ocean University, China
Birgitta Raaholt, Research Institute of Sweden, Sweden
Klaus Werner, pinkRF B.V., Netherlands

IMPI 56 Proceedings edited by Candice Ellison and Vadim Yakovlev

Purchasing Information: Copies of the Proceedings of the 56th Annual Microwave Power Symposium, as well as back issues from prior years, are available for purchase. Contact Molly Poisant, Executive Director of IMPI, by emailing molly.poisant@impi.org for details.

Table of Contents

Keynotes

MICROWAVE PLASMA

Microwave Chemistry

SOLID STATE TECHNOLOGIES

MICROWAVE PROCESSING OF MATERIALS

COMPUTER MODELING

DIELCTRIC PROPERTIES & MATERIALS

INDUSTRIAL MICROWAVES

MICROWAVES IN FOOD ENGINEERING

BIOLOGICAL APPLICATIONS

POSTERS

Notes

Notes

Notes

Overview of Radio Frequency and Microwave Driven Plasma Ion Sources for Particle Accelerators

Robert F. Welton[1], Olli Tarvainen[2], and Baoxi Han[1]

[1]Spallation Neutron Source, Oak Ridge National Laboratory, Oak Ridge, TN, USA
[2]UKRI-STFC-ISIS Pulsed Spallation Neutron and Muon Facility,
Rutherford Appleton Laboratory, Harwell, UK

Keywords: ion sources, microwave plasma, particle accelerators, particle beams, RF matching, RF plasma

ABSTRACT

Particle accelerators are among the most important scientific tools of the modern era. Large accelerator complexes, both hadron and lepton, have supported scientific user facilities which have had an enormous societal impact spanning many decades and enabling the work of 10's of thousands of scientific users worldwide [1]. Many of the large hadron facilities employ accelerator complexes which include cyclotrons, synchrotrons, storage rings, linear or tandem accelerators and deliver ion beams of very high-intensity and/or very high-energy to their user facilities. These accelerator complexes require the injection of positive or negative ions of varying charge states which are produced in bright ion sources where ions are typically formed within a plasma or through bombardment of surfaces [2, 3]. Increasingly, RF and microwave systems are being utilized, to generate these ion-rich plasmas due to their high reliability, minimal use of consumable components and ability to access very high charge states.

This report first discusses the basic mechanisms of ion formation and plasma generation as well as some specifics of RF/microwave generators, matching circuits and plasma coupling structures typically employed. A detailed discussion will be given of RF-driven negative ion source systems at the US Spallation Neutron Source. The ever-growing demands of microwave systems for electron cyclotron resonance ion sources, operating at frequencies from 2.45 GHz to 75 GHz, and producing high charge state ions for nuclear physics research and applications will be outlined. Finally, a summary table will be compiled of RF/microwave ion sources currently operational at large scale hadron facilities worldwide.

REFERENCES

[1] V. Shiltsev, "Particle beams behind physics discoveries", *Physics Today*, vol. 73, no 4, p. 32, 2020.

[2] R. Welton, D. Bollinger, M. Dehnel, I. Draganic, D. Faircloth, B. Han, J. Lettry, M. Stockli, O. Tarvainen, and A. Ueno, "Negative hydrogen ion sources for particle accelerators: Sustainability issues and recent improvements in long-term operations", *J. of Physics: Conference Series*, vol. 2244, 012045, 2022.

[3] R. Pardo, "Review of high intensity ion source development and operation", *Review of Scientific Instruments*, vol. 90, 123312, 2019.

Path Toward Multi-Megawatt Microwave Reactors for the Production of Low Carbon Hydrogen

Jan H.D. Boshoff and James M. Tranquilla

Nuionic Technologies (Canada) Inc., Fredericton, NB, Canada

Keywords: gas conversion, heterogenous catalysis, industrial microwave, microwave-assisted chemistry

INTRODUCTION

Electrification is an increasingly important element in a path toward net zero. The vast majority of new power capacity that has been brought on-line in recent years have been renewable, non-emitting electricity sources. Industrial heating represents an estimated 26% of global emissions [1]. However, while the availability of low-cost electricity is surging globally, direct electrification in industrial heating is limited by the availability of suitable process equipment that can readily make use of electricity.

Nuionic Technologies is developing novel applications of industrial microwave energy in the gas conversion industry to enable the use of non-emitting electricity as a clean energy source in industry at industrially relevant scale. This includes the development of chemical catalysts that are developed specifically for use in microwave energy [2], as well as large scale reactors that enables its use.

METHODOLOGY & MICROWAVE SYSTEM DEVELOPMENT

Nuionic is developing large scale microwave chemical reactors through the combination of a number of smaller reactor assemblies, employing principles widely used in chemical reaction engineering, as outlined in Table 1. As is the case for conventional multi-tubular chemical reactors, reactor design is driven by the development and scale-up of a single reactor "tube", which is then multiplied for larger reactors. This single unit, each of which may be representing as little as 1/1000th of the full commercial reactor scale, if properly designed, performance that is representative of the large-scale reactor.

Microwave system development encompasses all the elements including power generation, power delivery and reactor design. Over the past decades, the industrial applications of microwave power have resulted in current equipment "standards" that are based on the 100 kW continuous wave (CW) magnetron and associated electrical support systems. Multiples of this basic unit have resulted in plant installations up to a few MW; in most (or all) of

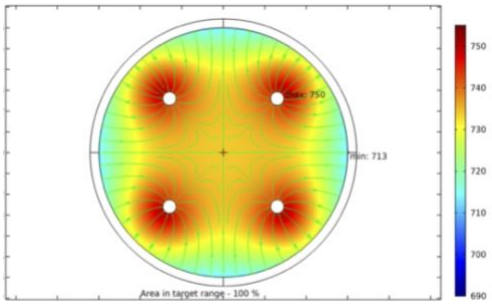

Figure 1. Example of a patent-pending multi-electrode 100kW single reactor assembly.

Table 1. Outline of Scale-up Methodology Followed for 1st Generation Reactor Systems Based on 100 kW Continuous Wave Magnetron Microwave Sources.

Stage	TRL	MW Power Level	Catalyst Inventory and Preparation Method
Lab	3	1 kW	< 100 g / Lab prepared
Pilot Phase I	4	6 kW	5 kg / Prepared at bench / lab scale
Pilot Phase II	5	6 kW	5 kg / Commercial preparation at bench / pilot scale
Technology Demonstration	6	100 kW	50 kg / Toll manufacturer on commercially relevant equipment.
Field Demonstration	7	N x 100 kW	N x 50 kg / Commercial catalyst preparation

these instances, the processes have been amenable to distributed, conveyorized configurations where they have worked well.

Microwave catalytic reactors require integrated development of the reactor assembly, catalyst and microwave energy field distribution up to the largest microwave generator point source that is used in the commercial reactor. For Nuionic, this implies developing and testing catalyst and reactor assemblies at 1 kW, 6 kW and 100 kW capacities; and while conventional multi-tubular reactors almost always consist of fixed tubes of catalyst, each microwave reactor assembly can be either a fixed or fluidized catalyst bed assembly (Fig. 1).

Nuionic is focused on industrial applications reaching to the multi-MW range which are not amenable to the distributed model. These applications require a new level of compaction and integration which are similar (in some ways) to the size and footprint of non-microwave processes against which they are competing. To be successful, the next generation of microwave system must be truly competitive both functionally as well as economically. This means pressing toward new performance limits and developing the building blocks needed to get there, including higher power CW generating devices, more efficient non-CW generating system as well simplification of the power delivery hardware that interfaces the generator and the chemical reactor.

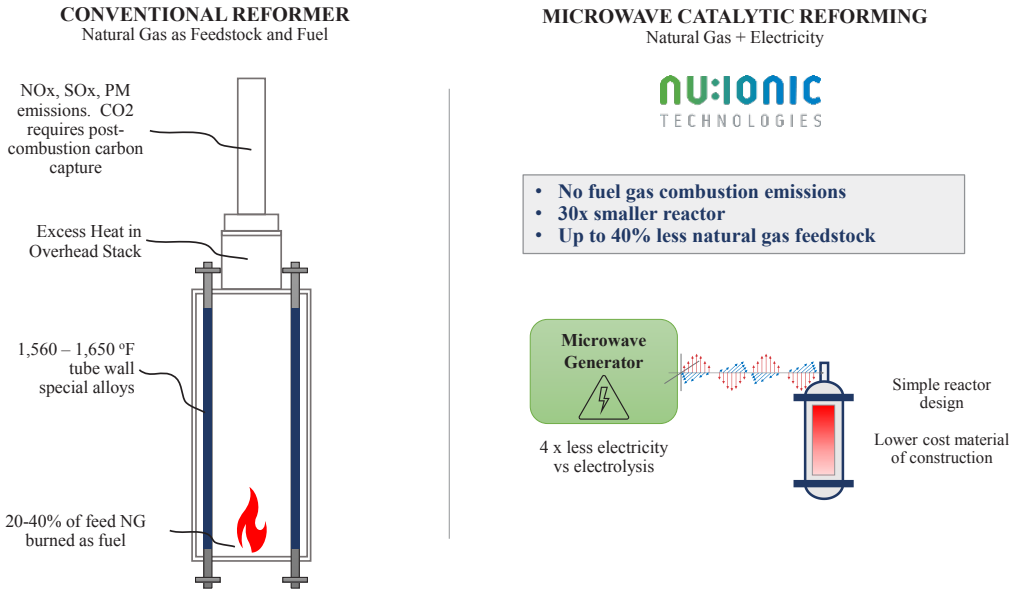

Figure 2. Schematic diagram comparing a conventional Steam Methane Reformer vs the Nuionic Microwave Catalytic Reformer for hydrogen production.

STEAM METHANE REFORMING FOR LOW CARBON HYDROGEN

Nuionic's first reactor design is for a Microwave Catalytic Reforming (MCR) process to allow for the elimination of the most polluting component of conventional hydrogen production, namely the combustion of natural gas (Fig. 2). This results in significant intensification and process simplification.

Nuionic has successfully developed an appropriate steam reforming catalyst and reactor design, and is currently at TRL 5, with plant designs for hydrogen production of up to 50 metric ton/day. Each reactor module consists of up to 4 MW of microwave energy, utilizing the scale-up principles mentioned above.

CONCLUSION

Nuionic's microwave catalytic reactor is an example of a multi-disciplinary approach to reactor development and scale-up. The company's reactor design for large scale hydrogen production effectively eliminates combustion emissions, allowing low carbon hydrogen production from natural gas / biogas and electricity with minimal greenhouse gas footprint. The company is also developing reactors for a number of other reaction chemistries.

REFERENCES

[1] IEA, *Renewables 2021*, https://www.iea.org/report/renewables-2021.
[2] V. Palma, D. Barba, M. Cortese, M. Martino, S. Renda, and E. Meloni, "Microwaves and heterogeneous catalysis: a review on selected catalytic processes," *Catalysts*, vol. 10, 246, 2020.

Atmospheric Pressure Plasma Source and Downstream Source: Characteristics and Industrial Applications

Robert Mueller[1], Klaus-Martin Baumgaertner[1], Markus Dingeldein[1], Moritz Gorath[1], Jens Hofmann[1], Andreas Schulz[2], and Matthias Walker[2]

[1]Muegge GmbH, Reichelsheim (Odenwald), Germany
[2]Institute of Interfacial Process Engineering and Plasma Technology, University of Stuttgart, Stuttgart, Germany

Keywords: atmospheric pressure plasma, downstream plasma, energy conversion, energy storage, microwave plasma, power-to-X, renewable energies

INTRODUCTION

Microwave-excited atmospheric pressure plasma sources and downstream sources are designed to generate a contact-free plasma while ensuring stable operation for a wide range of gas-types, gas flow and microwave power at 2.45 GHz and 915 MHz. These microwave-excited plasma sources are well suited for both the synthesis of special gases and for assisting chemical reactions with highly reactive gas species. This is the key for a wide range of industrial applications. Power-to-X applications such as Power-to-Gas and Power-to-Chemicals are prominent examples of industrial applications based on these microwave-excited plasma sources.

CHARACTERISTICS OF ATMOSPHERIC PRESSURE MICROWAVE PLASMA SOURCES AND DONWSTREAM SOURCES

High density of high-energy electrons, ions and highly reactive radicals in particular are the main characteristics of both microwave plasma torches operated at atmospheric pressure and downstream plasma sources working in the pressure range of a few mbar. This is due to the high field concentration formed in the resonant cavity of the microwave plasma sources. In this region, the plasma is ignited and sustained. Gas temperatures of up to 3500 K in the core of the plasma were determined by optical emission spectroscopy. Both types of plasma sources generate a contact-free plasma while ensuring stable operation in a wide range of gas types, working gas flow and microwave power (i.e., up to 10 kW at 2.45 GHz and 100 kW at 915 MHz).

These characteristics are prerequisites for significant enhancement of chemical kinetics and for thermal conversion of materials (e.g., heating and melting of metals and glass) in climate-neutral processes using energy from renewable sources.

POWER-TO-X APPLICATIONS USING MICROWAVE PLASMA TECHNOLOGIES

In periods with high output, generation of electrical energy from renewable energy sources (e.g., photovoltaics, wind, and water) can easily exceed the load. For maintaining stability of the public mains supply, surplus energy from renewable sources has to be stored, which poses a big challenge. “Power-to-X” is a general term summarizing technologies for conversion of this kind of surplus energy from renewable sources into matter that either can be stored and reconverted when required, or that will serve as basic materials for the production of, for example, more complex substances in the chemical industry or synthetic fuels replacing fossil fuels in the transport sector.

Power-to-X comprises generic technologies including Power-to-Heat, Power-to-Power, Power-to-Chemicals, Power-to-Gas and Power-to-Liquid, and also specific technologies including Power-to-Fuel, Power-to-Syngas, Power-to-Protein and Power-to-Ammonia. Power-to-X processes – inter alia applied for the decrease of greenhouse gases – are prominent industrial application fields of atmospheric pressure microwave plasma torches and downstream plasma sources. The following examples demonstrate the crucial role of microwave plasma technologies in Power-to-X applications.

MICROWAVE PLASMA TECHNOLOGIES FOR POWER-TO-GAS AND POWER-TO-CHEMICALS APPLICATIONS

Carbon dioxide (CO_2) conversion is a promising approach for storing surplus renewable energy (Fig. 1). The concept of CO_2 conversion is based on splitting CO_2 into oxygen (O) and carbon monoxid (CO) radicals in an atmospheric pressure plasma process. Highly energetic microwave plasma torches operated at the frequencies of 2.45 GHz and 915 MHz, which use excess electrical energy from regenerative sources, are well suited for efficient CO_2 dissociation. The process can be applied wherever CO_2 is produced in enriched form: in power plant combustion, in the cement and glass industries, and in breweries where CO_2 is a by-product of alcoholic fermentation.

CO is an industrial gas, which has numerous applications in chemical manufacturing. It can be converted into base chemicals and chemical energy stores such as methanol or methane in existing infrastructures using conventional chemical processes. By separation of the oxygen from the gas mixture, for example via a perovskite membrane, the remaining CO gas can be utilized for conversion into syngas or higher hydrocarbons and as fuel in some steel production processes. Hence, a zero-emission carbon cycle can be established.

A carbon-free, circular economy is required to decrease greenhouse gas emissions like CO_2. Carbon neutral hydrogen (i.e., H_2 produced by use of energy from renewable sources) is a commonly proposed alternative to the carbon-based economy. The conversion of natural gas like CH_4 into carbon neutral H_2 and acetylene (C_2H_2) as feedstock in the chemical industry – without formation of CO_2 – by application of microwave plasma sources has been successfully studied on the laboratory level for many years. CH_4 conversion rates of more than 90% and selective C_2H_2 yield of more than 80% with 2.45

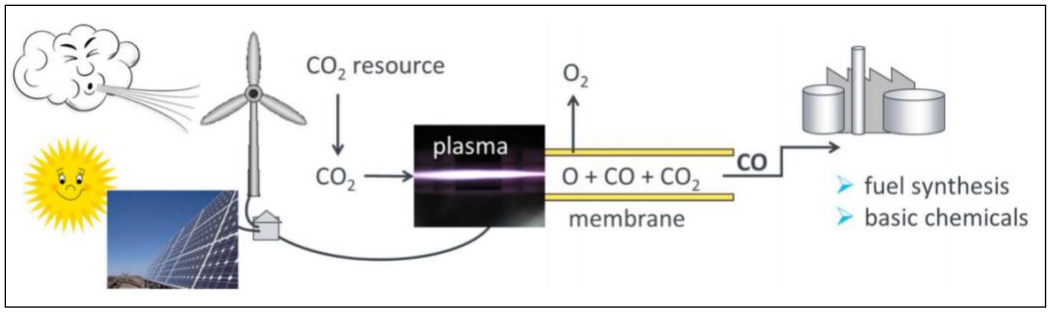

Figure 1. Concept of CO_2 conversion as an example of a Power-to-Chemicals application.

GHz plasma sources at power levels below 2 kW were reported [1]. New developments in microwave plasma torches and downstream plasma sources at much higher power levels of up to 100 kW using 915 MHz microwave technology enable successful upscaling and transformation of these Power-to-Gas and Power-to-Chemicals processes from laboratory level to industrial production. Compared to results achieved at the laboratory level, the proportionate energy consumption on an industrial scale could be reduced by approximately one order of magnitude, without losing efficiency in CH_4 conversion and in selective C_2H_2 yield [2].

CONCLUSION

Due to its wide and versatile utilization range, atmospheric pressure microwave plasma sources and downstream sources enable a wide range of industrial and research processes. The contactless plasma generation within a resonator structure is the key property of these microwave energy driven high temperature applications. At the same time, microwave plasma systems offer the best alternative to build decentralized supply networks with CO_2-neutral hydrogen-based fuel gases for energy storage or for direct and location-independent use.

Power-to-X technologies based on microwave plasma processes are innovative solutions to convert surplus electrical energy from renewable sources into material resources such as hydrogen, carbon monoxide, and synthetic gases for storage and recycling, e.g., conversion of electrical energy into gaseous or liquid fuels or chemicals for long-haul trucking, shipping and aviation.

REFERENCES

[1] M. Heintze and M. Magureanu, “Methane conversion into acetylene in a microwave plasma: optimization of the operating parameters,” *J. Appl. Phys.*, vol. 92, pp. 2276–2283, 2002.

[2] M. P. Bailey, “A microwave-plasma process that efficiently makes hydrogen and acetylene,” *Chemical Engineering*, Nov. 1, 2020, www.chemengonline.com/microwave-plasma-process-efficiently-makes-hydrogen-acetylene/.

Operational Experience with 1 MHz, 200 kW Free Running Oscillators for the ITER Neutral Beam Injectors Plasma Source

Alberto Maistrello

Consorzio RFX: CNR, ENEA, INFN, Università di Padova, Acciaierie Venete SpA, Padova, Italy

Keywords: neutral beam injector, RF plasma source, RF solid state amplifiers, self-excited oscillators

SUMMARY

This talk describes operational experience from a very special radio frequency power application: neutral beam injector (NBI) ion sources for fusion experiments. ITER will be the first fusion device to produce net energy and it is currently being constructed in Cadarache, France. ITER uses a mix of heating systems to reach high plasma temperature and to sustain fusion conditions. Most of the additional heating power will be delivered by two heating neutral beam injectors (NBI), each one expected to inject into the plasma a power of up to 16.5 MW by means of a beam composed of deuterium atoms accelerated up to the energy of 1 MeV, for a beam pulse length up to 3600 s [1,2].

The requirements for the ITER heating NBI were never met in a single device, thus the Neutral Beam Test Facility (NBTF) was required to make the future operation of the ITER heating neutral beam injectors efficient and reliable. This is fundamental for achieving thermonuclear-relevant plasma parameters in ITER.

The NBTF in Padova (Italy) includes two experiments: SPIDER (Source for the Production of Ions of Deuterium Extracted from a Radio Frequency Plasma), a full-size radio frequency negative-ion source [3] and MITICA (Megavolt ITer Injector & Concept Advancement), the full-scale prototype of the ITER heating neutral beam injector, based on the SPIDER ion source. SPIDER operated from June 2018 to the end of 2021 when a major shutdown started to improve the beam source, the power supplies and the pumping system. MITICA's plant systems, including the power supplies, have been installed and their integrated commissioning is underway. In the meantime, the procurement of in-vessel components is proceeding. MITICA's will begin operation by the end of 2024.

The SPIDER and MITICA ion source is composed of a 4x2 matrix of inductively coupled plasma drivers, surrounded by antennas, fed in pairs with RF power up to 200 kW at 1 MHz. Negative ions are mainly generated on the surface of a plasma grid (PG) covered

with caesium, while a set of grids (PG, extraction grid (EG) and grounded grid) working at different voltages extract and accelerate the beam up to 100 keV.

The Power Supply (PS) system is divided into two main parts: the acceleration grid PS (AGPS), feeding the main negative ion acceleration voltage, and the ion source and extraction grid PS (ISEPS) [4], installed within an air insulated Faraday cage called the high voltage deck (HVD) [5,6], biased at the AGPS voltage with respect to ground.

The four RF generators are based on push-pull Colpitts self-excited oscillators and a high voltage dc power supply; they are installed within the HVD along with the other ion source power supplies. The PS system is connected to the SPIDER beam source through a multi-conductor transmission line [7] which includes 4 coaxial RF lines and a matching network installed on the plasma source backside.

A key aspect of this application is that the impedance of the RF generator load varies from no-load to load conditions during the pulse in a not easily predictable way, since it is related to the plasma parameters. In other fusion experiments, a matching network composed of variable capacitors addresses this issue. However, this could not be adopted in ITER, due to the nuclear environment, along with the limited space available on board the plasma source. This limit was overcome by varying the operating frequency of the RF generators [8], in the range of 900-1100 kHz, with a variable capacitance in their tank circuit, thus in an easily accessible environment, while a normal L-type matching network with two fixed capacitances was provided on board the ion source.

In addition, free-excited oscillators were selected, on the basis of their supposed higher capability of adaptation to the load impedance variations. However, operation produced results quite different than expected: sudden frequency changes, called frequency flips, were observed when approaching the matching condition [9]. Analyses explanained the phenomenon, directly linking it to the inherent operational principle of the free-excited oscillators and to the presence of two resonances in the circuit (tank circuit & source load).

The frequency flip limits the operational space of the oscillators, producing an inhibited area around the best matching frequency (where the voltage standing wave ratio (VSWR) is the minimum) and stressing the system. The main drawback is the limitation in the power delivered to the load to about half the nominal load.

Operation made more evident the need for cleaning and conditioning the high voltage components in the oscillators, which were potential locations for insulation failure. This negatively impacted on availability. Both frequent unexpected flashovers in the oscillator were observed and significant maintenance was performed.

Another important lesson learnt from the operation of this complex system was the impact of the mutual coupling among the 4 pairs of antennas and surroundings passive structures. This caused cross-talking between the oscillators and produced intermodulation in the plasma. This can be mitigated by improving the connection layout, but could be more effectively addressed if all generators operate at the same frequency and phase. However, this is not possible for self-excited oscillators.

All these limitations can be overcome by changing the technology from tetrode-based oscillators to solid state amplifiers. Direct control of the RF amplifier output frequency can

allow optimal matching (lowest possible VSWR) [10], while phenomena like frequency flips are not expected since there are no competing resonant circuits. Modular amplifiers allows operating with faulted modules at reduced output power, thus increasing the availability of the plant. Furthermore, these RF amplifiers do not use high voltage components, avoiding the related problems.

Cross-talk among amplifiers is not expected since they can be driven at the same frequency and with a given phase displacement. However, the design and implementation of solid-state amplifiers for this special application required addressing several specific issues related to the frequency variation ranges, maximum power, interfaces, and cooling.

The talk will give an overview of the main interesting aspects coming from the operational experience of the SPIDER self-excited oscillators, the main outcomes of the accompanying analyses to better understand the observations, and key aspects of the new solid state amplifier design, planned to be installed in 2023, after the long on-going shutdown.

ACKNOWLEDGMENT

This work has been carried out within the framework of the ITER-RFX Neutral Beam Test Facility (NBTF) agreement and has received funding from the ITER Organization. This publication reflects the views only of the author, the views and opinions expressed herein do not necessarily reflect those of the ITER Organization.

REFERENCES

[1] ITER Physics Expert Group on Energetic Particles, Heating and Current Drive and ITER Physics Basis Editors, “Plasma auxiliary heating and current drive,” *Nucl. Fusion*, vol. 39, no. 12, 1999.
[2] ITER Technical Basis, International Atomic Energy Agency, Vienna, Austria, Section 5.3 DDD5.3, 2002.
[3] V. Toigo, et al., “Progress in the ITER neutral beam test facility”, *2019 Nucl. Fusion*, vol. 59, 086058.
[4] M. Bigi, et al., “Design, manufacture and factory testing of the Ion Source and Extraction Power Supplies for the SPIDER experiment”, *Fusion Engineering and Design*, vol. 96–97, pp. 405-410, 2015. es 405-410.
[5] E. Gaio, et al., “The alternative design concept for the ion source power supply of the ITER neutral beam injector”, Fusion Engineering and Design, vol. 83, Issue 1, pp. 21-29, 2008.
[6] M. Boldrin, et al., “The 100 kV Faraday cage (High Voltage Deck) for the SPIDER experiment”, *Fusion Engineering and Design*, vol. 96–97, pp. 411-415, 2015.
[7] M. Boldrin, et al., “The transmission line for the SPIDER experiment: from design to installation”, *Fusion Engineering and Design*, vol. 123, pp. 247-252, 2017.
[8] E. Gaio, et al., “Studies on the radio frequency power supply system for the ITER NB injector ion source”, *Fusion Engineering and Design*, vol. 82, Issues 5–14, pp. 912-919, 2007.
[9] A. Zamengo, et al., “Power supply system for large negative ion sources: Early operation experience on the SPIDER experiment”, Fusion Engineering and Design, vol. 173, 112790, 2021.
[10] W. Kraus, et al., “Solid state generator for powerful radio frequency ion sources in neutral beam injection systems”, Fusion Engineering and Design, vol. 91, pp. 16–20, 2015.
[11] L. Zanotto, et al., "Radio frequency generators based on solid state amplifiers for the NBTF and ITER projects", SOFE 2021.

Tuning Method for Improved Microwave Power Coupling into Frequency Tuned Plasma and Enhanced Reliability of High-Power Coaxial Transmission Line

Mohammad Kamarehi, Ilya Pokidov, Ken Trenholm, and Joe Desjardins

MKS Instruments / P&RGS, Wilmington, MA, USA

Keywords: coaxial cable, coupling, microwave, plasma, solid state, tuning

INTRODUCTION

In recent years, 2,450 MHz frequency-tuned microwave generators and the relevant delivery components have been utilized in applications such as microwave heating, material processing, research laboratories, as well as Semiconductor remote plasma sources. Semiconductor processing tools have begun to become much smaller in their footprint in order to increase the throughput of the Semiconductor Fabs by maintaining the same footprint of the Processing Fabs. As such, the Semiconductor tool manufacturers demand smaller footprint for the plasma generating systems, as well as added flexibility for installation.

MKS Instruments has been conducting advanced research in developing Solid State-based plasma systems of smaller footprint in order to provide the Semiconductor Industry with their recent footprint requirements. Such research has been focused on replacing waveguide delivery systems with coaxial-based delivery components of about 1,500 watts at 2,450 MHz. However, coaxial cables are primarily designed for applications where the cables do not use mechanical tuners in line and also terminated in a matched load. Mechanical tuners can be used as long as the coaxial cable is not located between the tuner and a highly mismatched load. The purpose of research at MKS is to provide a means of mechanical tuning that doesn't subject the cable to operation at high standing wave and consequently forming localized and excessive heating along the coaxial cable which could lead to premature and catastrophic failures.

This paper covers the extensive research conducted by MKS for developing a method for a) reducing or eliminating standing wave within the coaxial line, b) enhancing the coax cable reliability and life performance, and c) improving power coupled into a frequency-tuned microwave plasma source using a solid-state generator.

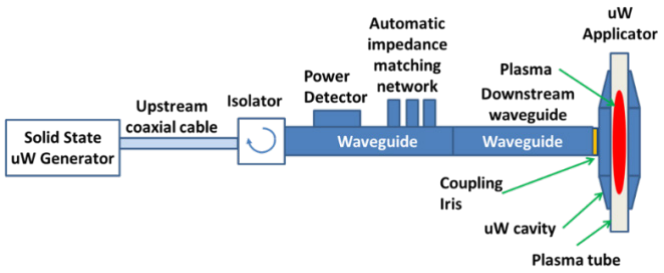

Figure 1. High-level illustration of MKS' solid-state downstream plasma system.

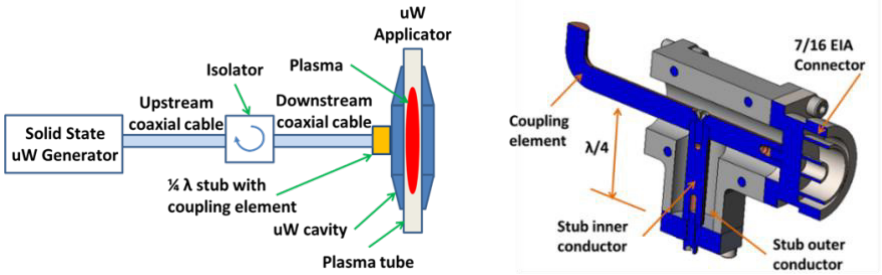

(a) (b)

Figure 2. Plasma system in reduced footprint (a) and tuning and coupling elements

METHODOLOGY

Fig. 1 shows a typical MKS' frequncy-tuned and waveguide-based downstream plasma system in which an automatic impedance matching network is used to tune out the reflected power caused by plasma impedances within the frequency band of 2.4-2.5 GHz. The methodology used to reduce the footprint of the system by designing delivery components into a coaxial-based system is shown in Figs. 2 and 3. Fig. 2 shows the plasma system with reduced footprint using 7/16" coaxial cable with a fixed coaxial-based tuner positioned immediately upstream of the microwave cavity.

Fig. 3 shows a 7/16" coaxial-based λ/4 wavelength fixed impedance matching stub integrated into the coupling antenna element, which combined, must be positioned immediately next to the microwave cavity to minimize any reflected power and standing wave in the transmission line downstream of the applicator. The method is intended for coarse tuning of the microwave energy being coupled to the resonant applicator. The final tuning is achieved by using the frequency-tuned capable solid-state generator. The coaxial-based tuner was also investigated for an adjustable inner conductor configuration which further provides flexibility of adjusting the impedance of the tuner to coarsely match that of the plasma impedance.

Fig. 4(a) shows COMSOL simulation results of power absorbed in the plasma at input power of 1 kW for the plasma source having a coaxial-based coarse tuner shown in Fig. 3. The simulation was done for a range of plasma conductivities covering 3 orders or magnitude. It shows that the coaxial-based tuner in conjunction with frequency tuning enable efficient

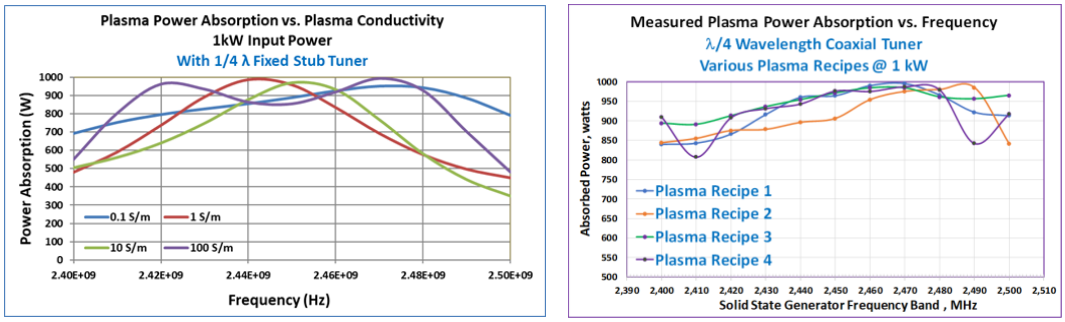

Figure 4. COMSOL simulation results (a) power absorption rest results (b).

It shows that the coaxial-based tuner in conjunction with frequency tuning enable efficient microwave coupling into the plasma with all plasma impedances or conductivities which fall between 2.4-2.5 GHz, the frequency band of the solid-state generator.

RESULTS AND DISCUSSION

Fig. 4(b) depicts the results of testing the microwave plasma system shown in Fig. 2 for several recipes. The results confirms the COMSOL simulation shown in Fig. 4(a). It is clear from the results that the combination of the coaxial-based λ/4 wavelength stub depicted in Fig. 3 and the solid-state microwave generator provide a viable and practical solution to designing a high-power coaxial-based plasma system. This system has a substantially reduced footprint. The peak absorption for all recipes tested was obtained between 2.46-2.49 GHz, indicating that plasma load impedances were relatively close.

Since the coaxial-based tuner is positioned immediately downstream of the microwave cavity, any reflected power and standing wave was minimized in the coaxial cable immediately upstream of the of coaxial-based tuner. This, in turn, eliminated overheating of the coaxial cable since the electric field hot spots were no longer present, therefore, substantially enhanced the reliability of the coaxial cable.

CONCLUSION

Extensive research has led to the design and development of a flexible and reduced footprint coaxial-based microwave plasma source. Furthermore, the incorporation of a fixed coaxial-based stub positioned immediately downstream of the plasma source has enabled the use of a high-power coaxial cable with enhanced reliability performance.

Radiofrequency Plasma Heating for Electrodeless Space Thruster Applications

Mario Merino, Jaume Navarro, Célian Boyé, Pedro Jiménez, Marco Inchingolo, Jiewei Zhou, and Eduardo Ahedo

[1]Equipo de Propulsión Espacial y Plasmas (EP2), Universidad Carlos III de Madrid, Leganés, Spain

Keywords: electrodeless plasma thrusters, radiofrequency plasma heating, space propulsion

INTRODUCTION

Radio frequency energization of plasmas offers several advantages for space propulsion applications, as it (1) eliminates the need for high-voltage sources onboard, (2) enables removing all life-limiting electrodes in contact with the plasma, and (3) allows using many propellant types, including those which are aggressive with typical electrode materials [1]. Existing concepts that exploit this idea, including the helicon plasma thruster (HPT) [2-4], the electron-cyclotron resonance plasma thruster (ECRT) [5, 6], the variable specific impulse magneto-plasma rocket (VASIMR) [7], and novel concepts like the magnetic arch thruster (MARCH), promise lower system-level complexity, longer lifetime, and higher mission versatility through enhanced thrust and specific impulse throttleability. Different power coupling strategies have been investigated, using frequencies from a few MHz to several GHz, and various electromagnetic coupler geometries. Different plasma absorption mechanisms, including resonant and non-resonant (collisional) are sought. However, to date these electrodeless devices do not provide good propulsive performance, in part due to the insufficient understanding of plasma-wave interaction [8].

Efficient power coupling depends directly on the plasma source and electromagnetic circuit design and geometry and requires exciting the correct wave modes in the plasma or seeking adequate resonances. Generally, it is desirable that the plasma absorbs most of the power near the center of the source volume and away from the source walls, to minimize hot plasma losses. The electromagnetic field response, in turn, depends strongly on the plasma density, collision frequency, and impedance seen by the electromagnetic circuit. These may change drastically across thruster operating modes. Indeed, the plasma transport and the electromagnetic problem are intimately coupled. Understanding the effect of design and operational parameters on the plasma-wave interaction is paramount in optimizing this key process of the operation of electrodeless space thrusters and is an ongoing endeavor in the space propulsion community.

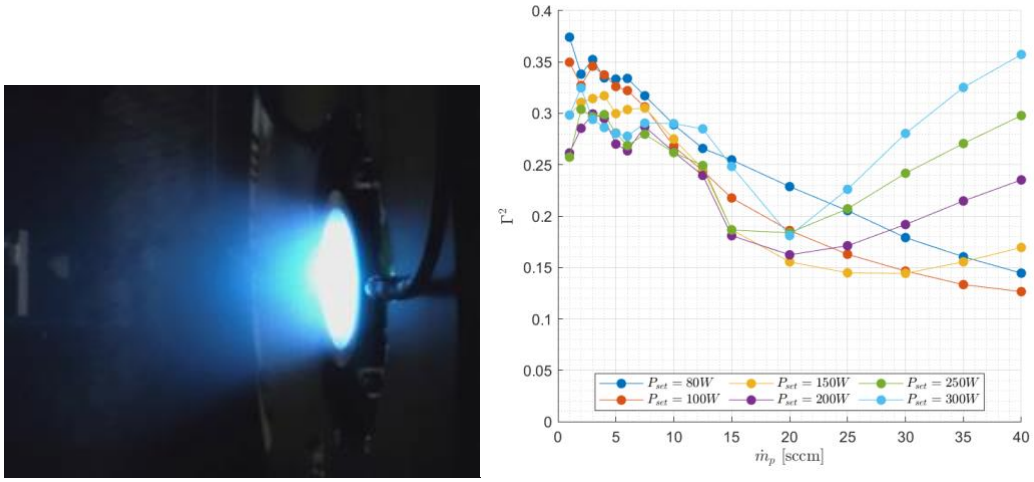

Figure 1: ECRT prototype in operation at EP2 facilities (a) and square of the measured reflection coefficient Γ in the ECRT for different values of the forward power and mass flow rate to the thruster (b).

METHODOLOGY AND RESULTS

This talk presents recent results from the EP2 research group in the area of electrodeless plasma thrusters, and exposes the main open questions relating to the plasma-wave interaction problem. Experimental results on HPT and ECRT prototypes [8, 9] are used to explain the multiplicity of approaches to electromagnetic power coupling. The ECRT in operation is shown in operation in Fig. 1. We discuss the sensitivity of the plasma properties and the MW reflection coefficient to changes in the operating point. The variation of the reflection coefficient Γ with the operating point of the thruster (mass flow rate, power) is presented and discussed (see Fig. 1), showing that a minimum occurs for each power at an intermediate mass flow rate in the investigated range.

Finite-differences frequency-domain (FDFD) and vector finite element method (FEM) simulations of the wave propagation in these devices [10, 11] are used to obtain the power absorption profiles in the plasma and assess the influence of the plasma parameters on the electromagnetic problem. The main parameters affecting the propagation and absorption are the applied magnetic field strength and direction, and the plasma density; the plasma collisionality plays a secondary role. Fig. 2 shows the power absorption profile in the plasma. Most of the power absorption happens inside the source region, where plasma density is highest, but non-negligible absorption exists also in the plume region. Interestingly, fields are evanescent and essentially no absorption occurs far from the thruster, once the electron-cyclotron resonance condition is crossed. This restricts the effective space where the fields are large to the vicinity of the device.

Finally, the geometric configuration of the novel MARCH thruster and its effect on the power propagation and absorption is briefly discussed.

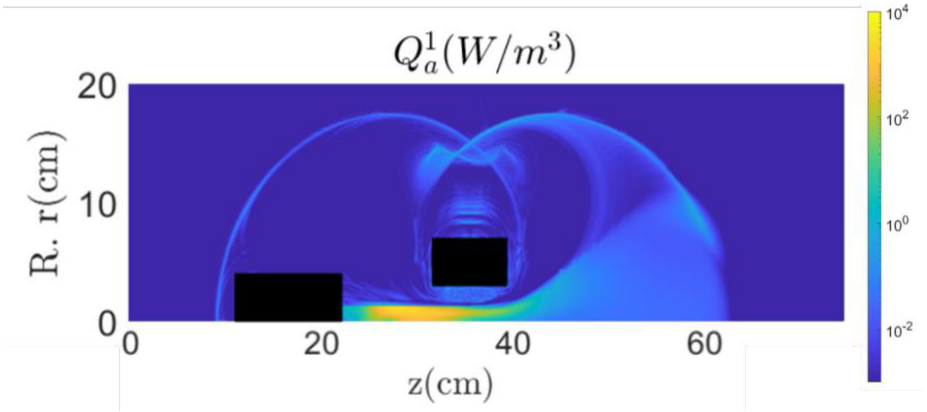

Figure 2: Simulated power absorption profile in the plasma, in the nominal operating point of the HPT prototype. Black boxes represent the magnetic coils and electronic boxes of the thruster.

REFERENCES

[1] E. Ahedo, "Plasmas for space propulsion," *Plasma Physics and Controlled Fusion*, vol. 53, no. 12, 124037, 2011.

[2] F. Chen, "Plasma ionization by helicon waves," *Plasma Physics and Controlled Fusion*, vol. 33, no. 4, pp. 339, 1991.

[3] M. West, C. Charles, and R. Boswell, "Testing a heli-con double layer thruster immersed in a space-simulation chamber," *J. Propulsion and Power*, vol. 24, no. 1, pp. 134–141, 2008.

[4] T. Ziemba, J. Carscadden, J. Slough, J. Prager, and R. Winglee, "High power helicon thruster," *41th AIAA/ASME/SAE/ASEE Joint Propulsion Conference & Exhibit*, AIAA 2005, 4119.

[5] D. Miller, E. Gibbons, and P. Gloersen, "Cyclotron resonance propulsion system,"In: *Electric Propulsion Conference*, 1962, p. 2.

[6] J.C. Sercel, "Electron-cyclotron-resonance plasma thruster research," In: *24th Joint Propulsion Conference*, 1988.

[7] F.R.C. Diaz, The VASIMR rocket, *Scientific American*, vol. 283, no. 5, pp. 90-97, 2000.

[8] J. Navarro-Cavallé, M. Wijnen, P. Fajardo, and E. Ahedo, "Experimental characterization of a 1 kW helicon plasma thruster," *Vacuum*, vol. 149, pp. 69–73, 2018.

[9] M.R. Inchingolo, J. Navarro-Cavallé, and M. Merino, "Design and plume characterization of a low-power circular waveguide coupled ECR thruster", In: *MPCS 2020 Conference.*

[10] B. Tian, M. Merino, and E. Ahedo, "Two-dimensional plasma-wave interaction in a helicon plasma thruster with magnetic nozzle," *Plasma Sources Science and Technology*, vol. 27, 114003, 2018.

[11] A. Sánchez-Villar, J. Zhou, E. Ahedo and M. Merino "Coupled plasma transport and electromagnetic wave simulation of an ECR thruster," *Plasma Sources Science and Technology*, vol. 30, 045005, 2021.

Mass Separation by the Ponderomotive Force Exerted by Standing Alfven Waves

A. Fruchtman and G. Makrinich

Holon Institute of Technology, Holon, Israel

Keywords: cyclotron frequency, mass separation, ponderomotive force, standing Alfven waves

INTRODUCTION

Mass separation, separation of particles of different mass, is a crucial process in a variety of societal applications [1]. In a significant number of techniques electromagnetic forces are exerted on charged particles or plasmas. These techniques rely on the difference in particle dynamics that results from mass difference. Methods in which the electromagnetic forces on the plasma involve electromagnetic waves have also been considered for mass separation. Such are the use of ion cyclotron resonance (ICR) [2, 3] and the ponderomotive force [4], which is the subject of this work. These waves are in the radio frequency range. In order to achieve high throughput, the process has to be realized in a plasma. Ways to introduce appropriate electromagnetic fields into the plasma have to be employed. A possible candidate is the shear Alfven wave or the ion cyclotron wave. In addition, the ponderomotive force modifies the plasma density and induces electrostatic space-charge fields. It is expected that these steady electrostatic fields will compete in an unfavourable way with the ponderomotive force and may destroy the mass separation process. Our goal was to study theoretically the combined effect of the ponderomotive force and the electrostatic self-fields.

THEORETICAL MODEL

This work is a theoretical analysis of the dynamics of two ion-species plasma under the ponderomotive force exerted by standing Alfven waves and the electrostatic self-fields. The plasma equations are the one-dimensional cold fluid equations for the two ion species combined with the assumption of quasi-neutrality, that determines the electrostatic fields. Ion velocity reaching the sonic velocity at both axial ends of the plasma is the imposed boundary condition [5]. For simplicity, the ponderomotive force by the Alfven waves is assumed uniform in the current study and the fields were determined by the dynamics of the majority ions.

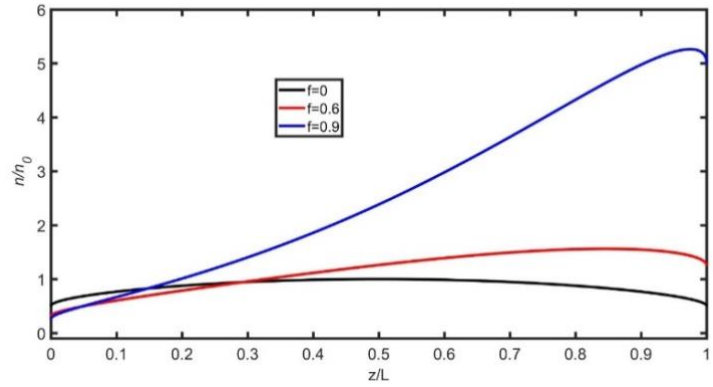

Figure 1: The calculated dimensionless electron density along the discharge, for three different values of f, the dimensionless ponderomotive force.

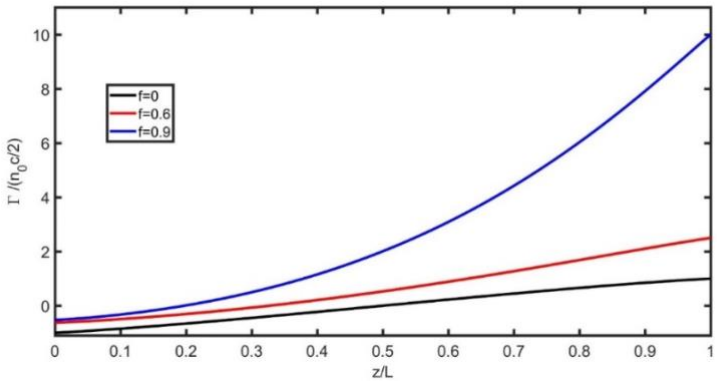

Figure 2: The calculated dimensionless flux density along the discharge of the majority ions, for three different values of f.

RESULTS OF CALCULATION

The formalism described above was applied to a two ion-species plasma (Ne^{22} and Ne^{20}, for example). The wave frequency was tuned to be in the vicinity of the cyclotron frequency of the majority ion. The majority ions were pushed by the ponderomotive force along the steady magnetic field towards one end of the discharge. Due to that force, the plasma density was modified. It was shown that the induced electrostatic field pushes the minority ions to the opposite end of the discharge, enhancing the mass separation effect. Thus, the electrostatic fields can be manipulated in a way that increases the mass separation process. Fig. 1 shows the calculated modification of the plasma density along the magnetic field due to the ponderomotive force. As f, the dimensionless ponderomotive force, increases, the density in the right-side increases. Fig. 2 shows the particle flux density of the majority ion, that becomes asymmetrical as f increases, larger to the right, while the flux to the left decreases. When f is near unity, most of the majority ions move to the right.

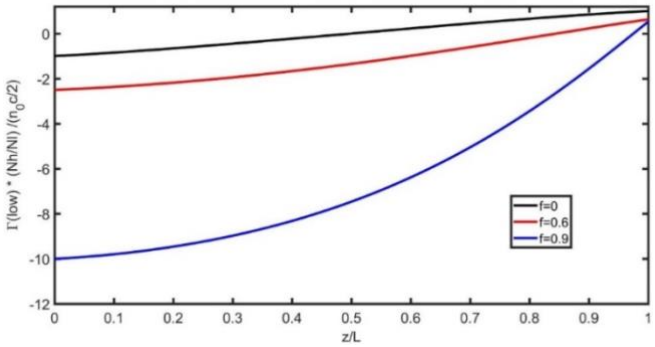

Figure 3: The calculated dimensionless flux density along the discharge of the minority ions, for three different values of **f** .

It is seen in Fig. 3, that as **f** increases, the flux of the minority ions also becomes asymmetrical, but larger to the left, while the flux to the right decreases. When **f** is near unity, most of the minority ions move to the left.

DISCUSSION

The calculation results, shown in the figures, demonstrate that the two species flow preferably towards opposite directions. The majority ions move mostly towards the right, while the minority ions move mostly to the left. The plasma density shown in Fig. 1 is larger at the right side due to the ponderomotive force on the majority ions. That modified electron density induces an electrostatic field that pushes the minority ions to the left. This result demonstrates that the electrostatic fields can be manipulated to play a positive role in a scheme for mass separation that is based on the ponderomotive force of the radio-frequency waves.

CONCLUSION

We presented a scheme for mass separation based on the combined effect of the ponderomotive force by Alfven waves and by space–charge fields. The results should motivate further research into the application to mass separation. Ways to excite a desired standing radio-frequency wave and to control its profile along the plasma should be explored.

REFERENCES

[1] S.Z. Zweben, R. Gueroult, and N.J. Fisch, ”Plasma mass separation,” *Phys. Plasmas*, vol. 25, pp. 090901-1-090901-23, 2018.

[2] J.M. Dawson, H.C. Kim, D. Arnush, B.D. Fried, R.W. Gould, L.O. Heflinger, C.F. Kennel, T.E. Romesser, R.L. Stenzel, A.Y. Wong, and R.F. Wuerker, ”Isotope separation in plasmas by use of ion cyclotron resonance,” *Phys. Rev. Lett.*, vol. 37, no 23, pp. 1547 – 1550, 1976.

[3] D.A. Dolgolenko and Yu.A. Muromkin, Plasma isotope separation based on ion cyclotron resonance, *Physics – Uspekhi*, vol. 52, no 4, pp. 345-357, 2009.

[4] E.S. Weibel, Separation of isotopes, *Phys. Rev. Lett.*, vol. 44, no 6, pp. 377-379, 1980.

[5] A. Fruchtman, Neutral depletion in a collisionless plasma, *IEEE Trans. Plasma Sci.*, vol. 36, no 2, pp. 403-413, 2008.

The Influence of Post-Plasma Species from Microwave Enhanced $CH_4/N_2/Ar$ Plasma on the Selectivity of Ethylene and Ammonia

Sarojini Tiwari, Brandon Robinson, Sean Brown, and Jianli Hu

West Virginia University, Morgantown, WV, USA

Keywords: microwave-enhance plasma, methane conversion, post-plasma catalysis

SUMMARY

Chemical processing industry is substantially dependent on natural gas as a feedstock. In the process, it has become one of the major contributors of green-house gas emissions [1]. Process intensification can substantially upgrade chemical industries to a carbon free and zero waste systems. The basic definition of an intensified chemical process has broadened from merely reducing the size of the processing plant to a holistic undertaking that can reduce waste and energy consumption with improved product yield [2, 3]. The direct conversion of Methane (CH_4), the major component in shale gas, to value-added chemicals can be qualified as an intensified process, if it is energy efficient, free of unwanted side products (CO_2), and leads to maximum conversion of CH_4 to useful products.

Microwave plasma (MWP) reactor is an emerging technology in line with the principles of process intensification. It offers several benefits such as fast process dynamics and flexibility, high product yield with least amount of unwanted by-products and low maintenance cost [4]. Additionally, MWP offers several advantages over other plasma sources [5]. It does not require electrodes, have the highest electron density in the discharge region, and high power-to-plasma efficiency [6]. In fact, the direct conversion of CH_4 to acetylene (C_2H_2) and hydrogen (H_2) in MWP reactors have been demonstrated to be energy efficient with high yield of the desired product [7, 8]. They can be optimized further by changing process parameters such as MW power and frequency [9], and composition of the feed gas mixture [10]. MWP, being a high energy discharge, converts CH_4 mostly to C_2H_2, H_2 and carbon soot [11]. The products can be upgraded by placing a catalyst in MWP reactors. Catalytic reactions in hot plasmas, such as MWP at atmospheric pressure, is only feasible in a post-plasma setup. In this kind of reactor, some of the plasma species created in the discharge region survive up to the post-plasma region [12]. Several studies have identified post-plasma species in MWP reactors generated from a feed gas mixture of CH_4 with Argon (Ar) or with Nitrogen (N_2), directed at surface coating and nitriding applications [13-15]. There has been no such study, as per our best knowledge, in direct methane conversion to valuable products such as C_2H_4 and NH_3.

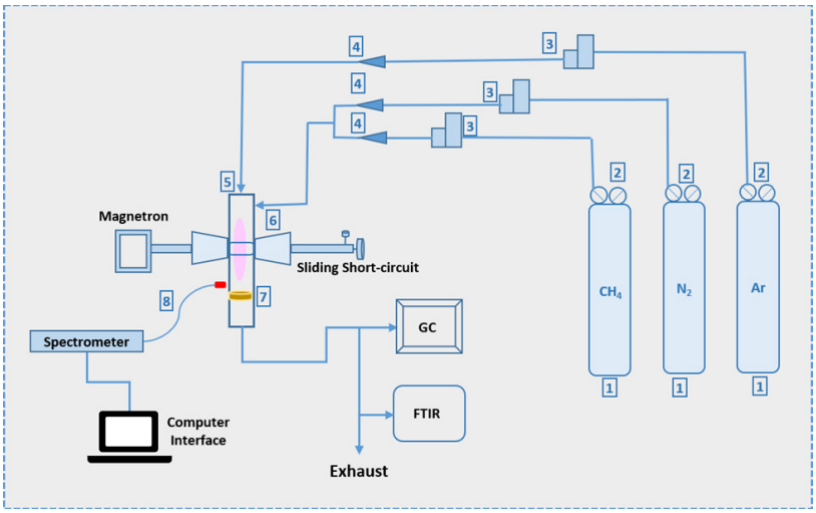

Figure 1. Reactor configuration.

A synergy of the plasma species with catalyst can be established if the post-plasma species influence the distribution and selectivity of the final products [16]. An optimum catalyst design can maximize the inter-molecular interaction of the plasma species. Hence, MWP catalytic reactor adheres to the principle of process intensification [3]. The reactive species with a plasma consist of free electrons, ions, radicals and excited states of gas molecules. An ideal catalyst would optimize the recombination of these species on its surface to modify the activity and the selectivity of the reaction [12, 17]. Based on numerous evidences of long-lived plasma species, a catalyst can be designed to influence the recombination of active radicals in the post-plasma region. The MW enhanced plasma made from CH_4 is known to be rich in CH_x and H radicals [18]. A catalyst, placed at the post plasma region, should be capable of hydrogenating these radicals to ethylene, while preventing over hydrogenation to ethane. The Ag-Pd bimetallic catalyst has been shown to be efficient in selective hydrogenation of acetylene in an ethylene rich stream [19–21]. Additionally, the surface defects on ceria nanoparticle is known to improve metal activity in hydrogenation reactions [22–24].

In order to achieve the broader goal of direct utilization of shale gas to make C_2H_4 and NH_3, the most valuable end products in chemical industry, through process intensification, a lab-scale proof of experiment is presented in this work (Fig. 1). MWP generated from methane is known to produce acetylene and hydrogen with high yield and can be optimized to be energy efficient. This article takes a step forward by identifying the post-plasma species in a MWP created by a gas mixture methane, nitrogen and Argon. The plasma reaction produced 0.1% hydrogen cyanide, 0.31% acetylene, 1.6% hydrogen. After placing the heated Ag-Pd/CeO_2 catalyst in the post plasma region, ethylene had the highest selectivity among the C_2 products and the amount of hydrogen cyanide was reduced by 40%, while the active nitrogen-based species simultaneously generated a steady amount of ammonia (~200 ppm). In absence of plasma, the catalyst over-hydrogenated the acetylene to ethane and no ammonia was produced. A thorough reaction chemistry was hypothesized to explain this plasma-catalyst synergy. The active metal sites on the catalyst, based on

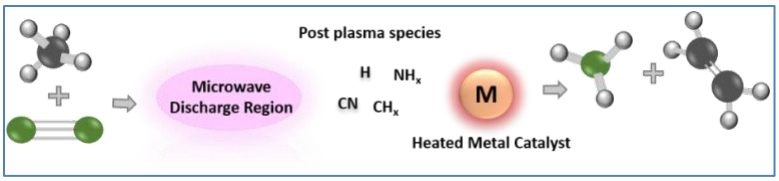

Figure 2: Figure 2: Reaction scheme of post-plasma species and catalyst synergy.

their preference to adsorb/desorb the post plasma species influence the reaction chemistry and product selectivity (Fig. 2).

REFERENCES

[1] P. Levi, T. Vass, H. Mandová, and A. Gouy, *Chemicals – Tracking Report*, IEA, 2020 https://www.iea.org/reports/chemicals.

[2] S. Sitter, Q. Chen, and I.E. Grossmann, An overview of process intensification methods, *Curr. Opin. Chem. Eng*., vol. 25, 87-94, 2019, doi.org/10.1016/J.COCHE.2018.12.006.

[3] T. Van Gerven and A. Stankiewicz, Structure, energy, synergy, time-the fundamentals of process intensification, *Ind. Eng. Chem. Res*., vol. 48, pp. 2465–2474, 2009, doi.org/10.1021/ie801501y.

[4] J.F. de la Fuente, A.A. Kiss, M.T. Radoiu, and G.D. Stefanidis, Microwave plasma emerging technologies for chemical processes, *J. Chem. Technol. Biotechnol*., vol. 92, pp. 2495–2505, 2017, doi.org/10.1002/jctb.5205.

[5] S. Tiwari, A. Caiola, X. Bai, A. Lalsare, and J. Hu, Microwave plasma-enhanced and microwave heated chemical reactions, *Plasma Chem. Plasma Process*., vol. 40, 1-23, 2020, doi.org/10.1007/s11090-019-10040-7.

[6] C.M. Ferreira and M. Moisan, *Microwave Discharges: Fundamentals and Applications*, Springer Science & Business Media, 2013.

[7] C. Shen, Y. Sun, D. Sun, and H. Yang, A study on methane coupling to acetylene under the microwave plasma, *Sci. China Chem*., vol. 53, pp. 231–237, 2010, doi.org/10.1007/s11426-010-0016-0.

[8] C. Shen, D. Sun, and H. Yang, Methane coupling in microwave plasma under atmospheric pressure, *J. Nat. Gas Chem*., vol. 20, pp. 449–456, 2011, doi.org/10.1016/S1003-9953(10)60209-5.

[9] M. Heintze and M. Magureanu, Methane conversion into acetylene in a microwave plasma: Optimization of the operating parameters, *J. Appl. Phys*., vol. 92, pp. 2276–2283, 2002, doi.org/10.1063/1.1497457.

[10] M. Wnukowski, A.W. van de Steeg, B. Hrycak, M. Jasiński, and G.J. van Rooij, Influence of hydrogen addition on methane coupling in a moderate pressure microwave plasma, *Fuel*, vol. 288, 2021, doi.org/10.1016/j.fuel.2020.119674.

[11] M. Scapinello, E. Delikonstantis, and G.D. Stefanidis, The panorama of plasma-assisted non-oxidative methane reforming, *Chem. Eng. Process. Process Intensif.,* vol. 117, pp. 120–140, 2017, doi.org/10.1016/J.CEP.2017.03.024.

[12] A. Bogaerts, X. Tu, J.C. Whitehead, G. Centi, L. Lefferts, O. Guaitella, F. Azzolina-Jury, H.H. Kim, A.B. Murphy, W.F. Schneider, T. Nozaki, J.C. Hicks, A. Rousseau, F. Thevenet, A. Khacef, and M. Carreon, The 2020 plasma catalysis roadmap, *J. Phys. D. Appl. Phys*., vol. 53, 2020, doi.org/10.1088/1361-6463/ab9048.

[13] J.L. Jauberteau and I. Jauberteau, Synthesis of cyanides in N2-CH4 discharge afterglow, *J. Phys. D. Appl. Phys*., vol. 51, 2018, doi.org/10.1088/1361-6463/aaccc2.

[14] A.M. Diamy, R. Hrach, V. Hrachová, and J.C. Legrand, Influence of C atom concentration for acetylene production in a CH_4/N_2 afterglow, *Vacuum*, vol. 61, pp. 403–407, 2001, doi.org/10.1016/S0042-207X(01)00151-8.

[15] J.L. Jauberteau, L. Thomas, J. Aubreton, I. Jauberteau, and A. Catherinot, High reactivity of CH_2 radical in an AR-CH4 post-discharge, *Plasma Chem. Plasma Process*., vol. 18, pp. 137–151, 1998, doi.org/10.1023/A:1021797428416.

Microwave Plasma Conversion of Natural Gas for Hydrogen and Carbon Production

Alvaro Martin Ortega[1], Gérard Gatt[1], Arnaud Boutibonnes[2], Ariel Mello[3], and Marilena Radoiu[3]

[1]Sakowin SAS, Fréjus, France
[2]Polytech de Marseille, Filière Mécanique et Energétique, Marseille, France
[3]Microwave Technologies Consulting SAS, Lyon, France

Keywords: cavity, energy, microwave, plasma application, processing, renewable energy

INTRODUCTION

The extensive use of fossil fuels as an energy source for power generation and transport results in the emission of large amounts of CO_2 into the atmosphere, up to ~32 billion metric tons per year [1], emissions that are responsible for the global warming. According to the *Hydrogen Roadmap Europe* [2], hydrogen gas (H_2) will play an important role for achieving the transition to a carbon-free energy, by replacing fossil fuels in industrial processes and in transportation.

The traditional H_2 production process is the steam reforming $CH_4+H_2O\rightarrow CO+3H_2$ (ΔH=206 kJ/mol), followed by the water-shift reaction $CO+H_2O\rightarrow CO_2+H_2$ (ΔH=-41.17 kJ/mol). Due to emission of large amounts of CO_2, this process is not a suitable CO_2-free energy source. The alternative methods for H_2 production are the water electrolysis and direct CH_4 decomposition, in which each compound is decomposed into its constituent elements: $H_20\rightarrow H_2+½O_2$ (ΔH=285.82 kJ/mol) and $CH_4\rightarrow C(s)+2H_2$ (ΔH=-74.85 kJ/mol). The theoretical energy cost of the CH_4 decomposition is much lower than that of water electrolysis, and the solid carbon produced, usually in the form of micron-sized particles (carbon black) can find usages in tire manufacturing, pigment in inks, reinforcer and stabilizer of other mixtures. Today carbon black is produced mainly by partial combustion of heavy hydrocarbons; therefore, an efficient method for CH_4 decomposition would remove two current sources of CO_2 while consuming less energy than H_2 production by water electrolysis.

The advantages of using plasma to promote the decomposition reactions lay in the fact that gas molecules are excited, ionized and decomposed while the gas temperature remains low; the collisions between the electrons and molecules create reactive ions and radical species that are not accessible by thermal heating. Among the various plasma sources investigated for CH_4 decomposition, *e.g.,* DC-spark discharge, gliding arc, DBD, microwave (MW) plasmas have advantages with regards to the absence of discharge electrodes and the

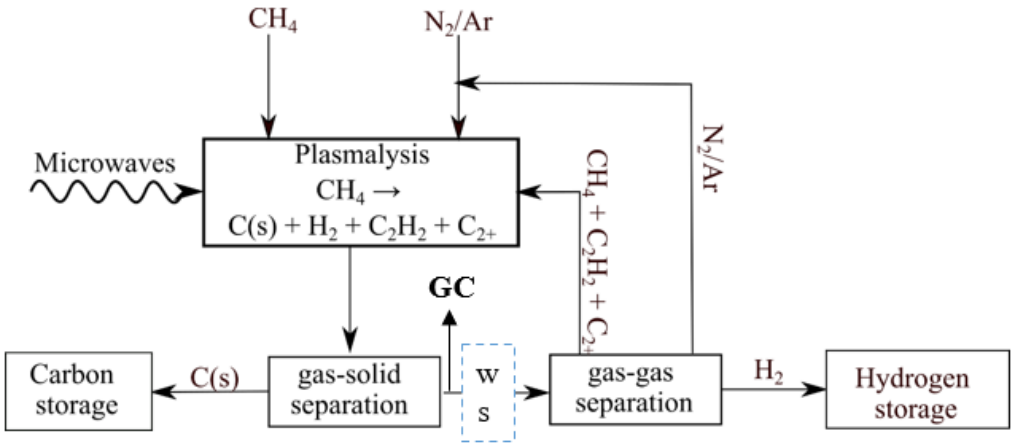

Figure 1. Schematic diagram of the South Beach process, including gas-solid and gas-gas separation stages and gas recycling; WS – water scrubber; GC- gas chromatograph

independent control of MW power and gas flow in the plasma reactor. Research on the use of MW sources include the "downstream sources", but also its use in combination with solar concentrators with a solid phase enhancing the reaction.

METHODOLOGY

The core of the South Beach plasma system is a resonant microwave cavity excited at 2.45 GHz, within which the plasma is created. The MW power is supplied by a 2.45 GHz, 2 kW CW water-cooled magnetron and a switch-mode HV power supply; the MW transmission line includes an isolator (water load + circulator), a 3-stub tuner and a sliding short-circuit. Plasma ignition at atmospheric pressure is achieved *via* a pneumatic system that briefly introduces a metallic needle in the center of the MW cavity. Downstream the plasma reactor a gas-solid separation system recovers the solid carbon product; at this stage of development the separation also includes a water scrubber (WS) which also cools down the gas stream exiting the reactor. In the industrial versions of the South Beach module, the gas-solid separation will be made using dry filters; further downstream, a gas-gas separation system separates the H_2 and recycles any non-decomposed CH_4 and by-products – see Fig. 1. The performance of the process is measured using a gas chromatograph (GC) Micro GC Fusion, which measures the inlet/outlet concentrations of N_2, CH_4, H_2, C_2H_2 and other gas molecules produced in the process.

RESULTS AND DISCUSSION

An example of results obtained for the conversion of CH_4 (introduced as natural gas, GRDF quality) are presented in Figure 2. The plasmagen N_2 is inert and therefore does not take part in the decomposition reaction; N_2 peak remains the same at the inlet and outlet of gas analysis. Part of the CH_4 (around 50% in this example) is decomposed in hydrogen, C_2H_2 and higher hydrocarbons, which can be measured by GC, and in solid carbon. The natural gas carries a small but noticeable amount of C_2H_6 which is also decomposed into the same products as the CH_4; the decomposition reaction is not sensitive to the presence of other hydrocarbons and in fact the performance obtained was similar when using pure CH_4.

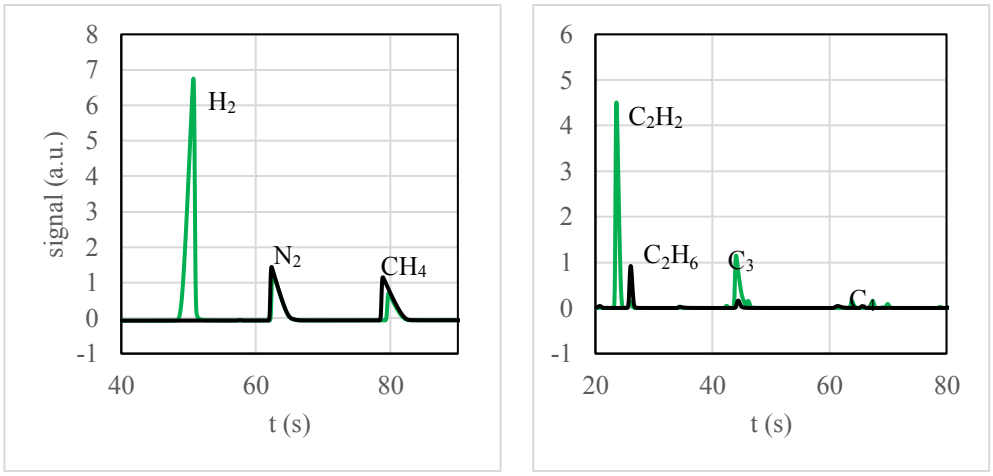

(a) (b)

Figure 2: Comparison of chromatogrammes of the inlet (black line) and outlet (green line) gas flow, taken from a Rt-Molsive column (left, H_2, N_2 and CH_4) and an Rt-Q-bond (right, C_2H_2 and other hydrocarbons); MW power 1.8 kW, 2.45 GHz

gas carries a small but noticeable amount of C_2H_6 which is also decomposed into the same products as the CH_4; the decomposition reaction is not sensitive to the presence of other hydrocarbons and in fact the performance obtained was similar when using pure CH_4.

CONCLUSION

The South Beach 2.45 GHz microwave plasmalysis system takes advantage of the lower energy requirement for CH_4 decomposition (in comparison to H_2O electrolysis) to provide a low-cost H_2 gas source. In addition to H_2, the co-product, solid carbon, will be collected and valorized. The use of a 2.45 GHz microwave plasma reactor to perform CH_4 plasmalysis allows the reaction to take place at lower temperatures than pyrolysis, without needing to use a catalyst. The current prototype allows for the optimization of CH_4 decomposition reaction with respect to the various operation parameters (gas flows, microwave power) as to achieve the highest efficiency for H_2 production.

Further development includes the precise characterization of the output gas and of the solid carbon, as well as the scale-up to 6 kW microwave power, which will allow to process larger volumes of gas.

REFERENCES

[1] T.A. Boden, G. Marland, and R.J. Andres, *2012 Global, Regional and National Fossil-Fuel CO2 Emissions,* Oak Ridge National Laboratory, cdiac.ess-dive.lbl.gov/trends/emis/overview.

[2] *Fuel Cell and Hydrogen: Hydrogen Roadmap Europe: A Sustainable Pathway for the European Energy Transition*, www.fch.europa.eu/publications/hydrogen-roadmap-europe-sustainable-pathway-european-energy-transition.

Selective Microwave Heating of Organic Reaction Mixtures

Gregory B. Dudley

West Virginia University, Morgantown, WV, USA

Keywords: chemical synthesis, selective microwave heating, microwave chemistry, kinetics, microwave effects

INTRODUCTION

Research in the Dudley Lab focuses on the development of emerging and enabling technologies for chemical synthesis, including microwave-assisted organic synthesis. This paper focuses on the strategic use of microwave electromagnetic radiation to accelerate thermochemical processes [1]. Modern physical organic reaction theory is based on the physics of convective heating and generally assumes uniform constant temperatures.

Microwave energy produces heat by a dielectric heating mechanism [2], which can enable selective heating and create opportunities for chemical synthesis. These mechanisms need to be understood and incorporated into reaction design in order to gain maximum benefit from this emerging and enabling technology. Collaborative efforts from within and beyond the Dudley lab to develop and apply selective heating in homogeneous solution have led to identification and characterization of reaction systems in which microwave-specific rate enhancements have been documented both qualitatively and quantitatively. These results, a physical model, and recent strategic applications in synthesis will be discussed.

METHODOLOGY

Commercial microwave reactors designed for organic synthesis were used. Most microwave experiments were performed in CEM Discover reactors using quartz glassware, in high boiling solvents, and at ambient pressure. Reaction temperatures were measured using internal fiber-optic probes, external IR sensors, and/or thermal imaging cameras.

Reaction systems typically feature polar, microwave-absorbing solutes in non-polar, non-absorbing solvents reacting in nearly transparent quartz vessels (Fig. 1). The ideal system is one in which heat introduced into the system during the course of the reaction arises uniquely by interaction of the polar solute with microwave energy, consistent with the molecular radiator [3] model of microwave-specific selective heating. Comparison and control experiments under conventional heating generally feature otherwise-identical reaction mixtures in pre-heated oil baths or heating blocks.

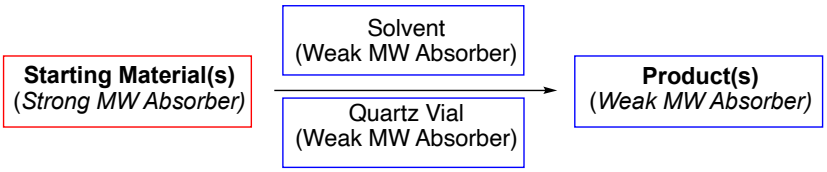

Figure 1. Methodology design of reaction systems for selective microwave heating.

RESULTS

In this section, three reaction systems are presented and discussed. The first is a thermal ***Friedel-Crafts benzylation*** of non-polar aromatic solvents using strongly absorbing and poorly soluble ionic benzyl-transfer reagents (Fig. 2) [4]. Data from monophasic and biphasic reaction mixtures include data from new technology allowing for simultaneous microwave and convective heating. The roles of temperature, microwave heating, and solubility in reaction outcomes including rate and efficiency are also discussed.

The second reaction system is a thermal ***aryl Claisen rearrangement*** of a polar covalent substrate in a non-polar aromatic solvent [5]. Comparisons of kinetic data at various temperatures and heating protocols suggest that dynamic microwave heating profiles can be advantageous. For example, applying microwave power periodically with intermittent cooling provided significant rate enhancements over other heating protocols (Fig. 3).

Third is an ***oxidative cycloisomerization*** reaction [6] from a recent synthesis of the natural product illudinine (Fig. 4) [7]. This reaction was optimized empirically and later found to be more efficient using microwave heating as compared to conventional heating. The reaction requires high temperatures at which the product is thermally unstable. Increases in reaction yield here are consistent with the intriguing possibility of selective microwave heating of the reactant in a solution in which the product is kept relatively cool. In many cases, deviations from classic Arrhenius kinetics are documented and discussed in the context of selective microwave heating.

DISCUSSION

The observations consistent with selective microwave heating can be rationalized by considering a physical model in which polar solutes aggregate in non-polar solvents to create nano-phases within a macroscopically homogeneous mixture. Polar nanophases are expected to heat more efficiently than the bulk solvent, raising the local temperature within the nanophase rapidly and selectively compared to the bulk solution. Heat subsequently flows, perhaps by convective heat transfer mechanisms, from the polar nanophase to the bulk solution and then out of the system, establishing a persistent thermal gradient and distinct temperature domains between the nanophases and bulk solution. Polar solutes in the nanophase react in accord with the temperature of their immediate surroundings, which inside the nanophase is higher than what is measured as the bulk solution temperature.

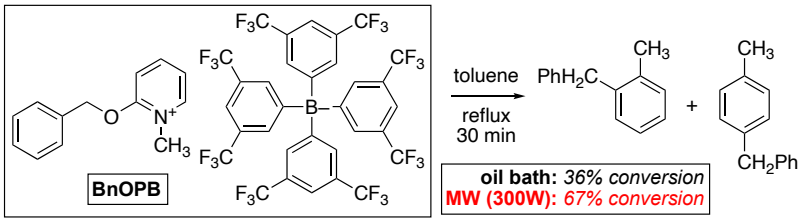

Figure 2. Friedel–Crafts benzylation.

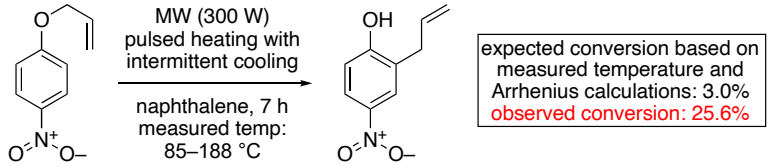

Figure 3. Aryl Claisen rearrangement.

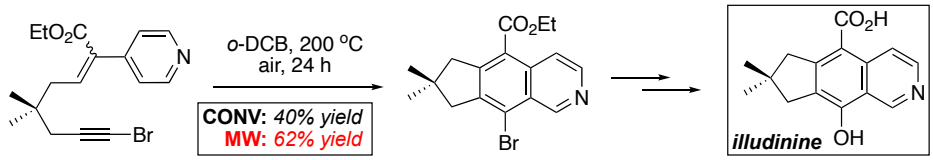

Figure 4. Oxidative cycloisomerization *en route* to synthetic illudinine.

CONCLUSION

Selective microwave heating creates potential opportunities for strategic advances in chemical synthesis, provided that sufficient magnitude, reproducibility, and generality of selective heating effects can be realized.

REFERENCES

[1] G.B. Dudley and A.E. Stiegman, "Changing perspectives on the strategic use of microwave heating in organic synthesis," *Chem. Rec.*, vol. 3, pp. 381-389, 2018.

[2] G.B. Dudley, R. Richert, and A.E. Stiegman, "On the existence of and mechanism for microwave-specific reaction rate enhancement," *Chem. Sci.*, vol. 6, pp. 2144-2152, 2015.

[3] A.M. Rodríguez, P. Prieto, A. de La Hoz, A. Díaz-Ortiz, and J.I. García, "The issue of 'molecular radiators' in microwave-assisted reactions. Computational calculations on ring closing metathesis (RCM)," *Org. Biomol. Chem.*, vol. 12, pp. 2436-2445, 2014.

[4] M.R. Rosana, J. Hunt, A. Ferrari, T. Southworth, Y. Tao, A.E. Stiegman, and G.B. Dudley, "Microwave-specific acceleration of a friedel–crafts reaction: evidence for selective heating in homogeneous solution," *J. Org. Chem.*, vol. 79, pp. 7437-7450, 2014.

[5] P.-K. Chen, M.R. Rosana, G.B. Dudley, and A.E. Stiegman, "Parameters affecting the microwave-specific acceleration of a chemical reaction," *J. Org. Chem.*, vol. 79, pp. 7425-7436, 2014.

[6] C. Duangkamol, P. Batsomboon, A.E. Stiegman, and G.B. Dudley, "Microwave heating outperforms conventional heating for a thermal reaction that produces a thermally labile product: Observations consistent with selective microwave heating," *Chem.–Asian J.*, vol. 14, pp. 2594–2597, 2019.

[7] A.E. Morrison, T.T. Hoang, M. Birepinte, and G.B. Dudley, "Synthesis of illudinine from dimedone," *Org. Lett.*, vol. 19, pp. 858–861, 2017.

Effect of Microwave-Assisted Gasification on the Chemical and Physical Properties of Coal Chars

Candice Ellison[1,2], Victor Abdelsayed[1,2], Mark Smith[1], and Dushyant Shekhawat[1]

[1]National Energy Technology Laboratory, Morgantown, WV, USA
[2]NETL Research Support Contractor, Morgantown, WV, USA

Keywords: char characterization, microwave gasification

INTRODUCTION

Microwave technology may play a crucial role in electrifying the chemical industry, enabling the use of renewable energy to drive thermal processes. While coal gasification is an industrially established process for production of syngas, the application of microwaves to the gasification process is a relatively nascent field of study. Microwave selective heating may offer unique advantages to the gasification process by enabling gasification at lower bulk reaction temperatures, accelerating reaction rates, increasing syngas yield, and increasing overall process efficiency compared to traditional gasifiers [1].

As the feedstock chemical and physical properties dictate the gasification reactivity of a particular feedstock, analysis of the feedstock and char properties may lead to a better understanding of microwave effects on the gasification process [2]. By comparison of residual char properties after microwave and conventional gasification, the influence of microwave heating on char structure development during gasification will be elucidated. In this study, the structure and composition of feedstock coal samples and the residual char after microwave and conventional gasification were analyzed.

METHODOLOGY

Coal samples were gasified under microwave and conventional heating to study the effect of microwave gasification on char chemical and physical properties. Microwave coal gasification was carried out at 700 °C in a single mode microwave waveguide cavity (2.45 GHz, 2 kW) under a mixed flow of 100 cm^3/min CO_2 and 50 cm^3/min Ar (Fig. 1(a)). For comparison, traditional thermal gasification was carried out by gasifying samples under the same flow and temperature conditions in a resistive furnace (Fig. 1(b)). The produced char samples were analyzed by BET surface area analysis, scanning electron microscopy (SEM), Fourier transform infrared (FTIR) spectroscopy, elemental analysis, and dielectric characterization.

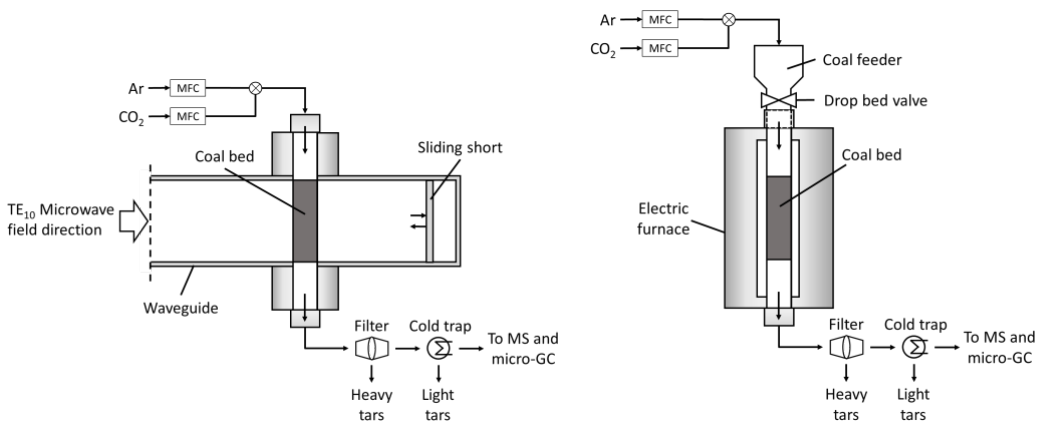

Figure 1: Schematic diagram of the experimental microwave gasifier (a) and the conventional gasifier (b).

RESULTS

Coal undergoes a number of chemical and physical changes as it is converted to char during gasification. The mode of heating (microwave or conventional) was found to have a significant effect on the residual char properties. The microwave gasified chars were found to have lower surface area, in general, compared to the conventionally gasified chars, which may suggest the collapse of the porous structure and ash melting. Evidence of ash melting was also observed in the SEM images of the microwave gasified chars by the presence of micron-scale spherical ash particles, which were not present in the conventionally gasified chars. The FTIR spectra indicate loss of surface functional groups compared to the parent coal. As indicated by the FTIR spectra and elemental analysis, chars from microwave gasification resulted in a greater degree of carbon conversion compared to those generated by thermal gasification.

DISCUSSION

The observed compositional and structural differences between microwave and conventionally gasified chars are evidence of microwave selective heating. Under microwave gasification, the char characteristics, (i.e., collapsed porous structure, ash melting, and greater carbon conversion) indicate that greater temperatures were reached under microwave gasification compared to conventional gasification despite both microwave and conventional gasification processes being controlled to the same reaction temperature (700°C). This may suggest the presence of hot spots within the fixed bed with localized areas of higher temperature relative to the bulk measured temperature, which may arise as a result of microwave selective heating of some phases within the heterogeneous coal sample [1].

CONCLUSION

Investigations of the chemical and physical properties of microwave and conventionally gasified chars offer insights into microwave-specific effects on the gasification process. The microwave-assisted gasification offers unique processing advantages, which were mainly attributed to microwave selective heating and formation of hotspots. These phenomena enabled gasification at lower bulk temperatures than required by conventional gasifiers, which may lead to improved process efficiency. These results, along with prior reaction studies, may be used to design and optimize a microwave-based gasification process for coal or other carbon-based fuels, such as biomass or plastics.

REFERENCES

[1] V. Abdelsayed, C. Ellison, A. Trubetskaya, M.W. Smith, and D. Shekhawat, "Effect of microwave and thermal co-pyrolysis of low rank coal and pine wood on product distributions and char structure, *Energy and Fuels*, vol. 33, no.8, pp. 7069-7082, 2019.

[2] L. Liu, Y. Cao, and Q. Liu, Kinetics studies and structure characteristics of coal char under pressurized CO_2 gasification conditions, *Fuel*, vol. 146, pp. 103-110, 2015.

Microwave-Assisted Ammonia Synthesis Over Cs-Ru/CeO_2 Catalyst at Ambient Pressure: Effects of Metal Loading and Support Particle Size

Alazar Araia[1], Yuxin Wang[1], Brandon Robinson[1], Changle Jiang[1], Sean Brown[1], Christina Wildfire[2], Dushyant Shekhawat[2], and Jianli Hu[1]

[1] Department of Chemical and Biomedical Engineering, University of West Virginia, Morgantown, WV, USA
[2] U.S. Department of Energy, National Energy Technology Laboratory, Morgantown, WV, USA

Keywords: ammonia synthesis, Cs-Ru/CeO_2 catalyst, microwave irradiation, Ru particle size and dispersion

INTRODUCTION

Ammonia is a highly produced and consumed chemical in the world. It is widely used as a raw material for nitrogen containing chemicals, fertilizers, and intermediates for pharmaceutical [1]. Ammonia is emerging as an energy source of choice for fueling the shipping industry to transition away from conventional fuels and reduce GHG emission [2]. Industrially, ammonia is produced by Haber-Bosch process under high temperature (400–500 °C) and high pressure (150–300 bar) over Iron-based catalyst. This process requires high energy and is capital intensive as it operates at high temperature and pressure. Microwave is a promising technology to produce ammonia at low temperature and pressure with the use of an electromagnetic sensitive catalyst [3]. Microwave offers instantaneous and volumetric heating via interaction with electromagnetic radiation, which is fundamentally different from conventional thermal heat conductive or convective transfer through direct heating [4]. Microwave's irradiation selectively heats active sites on the surface of heterogeneous catalyst, facilitating the transfer of electrons between catalyst and reaction intermediates [3]. A catalyst with high activity under microwave condition is much desired to further improve the energy efficiency and ammonia production. Ru-based catalyst exhibited higher activity than Fe-based catalyst under similar reaction condition. Cs promoted Ru catalyst supported on cerium oxide with different metal loading (4-24 wt.% Ru) and support particle size (25nm, 50nm and 5μm) was investigated at ambient pressure and temperature from 260-360^{o}C under microwave reactor for ammonia synthesis.

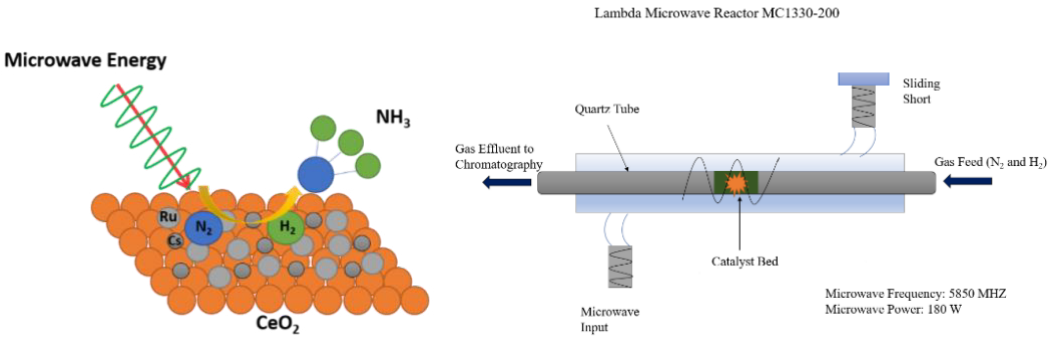

(a) (b)

Figure 1. Reaction mechanism for ammonia synthesis over Cs-Ru/CeO_2 catalyst (a) in a microwave reactor (b).

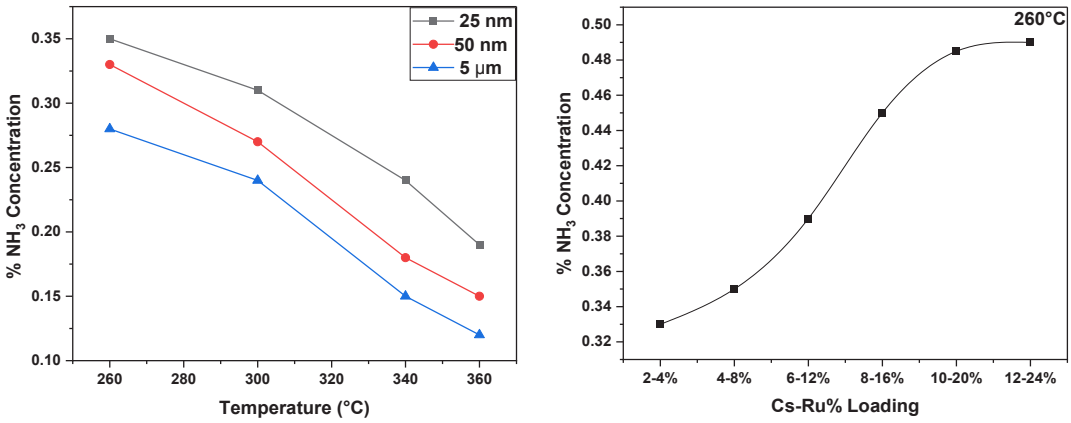

(a) (b)

Figure 2. Ammonia concentration (%): different sized cerium oxide support (a) and different metal loading (b).

METHODOLOGY

Cs-Ru/CeO_2 catalyst is prepared by incipient wetness impregnation method. The catalytic activity for ammonia synthesis was tested in a variable frequency microwave reactor system (Lambda MC1330-200) at a frequency of 5850 MHz. The microwave reactor has two IR sensors, one is used to measure reactor tube temperature, the other is used to measure catalyst surface temperature. The system was tuned so that the reflective power was minimized to basically zero. The catalytic performance test was conducted in a continuous-flow quartz tube reactor with 8 mm internal diameter. CO chemisorption, H_2-TPR and Raman Spectroscopy were utilized to determine Ru particle size, dispersion, and cerium oxide oxygen vacancy.

RESULTS

Cs-Ru/CeO_2 catalyst with (25 nm) CeO_2 support showed the highest ammonia concentration at all reaction temperatures. CeO_2 support with 50 nm particle size exhibited lower activty as compared to the 25 nm support and 5 µm cerium oxide support showed the lowest activity at 260 °C reaction temperature. The highest activity for the small sized cerium oxide support (25 nm CeO_2) is mostly related to higher oxygen vacancy forming low crystalline Ru species, and Ru is highly dispersed, as compared to the 50 nm and 5 µm cerium oxide support. As shown in Fig. 1(b), a significant increase in ammonia concentration can be noticed on going from 4 wt.% Ru loading to 20 wt.% Ru loading at 260 °C, while for higher than 20 wt.% Ru loading activity seems to attain a plateau.

DISCUSSION

Based on different characterization techniques and ammonia synthesis experimental data, cerium oxide particle size significantly affects the dispersion and size of Ru, affecting the ammonia production. The small sized cerium oxide support exhibited the highest ammonia production at 260 °C due to high Ru dispersion and small size of Ru species as compared to 50 nm and 5 µm cerium oxide support. Beside the effect of cerium oxide support particle size, Ru loading also significantly affects the size of Ru and its dispersion over cerium oxide support. As Ru loading increased, due to the presence of large content of Ru metal species the number of active sites is increased resulting an increase in ammonia production. At higher metal loading the size of Ru species increased while dispersion was reduced resulting a low Ru catalyst utilization.

CONCLUSION

The small sized cerium oxide support has the highest activity towards ammonia synthesis, due to low crystalline Ru species and high dispersion. Higher metal loading increased the ammonia concentration, but the utilization of Ru is decreased. The increase in ammonia concentration with increase in Ru loading is largely associated to high Ru metal content present in the catalyst.

REFERENCES

[1] M.Y. Aslan, *Supported Ru Based Ammonia Synthesis Catalyst*, M.S. Thesis, Middle East Technical University, 2012.

[2] Y. Guo, S. Mei, K. Yuan, D.J. Wang, H.C. Liu, C.H. Yan, and Y.W. Zhang, "Low-temperature CO_2 methanation over CeO_2-supported Ru single atoms, nanoclusters, and nanoparticles competitively tuned by strong metal-support interactions and H-spillover effect," *ACS Catal.*, vol 8, no 7, pp. 6203–6215, 2018.

[3] Y. Wang, C. Wildfire, T.S. Khan, D. Shekhawat, J. Hu, P. Tavadze, R. Quiñones-Fernández, and S. Moreno, "Effects of support and promoter on Ru catalyst activity in microwave-assisted ammonia synthesis," *Chem. Eng. J.*, vol. 425, no 3, pp. 1–11, 2021.

[4] J. Hunt, A. Ferrari, A. Lita, M. Crosswhite, B. Ashley, and A,E, Stiegman, "Microwave-specific enhancement of the Carbon-Carbon dioxide (Boudouard) reaction," *J. Phys. Chem. C,* vol. 117, no 51, pp. 26871–26880, 2013.

Chemical Looping Ammonia Synthesis: Microwave and Thermal Fixed Bed Systems

Sean W. Brown[1], Candice Ellison[2], Dushyant Shekhawat[2], and Jianli Hu[1]

[1]Department of Chemical and Biomedical Engineering, West Virginia University, Morgantown, WV, USA
[2]US DOE National Energy Technology Laboratory, Morgantown, WV, USA

Keywords: ammonia, chemical looping, Haber-Bosch, nitride, microwave catalysis

INTRODUCTION

Modern industrial ammonia synthesis proceeds by the Haber-Bosch process, this high temperature, 300-500 °C, and high pressure, 20-100 MPa, reaction relies on multi-promoted iron or ruthenium on carbon catalyst systems to overcome equilibrium limitations [1]. The ammonia synthesis process as currently practiced consumes 1-2 % of global energy per year, which corresponds to 2.5 % of the global CO_2 emissions [1, 2]. Chemical looping ammonia synthesis is a reaction scheme to decouple the ammonia synthesis reaction as traditionally understood in Haber-Bosch, theoretically allowing these equilibrium limitations to be overcome [3, 4]. Similarly, microwave heating and microwave catalysis allow for volumetric heating and for enhanced catalytic activity by the formation of localized high temperature "hot spots," among other effects [5, 6].

METHODS AND MATERIALS

To compare the efficacy of traditional thermal fixed bed and microwave heating, each candidate material was evaluated for three chemical looping ammonia synthesis (CLAS) cycles. One chemical looping cycle is defined as Equation 1, the nitridation step, followed by Equation 2, the hydrogenation step.

Equation 1: $Fe_x + N_2 \rightarrow Fe_xN_y$ (450 °C)

Equation 2: $Fe_xN_y + H_2 \rightarrow Fe_xN_{y-z} + {}_zNH_3$ (450 °C)

A continuous flow conventional tubular thermal fixed bed and a continuous flow microwave fixed reactor were used to evaluate chemical looping ammonia synthesis materials at atmospheric pressure. Quartz tubes (406.4 mm L, 10 mm I.D., 12 mm O.D.) were used to contain the materials between quartz wool supports in the center of the tube. Iron powder (Fe, <10 μm, >99.9%, Aldrich) was used as an ammonia synthesis material and Silicon Carbide (SiC, 325 mesh, 98%, Aldrich) was used as a microwave sorbent to enhance heating. The materials were physically mixed before loading into the reactor. Inlet

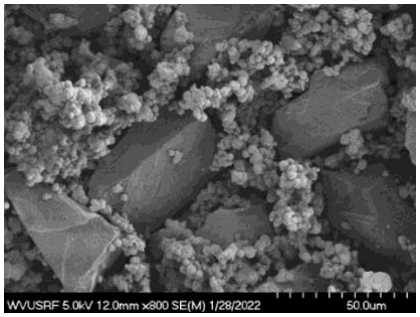

Figure 1. SEM imagery of spent 1:1 Fe:SiC spent microwave sample.

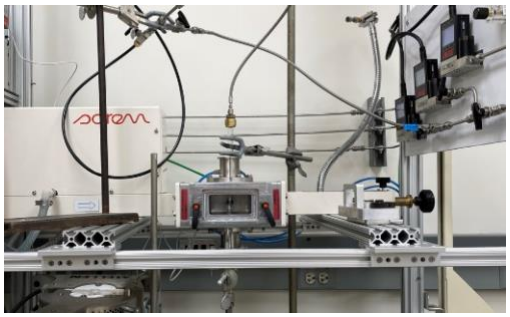

Figure 2. Microwave reactor with waveguide, quartz tube, gas supply

reactant gases were of ultra-high purity grade (99.999%, Matheson and Air Gas, Inc.): H_2, N_2, and Ar.

Microwave testing was performed in a fixed frequency, 2.45 GHz, 3 kW, magnetron power, single mode cavity microwave from Sairem (model GMP20K). The temperature was measured using a laser aligned infrared pyrometer from Micro-Epsilon (model CTLM3) with a pre-calibrated temperature range of 200 to 1500 ℃. The pyrometer measures the surface temperature of the reaction tube and contents. A manual sliding short was tuned to minimize microwave leakage and to focus the beam onto the sample. The basic reactor setup is shown in Fig. 2.

Outlet gas concentrations from both the thermal fixed bed and the microwave fixed bed reactors were measured by CAI 600 Fourier Transform Infrared Spectroscopy (FTIR) with a gas flow cell. Temperature of microwave catalyst beds were analyzed in-situ using a FLIR camera.

RESULTS AND DISCUSSION

Iron was selected as a CLAS material for comparison between microwave and thermal heating modes due to its efficacy as an ammonia synthesis catalyst and its heating properties in the microwave.

Time on stream experimental results presented in Fig. 3, show an advantage to microwave heating on CLAS Cycle 1 ammonia synthesis reaction, on CLAS Cycle 2 the microwave shows distinct advantage, while on the final CLAS Cycle 3, there is an indeterminate advantage between heating modes with spent sample deactivation.

Microwave heating in bulk metals typically proceeds by both dielectric and magnetic heating modes, with magnetic heating typically thought to dominate [7]. The “skin-effect” in metals typically prevents bulk particle heating, but in this case the particle size is on the same order as the penetration depth of the microwave energy, for Fe, 1.3 μm [7]. This allows tradition volumetric heating to dominate, when paired with the insulating microwave sorbet SiC, heating is further enhanced by conduction to Fe particles.

External temperature validation was performed with a FLIR camera, the average temperature under N_2 was found to be 492 ℃ and the average temperature under H_2 was

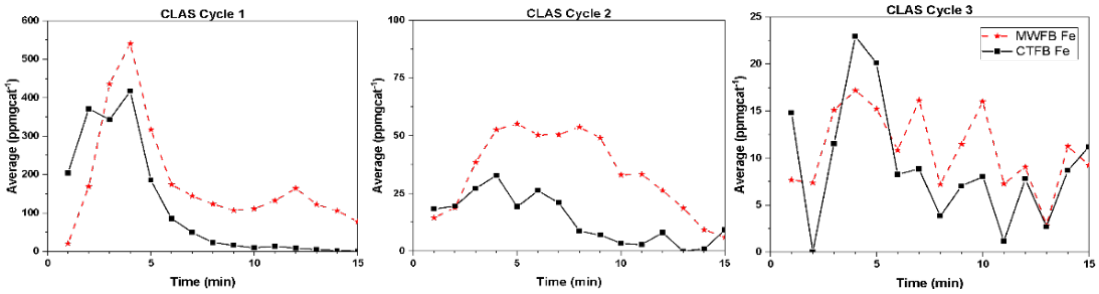

Figure 3. Three cycle ammonia synthesis results for the microwave (red) and conventional thermal fixed bed (black) time on stream ammonia synthesis results.

found to be 490 °C during ammonia synthesis. Ammonia synthesis is an exothermic process, so it is logical that the overall temperature is lower and requires less input energy. Overall, the average temperatures reported by thermal imaging are on the order of ~ 40 °C higher than the set point. However, a large variability exists between Q1 and Q3; 506 °C and 467 °C for nitridation, and 503 °C and 465 °C for hydrogenation. This means that while Fe temperature exceeds the setpoint, it is possible to heat and maintain reaction in the system with reasonable temperature control, where 40 °C is ~10% of the temperature set point.

Future work will explore other CLAS materials under microwave and thermal heating.

REFERENCES

[1] M. Appl, Ammonia, In: *Ullmann's Encyclopedia of Industrial Chemistry*; Wiley-VCH Verlag, 2006.

[2] P.H. Pfromm, "Towards sustainable agriculture: fossil-free ammonia," *J. Renew. Sustain. Energy*, vol. 9, no 3, 034702, 2017, doi.org/10.1063/1.4985090.

[3] H. Yan, W. Gao, Q. Wang, Y. Guan, S. Feng, H. Wu, Q. Guo, H. Cao, J. Guo, and P. Chen, "Lithium palladium hydride promotes chemical looping ammonia synthesis mediated by lithium imide and hydride," *J. Phys. Chem. C*, vol. 125, no 12, pp. 6716–6722, 2021, doi.org/ 10.1021/acs.jpcc.1c01230.

[4] R. Michalsky and P.H. Pfromm, "An ionicity rationale to design solid phase metal nitride reactants for solar ammonia production," *J. Phys. Chem. C*, vol. 116, no 44, pp. 23243–23251, 2012, doi.org/10.1021/jp307382.

[5] C. Wildfire, V. Abdelsayed, D. Shekhawat, and M.J. Spencer, "Ambient pressure synthesis of ammonia using a microwave reactor," *Catalysis Communications*, vol. 115, pp. 64–67, 2018, doi.org/10.1016/j.catcom.2018.07.010.

[6] R.R. Mishra and A.K. Sharma, "Microwave–material interaction phenomena: heating mechanisms, challenges and opportunities in material processing," *Composites Part A: Applied Science and Manufacturing*, vol. 81, pp. 78–97, 2016, doi.org/10.1016/j.compositesa.2015.10.035.

[7] J. Sun, W. Wang, and Q. Yue, "Review on microwave-matter interaction: fundamentals and efficient microwave-associated heating strategies, *Materials*, vol. 9, no 4, p. 231, 2016, doi.org/10.3390/ma9040231.

A Miniature Electron Cyclotron Resonance Ion Source for Neutron Generators

David L. Williams, Allan X. Chen, Craig Brown, Adam Amoroso, Veronica Smith, Mashal Elsalim, and Charles K. Gary

Adelphi Technology, Inc., Redwood City, CA, USA

Keywords: electron cyclotron resonance, Deuterium-Deuterium, Deuterium-Tritium, neutron generator

INTRODUCTION

High yield neutron generators can be used for applications such as neutron imaging [1], materials analysis, isotope generation [2] and Boron Neutron Capture Therapy [3, 4]. Deuterium ions from an RF driven ion source are accelerated through a high voltage, such as 250 kV, onto a target. Collisions between ions from the ion beam and ions that have previously been implanted in the target result in fusion reactions that produce neutron emission. A neutron yield of around 5×10^{10} neutrons/s can be achieved in this way via the Deuterium-Deuterium (D-D) reaction (which leads to the production of 2.45 MeV neutrons). In comparison, this is approximately 500× higher yield than is provided by Penning ion source-based tubes that are commonly used for well logging applications despite that they almost exclusively use a mixture of deuterium and tritium gas. The Deuterium-Tritium (D-T) reaction has approximately a 100× greater fusion cross section than D-D, and the D-T reaction also produces more penetrating 14.1 MeV neutrons. The choice of D-D vs. D-T is typically dictated by the application.

The neutron generators described in this work employ an Electron Cyclotron Resonance (ECR) ion source consisting of a gas volume with an axial magnetic field. For the ECR condition to be met, the ion source is operated on resonance: $2\pi f = eB/m$, where f is the frequency B is the applied magnetic field and e/m is the charge-to-mass ratio of the electron. The RF energy causes electrons to exhibit circular motion within the ion source, which ionizes the gas.

In current high-yield D-D neutron sources, solid-state RF sources have replaced magnetrons because they provided more stable, higher beam current operation. Magnetron RF sources tended to suffer from frequency instabilities (mode hopping) and the highest beam current occurs only when operated at resonance. Laboratory-based high-yield D-D neutron sources employ a 200 W 2.45 GHz RF source. The microwave power is launched into a WR340 waveguide and is subsequently transmitted through a window into the ion

(a) (b) (c) (d)

Figure 1. Ion source (a) without magnets installed (b), with magnet holder (c) ion source exit aperture mounted in a DN35CF (2¾") Conflat flange, (d) operating ion source

chamber (coupled via stubs) [5]. In these older designs the solid-state RF source simply replaced the magnetron.

We present a small, direct antenna-coupled ion source. The ion source fits within a modified 2.75" Conflat flange footprint, and the ion source inside diameter (I.D.) is less than 1 cm. The antenna is located directly within the ion source volume, in contact with the plasma. Materials lining the plasma chamber walls are chosen for their material properties: Good electron emitters to promote plasma formation, and poor at catalyzing the recombination from atomic to molecular ion species. Additionally, the gas diameter is restricted to be only a little larger than the ion source exit aperture diameter, reducing energy wasted producing ions that do not subsequently contribute to the ion beam current.

The ion source dimensions were chosen so that it would operate at 10 GHz. The source was also found to operate at lower frequencies, including 2.45 GHz despite these small dimensions. In this design, the RF power enters through an SMA feedthrough. For R&D purposes a small coax terminated stub tuner was used for RF matching to the ion source. This had stubs that protruded radially. Inline, rotatable stub tuners offer some size improvement [6]. However, a production version is expected to employ discrete components forming, for example, a π or T network.

Portable applications require miniature ion sources that are also efficient (since the neutron generator will be battery operated). The ion sources also need to produce ions with a high fraction of atomic species in order to achieve high neutron yields.

METHODOLOGY

The magnetic field within the ion source was chosen to meet the ECR condition for each frequency used. The ion source was placed in a vacuum system and the deuterium pressure set to a few millitorr. The resulting plasma was then viewed through a vacuum window. The miniature ion source is shown in Fig. 1. High frequency (up to 10 GHz) sources were designed and constructed using components from both Cree and Quorvo, as shown in Fig. 2. The block diagram of the Quorvo RF source is shown n Fig. 3.

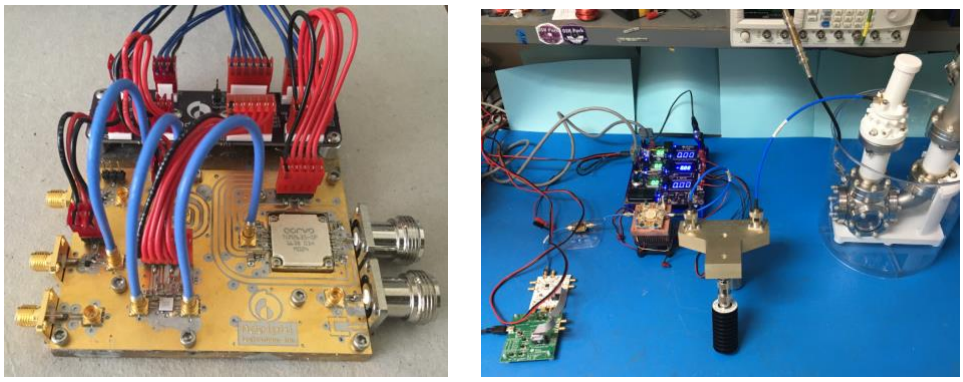

(a) (b)

Figure 2. Power amplifier circuitry: Quovo (a) and Cree (b).

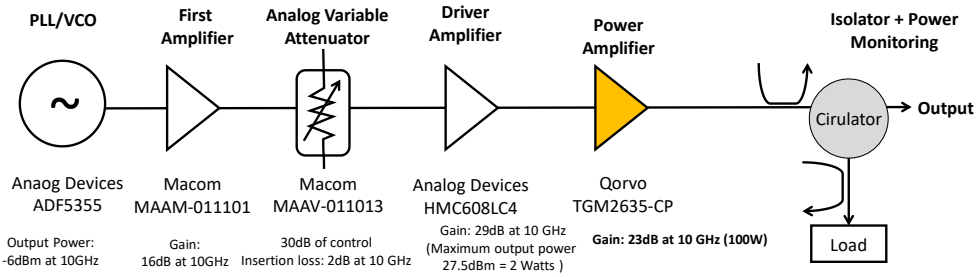

Figure 3. Block diagram of the amplifier chain using a Quorvo 100 W, 10 GHz power amplifier.

RESULTS AND CONCLUSIONS

Ion sources were successfully operated at several frequencies. RF sources capable of approximately 100 Watts were built and operation of the ion sources down to approximately 10 Watts of RF power was demonstrated. These ion sources were designed for use on portable neutron generators employing D-D and D-T reactions to produce 2.45 MeV and 14.1 MeV neutrons respectively.

REFERENCES

[1] D.L. Williams, C.M. Brown, D. Tong, A. Sulyman, and C.K. Gary, "A fast neutron radiography system using a high yield portable DT neutron source," *J. of Imaging*, vol. 6, no 12, p. 128, 2020, www.mdpi.com/2313-433X/6/12/128/pdf

[2] E.J. Mausolf, E.V. Johnstone, N. Mayordomo, D.L. Williams, E.Y.Z. Guan, and C.K. Gary, "Fusion-based neutron generator production of Tc-99m and Tc-101," *Pharmaceuticals*, vol. 14, no 9, p. 875, 2021, doi.org/10.3390/ph14090875.

[3] US Patent 11,090,509 "Neutron source with beam shaping apparatus for cancer treatment".

[4] US Patent 10,955,365 "Neutron source with beam shaping apparatus for radiography".

[5] D.L. Williams, et al., "Neutron generators employing solid state microwave sources," *Proc. IMPI's Intern. Microwave Power Symp., Long Beach, California, June 2018*.

[6] US Patent 2,966,642 "Double stub tuner".

Effective Microwave Heating of Catalysts: Comparison of Electric and Magnetic Fields

Daniel R. Slocombe[1], Alex J. L. Morgan[1], Xiangyu Jie[2], and Peter P. Edwards[2]

[1]School of Engineering, Cardiff University, Queen's Building, The Parade, Cardiff, UK
[2]Inorganic Chemistry Laboratory, University of Oxford, South Parks Road, Oxford, UK

Keywords: catalysts, electric field heating, microwave, magnetic field heating

INTRODUCTION

Important heterogeneous catalytic reactions can be driven efficiently using microwaves, often leading to very different results from conventional heating due to the fundamentally different, and highly selective heating mechanisms. The effective complex permittivity and permeability of catalyst particles can vary greatly depending upon preparation conditions and throughout the reaction as it proceeds. Research in this area has often focused on heating using the electric field in single mode, or multi-mode cavities, whilst there has been far less focus upon using microwave magnetic fields in catalysis [1-3]. Using magnetic field heating can present advantages over electric field heating in some cases as the selectivity of microwave absorption becomes dramatically different because of the complex interaction mechanisms and also depending upon their structure and size [4]. In a reaction mixture, it is common to find fewer materials with a high imaginary permeability μ_2, and so will not be wasted heating materials that we do not want to heat, but instead, energy can be delivered exclusively to the site of the catalytic reaction (i.e., the surface of our heterogeneous catalyst). In this work, we examine the heating behaviors of selected catalyst materials in microwave magnetic fields and compare them to heating in the microwave electric field. The added selectivity brings another tool with which catalyst materials can be designed to make use of the advantageous effects of microwave heating in heterogeneous catalysis.

EXPERIMENTAL APPARATUS AND PROCEDURE

Samples were placed in a 6mm inner diameter quartz tube and then placed on a vibrating stage to ensure consistent packing between catalyst powder particles. The sample is placed into a TM_{010} cylindrical cavity resonator operating at 2.45 GHz. For *E*-field heating, the sample is placed through a sample insertion hole along the axis at the antinode of the electric field (and the node of the magnetic field). For *H*-field heating, the sample is placed in a sample insertion hole at the edge of the cylindrical cavity where the magnetic field is at its maximum (and the electric field is minimum) and is azimuthally polarized (see Fig. 1). Nominally 30 W of power was applied at 2.5 GHz using a bespoke solid-state

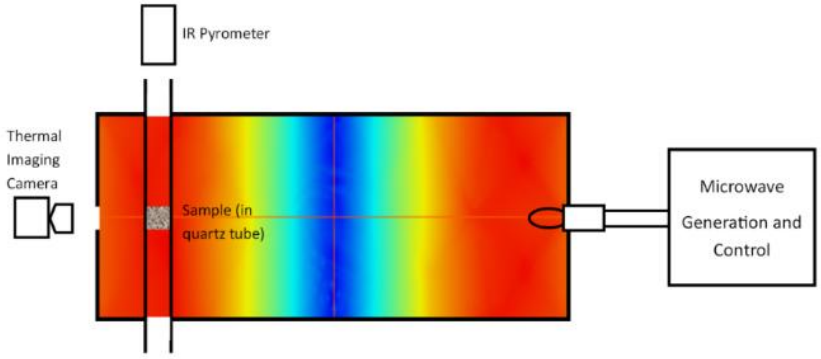

Figure 1. Experimental setup – A 2.495 GHz, 30 W signal is generated and delivered to a TM_{010} cavity resonator; sample held within a quartz tube; colour gradient represents the magnetic field (red = high magnetic field); temperature measurements taken using thermal imaging camera and IR pyrometer.

microwave power applicator. The resonance is monitored and tracked rapidly using S_{11} measurements in order to maintain critical coupling. Measurements of temperature were taken using a Micro-Epsilon CT-SF22-C1 IR pyrometer in parallel with a Micro Epsilon TIM640 thermal imaging camera. Catalyst materials were produced at the Inorganic Chemistry Laboratory, University of Oxford, UK. The sample materials used were $FeAlO_x$, Fe_3O_4, Fe_2O_3 and Fe. A range of Fe particle sizes were used: ~25 nm, 35-45 nm, 60-80 nm, 200 mesh (~74 μm), 70 mesh (~210 μm) and 20 mesh (~840 μm).

RESULTS

Fig. 2(a) shows the maximum temperature achieved when the sample powders were placed in the electric and magnetic field maxima respectively. In the magnetic field heated samples shown in blue, $FeAlO_x$ and Fe_2O_3 achieve a higher temperature than when heated using the electric field, whereas Fe_2O_3 samples achieve a higher maximum temperature in the electric field. Fig. 2(b) shows the temperature achieved and the corresponding Q factor of the resonant cavity when $FeAlO_x$ is heated in the magnetic (*H*) field and the electric (*E*) field.

DISCUSSION

From Fig. 2(a) we see that there is a greater difference in maximum temperature in magnetic field heating, with over 350°C variation between $FeAlO_x$ and Fe_2O_3 in contrast to less than 25°C difference across all 3 catalysts in the electric field. Fe_2O_3 is a non-magnetic ferrous oxide so the poor heating in the magnetic field is to be expected. In the electric field, the absorption is due to the moderate dielectric loss of the samples. It is also worth noting that whilst the maximum temperature reached in the magnetic field by $FeAlO_x$ and Fe_3O_4 are relatively similar, the heating rates for these catalysts were dramatically different with $FeAlO_x$ taking over 6 minutes to reach its peak whilst Fe_3O_4 reach maximum temperature in just over a minute. It can also be seen that the maximum temperature achievable was greater with the magnetic field. A significant factor in this was the loss of

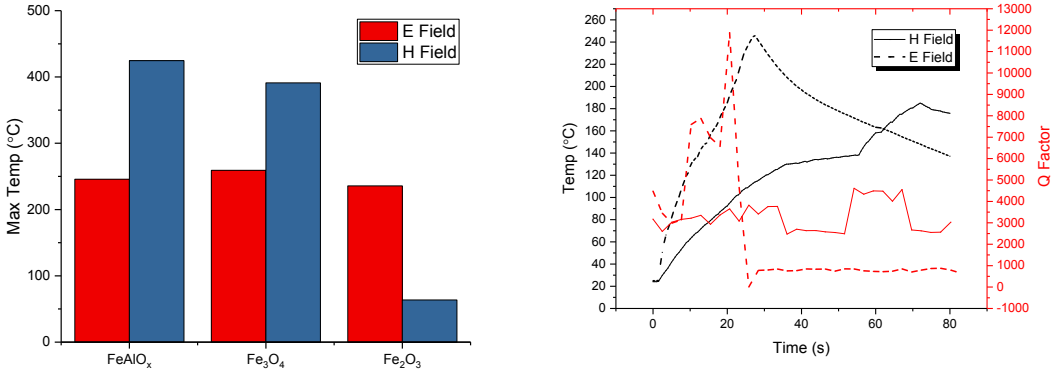

Figure 2. Maximum temperature reached in *E* (red) and *H* (blue) fields in the TM_{010} mode cavity resonator at 2.45GHz. In the electric fields the samples reach similar temperatures, but in the magnetic fied there is a difference of over 350°C (a). Temperature (Black) and Q Factor (Red) during heating of $FeAlO_x$ in the magnetic (solid) and electric (dashed) field. Sudden drop in Q factor causes the powder to stop heating in the electric field (b).

coupling occurring at approximately 250°C when heated using the electric field, causing a dramatic drop in the Q factor. This is not the case in the magnetic field as can be seen in Fig. 2(b). The loss of coupling is due to a shift in sample permittivity as a result of the increasing temperature. This in turn leads to a shift in resonant frequency and a loss of coupling.

CONCLUSION

In this work we show that heating rates in iron-based catalyst particles vary dramatically in the magnetic field unlike in the electric field. Being able to heat selectively based on magnetic loss opens a range of possibilities to improve efficacy and efficiency of microwave driven heterogeneous catalytic processes. Better understanding of the differences between heating in electric and magnetic fields in microwave catalysis will enable better system design and catalyst selection and can lead to hyper-selective heating where catalysts are effectively targeted in mixed feedstocks.

REFERENCES

[1] D.R. Slocombe and A. Porch, "Microwaves in chemistry," *IEEE J. of Microwaves*, vol. 1, no. 1, pp. 32-42, 2021.

[2] X. Jie, W. Li, D. Slocombe, Y, Gao, I. Banerjee, S. Gonzolas-Cortes, B. Yao, H. AlMegren, S. Alshihri, J. Dilworth, J. Thomas, T. Xiao, and P. Edwards, "Microwave-initiated catalytic deconstruction of plastic waste into hydrogen and high-value carbons," *Nature Catalysis*, vol. 3, pp. 902-912, 2020.

[3] H. Nguyen, J. Sunarso, C. Li, G. H. Pham, C. Pham, and S. Liu, "Microwave-assisted catalytic methane reforming: a review," *Applied Catalysis A: General*, vol. 599, no. 5, 2020.

[4] A. Porch, D. Slocombe, and P. Edwards, "Microwave absorption in powders of small conducting particles for heating applications," *Physical Chemistry and Chemical Physics,* vol. 15, no. 8, pp. 2757-2763, 2013.

Material/Chemical Recycling *via* CO_2-Free Emissions by Using Microwave Flash Pyrolysis of Waste Plastics

Anna Sawai and Satoshi Horikoshi

Sophia University, Tokyo, Japan

Keywords: chemical recycling, microwave, pyrolysis, waste plastics

INTRODUCTION

Plastics are typical chemical products that have made our lives easier. However, the long stability of chemical structures of plastics has made post-use processing difficult. For example, in Japan, which has a small land area, more than 50% of waste plastics are treated by thermal recycling, and thermal energy is recovered by burning them. However, since this recycling method produces CO_2 gas, it cannot be sustained from the viewpoint of global warming. Furthermore, the most noticeable recycling is chemical recycling, but it is not a major recycling method due to its difficulty and process complexity. Pyrolysis is known as one of the most feasible ways to convert waste plastic into chemical materials easily. But in general, pyrolysis requires a large amount of energy to breakdown polymers and the use of energy-efficient heat sources is essential to build novel recycling processes. Additionally, when waste plastic is thermally decomposed by conventional heating, tar is usually generated, and resources can hardly be obtained. Therefore, we were challenged to solve the problem of material and/or chemical recycling by using microwaves and microwave absorbers.

In this study, polyethylene and polypropylene powders were used as the model waste plastic because they form a large amount of production and waste [1]. Because of transparency of these plastics to microwaves, direct pyrolysis does not take place by itself under microwave irradiation. Therefore, we investigated the possibility of a heating element that absorbs various microwaves. Carbon susceptor showed good performance, so carbon material and plastic were blended and used as a sample. In this novel pyrolysis method, a gas containing a monomer as a main component was obtained as a decomposition product from polyethylene and polypropylene.

METHODOLOGY

In this study, an experiment was conducted using a single-mode applicator connected to a semiconductor-microwave generator to clarify the characteristics of the recycling of plastics by microwave flash heating. The sample temperature was monitored using an

(a) (b)

Figure 1. Pictures of reactor with carbon materials and polyethylene pellets before (a) and after microwave heating (b).

infrared thermometer (~ 2100 °C) that transmits quartz. A material containing a mixture of carbon material and model plastic pellet was enclosed in a synthetic quartz pipe (reactor) and irradiated with microwaves under nitrogen gas flow condition. The reaction vessel was installed at the maximum position of the electric field (***E***-field) in the single mode applicator and continuously irradiated with microwaves. The gas discharged from the reactor together with nitrogen carrier gas were collected by gas bag and subsequently analyzed by gas chromatography in order to quantify various decomposition gases. As a control experiment, the behavior during normal heating was observed using an electric furnace.

RESULTS AND DISCUSSION

When microwave heating was performed for 3 min using 7 mg of carbon material with respect to 70 mg of polyethylene pellets, a gas containing ethylene as a main component was obtained with a gas yield of 84%. Immediately after irradiation with microwaves, the temperature of the sample increased significantly and reached ca. 1500 °C or higher in a few sec. Observing the inside of the reactor after the microwave irradiation at 3 min, polyethylene is decomposed to the extent that it cannot be visually confirmed after microwave heating (Fig. 1). Ethylene could be obtained with high yield and high selectivity from polyethylene. Furthermore, it has been confirmed that almost no CO_2 is generated. In addition, it was not possible to identify commonly occurring “tar”.

On the other hand, when the decomposition of polypropylene was attempted by the same method as that of polyethylene, a gas containing propylene as a main component was obtained with a gas yield of 82.7%. The propylene could be obtained with high yield and high selectivity.

The polyethylene was heated in an electric furnace at 1500 °C for 3 min under a nitrogen carrier gas, but the polyethylene remained as a solid, and the gas could not be recovered. Therefore, further heating was continued, but polyethylene was obtained only as a solid (tar), not as a gas.

Why did the microwave method succeed in gasification? Generally, once tar-like substances are produced, further decomposition was hard to occur. However, with microwave heating, the temperature of the plastic reaches 1500 °C in a very short time, so it is thought that it was gasified without passing through tar-like substances. Furthermore, microwave heating creates a microscopic high temperature field (hot spot) of more than 1500 °C [2]. It is also considered that such a microscopic high temperature was generated on the surface of the carbon material.

CONCLUSION

In the thermal decomposition of polyethylene and polypropylene, when microwave heating was used, the plastic was decomposed into a monomer-based gas in high yield. On the other hand, the decomposition product could not be obtained as a gas by normal heating using an electric furnace. The microwave heating enables decomposition of plastics, which is difficult with normal heating, and a gas containing a monomer as a main component can be obtained in an energy-effective manner.

REFERENCES

[1] Ministry of the Environment in Japan, “Toward the situation surrounding plastics and the construction of a resource recycling system,“ 2019.

[2] S. Horikoshi, A. Osawa, M. Abe, and N. Serpone, “On the generation of hot spots by microwave electric and magnetic fields and their impact on a microwave-assisted heterogeneous reaction in the presence of metallic Pd nanoparticles on an activated carbon support," *J. Phys. Chem. C*, vol. 115, pp. 23030–23035, 2011.

Microwave Catalytic Non-Oxidative Conversion of a Model Natural Gas to Hydrogen and Carbon Nanotubes

Changle Jiang, Sonit Balyan, Brandon Robinson, Alazar Araia, Yuxin Wang, and Jianli Hu

West Virginia University, Morgantown, WV, USA

Keywords: carbon nanotube, hydrogen, microwave catalysis, natural gas, pyrolysis

INTRODUCTION

The steam methane reforming (SMR) has been the main sources for current hydrogen production. However, the reaction was creating CO/CO_2 during the process. The generation of these gases was not preferred by the current emission policies. In this work, a CO_x free process was presented as a possible alternative for the SMR. More importantly, the hydrogen process was fully driven by microwave. In addition, carbon nanotube was generated as a by-product, which could compensate the overall cost. Our group has proved that carbon nanotube supported Ni-Pd bimetallic catalyst could convert the methane to CO_x free hydrogen and carbon nanotubes under conventional heating in an electrical furnace [1]. We have further discovered in one yet published work that microwave heating could replace the conventional heating for this specific reaction and show competitive results as well [2]. In this work, we expanded the reaction for a model natural gas that including ethane, which was the second most composition in the natural gas.

METHODOLOGY

The catalyst used in this work was a multi-walled carbon nanotube (MWCNT) supported Ni-Pd bimetallic catalyst. The weight percentages of Ni, Pd, and MWCNT were 10%, 1% and 89%, respectively. The Ni-Pd was loaded on the MWCNT by a solvothermal preparation. The nickel nitrate and palladium nitrate (Sigma Aldrich) were used as precursors. Acetone was used as solvent. The nitrate salts of Ni and Pd were dissolved in acetone, mixed with MWCNT, and undergone a solvothermal process in a sealed autoclave. The temperature of the solvent was 110 °C and the pressure inside the autoclave was 150 psi. The MWCNT loaded with Ni and Pd precursor were dried in the oven at 80 °C for 24 hours. The dried solid was reduced in pure hydrogen for 4 hours, resulting in 10Ni-1Pd-CNT catalyst. This catalyst was used in all the microwave driven methane or ethane conversion reactions for this work.

The reaction was carried out in a microwave reactor (MC1330, Lambda Technologies Inc., Morrisville, NC, USA). The microwave frequency was 5.85 GHz. The reaction

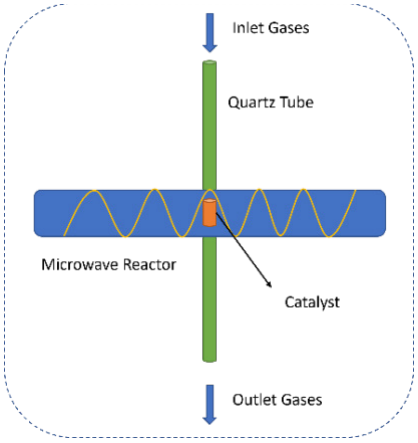

Figure 1. Schematic diagram of the microwave reactor

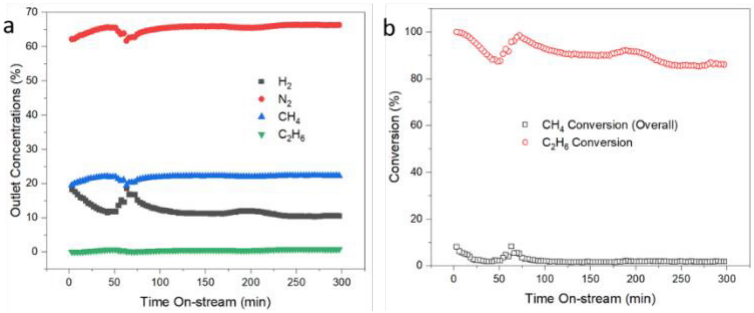

Figure 2. Conversion of model natural gas to hydrogen and CNT

temperature was 550 °C. The layout of the reactor, catalyst, and gas flows were shown in Fig. 1. The residence time was 6 hours. The outlet gases were detected by a four-column micro gas chromatography (Micro GC Fusion, Inficon, Inc.). The inlet gases were a mixture of nitrogen and a model natural gas with methane/ethane ratio of 4.0 by volume. Nitrogen has a flow rate of 70 ml/min. The model natural gas has a flow rate of 30 ml/min (Methane 24 ml/min; Ethane 6 ml/min). Separated tests using methane or ethane only as feed were carried out as well. Either test has a methane/ethane 30 ml/min flow rate and a 70 ml/min nitrogen flow. 0.2 gram of 10Ni-1Pd-CNT was loaded to the fixed-bed microwave reactor for the reaction.

RESULTS

The gas chromotography result of the outlet gases has shown the presence of nitrogen, hydrogen, methane, and ethane (Fig. 2(a)). None other gases were detected with a visible amount. Upon caculation of the conversion, the ethane has a conversion around 85% while methane has very low converion overall. Futher tests on methane or ethane only feed have been conducted. The results confirmed that ethane has a similar high conversion like in the conversion of model natural gas. However, we did observe a methane conversion around 25% in methane only feed test.

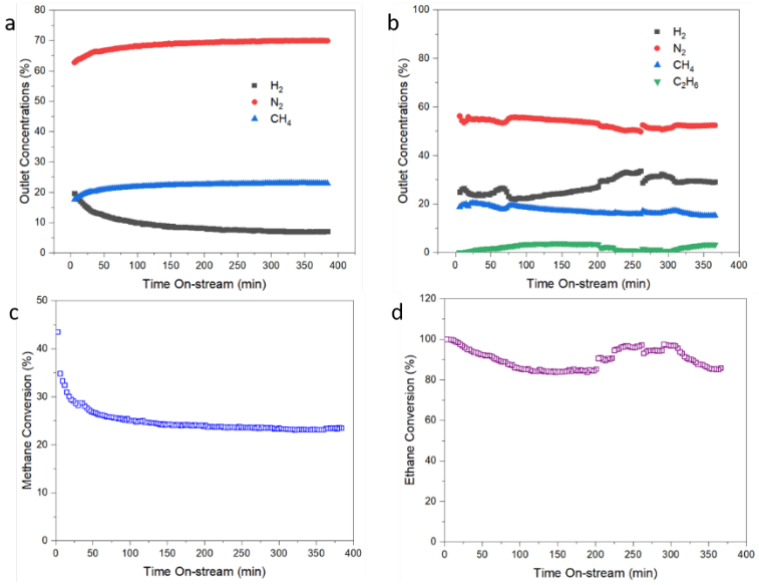

Figure 3. Separate tests using methane only flow (a,c) and ethane only flow (b,d): flow rates remain 100 ml/min total; 30% reactant gas and 70% nitrogen as balance flow.

DISCUSSION

There are two possible interpretations of the results. One is that there was competition between ethane and methane when it came to occupying the active catalytic sites. Ethane has outcompeted the methane when approaching metallic surface. The other explanation is that ethane was dehydrogenated to carbon and methane, thus, compensating the methane consumed during the reaction, leading to an observation of much lower methane conversion.

CONCLUSION

The conversion of model natural gas was different from pure methane feed. The catalyst remained active toward natural gas. However, ethane was dehydrogenated much easier and faster than methane. The mechanism regarding this combined reaction will be further explored.

REFERENCES

[1] I.W. Wang, R.A. Dagle, T.S. Khan, J.A. Lopez-Ruiz, L. Kovarik, Y. Jiang, M. Xu, Y. Wang, C. Jiang, S. Davidson, and P. Tavadze, "Catalytic decomposition of methane into hydrogen and high-value carbons: combined experimental and DFT computational study," *Catal. Sci. Technol.*, vol. 11, pp. 4911-4921, 2021.

[2] C. Jiang, I.W. Wang, X. Bai, S. Balyan, B. Robinson, J. Hu, W. Li, A. Deibel, X. Liu, F. Li, L. Neal, J. Dou, Y. Jiang, R.A. Dagle, J.A. Lopez-Ruiz, and G. Skoptsov, "Methane catalytic pyrolysis by microwave and thermal heating over CNT supported catalysts: productivity, kinetics, and energy efficiency," *Ind. Eng. Chem. Res.,* 2022 (under review).

Microwave-Enhancement Conversion of Methane into Aromatics over Mo/ZSM-5 Catalysts

Victor Abdelsayed[1,2], Ashraf Abedin[1,2], Pranjali D. Muley[1,2], Hari P. Paudel[1,2], and Daniel J. Haynes[1]

[1]National Energy Technology Laboratory, Morgantown, WV, USA
[2]NETL Research Support Contractor, Morgantown, WV, USA

Keywords: catalyst activation, microwave dehydroaromatization, methane non-oxidative conversion

INTRODUCTION

Microwave-assisted chemical conversion processes offer many advantages such as rapid and volumetric heating. These processes can be used to convert remote associated flaring gases into value-added chemicals near oil fields due to their low cost and modularity compared to large scale thermal reactors. Nonoxidative conversion of methane is a direct chemical process to produce value-added chemicals and gases such as aromatics and hydrogen. However, challenges of rapid catalyst coking and low thermodynamic conversions represent a major challenge towards commercialization. A better understanding of the material performance under microwaves is needed to control the reaction chemistry and design more efficient microwave catalysts.

In this work, Mo/ZSM-5 was used as benchmark catalyst to evaluate the effect of material activation between thermal and microwave reactions. Catalyst activation is required in-situ to generate dispersed active Mo species and intermediate carbon pools in the pores to produce benzene. We also demonstrate how the catalyst was activated under CO or methane prior to reaction under thermal or microwave towards methane dehydroaromatization reaction. Modeling and characterization work are presented to determine the activity-structure relationship and differences under microwave reactions.

METHODOLOGY

Mo/HZSM-5 catalyst with different Mo loadings were used in this study. The catalysts were activated under different gases: CO, syngas, and methane followed by methane dehydroaromatization reaction using microwave-assisted and conventional thermal heating. Fig. 1. Shows the experimental setup for microwave and conventional thermal fixed bed reactor. A single mode microwave cavity with a fixed frequency (2.45 GHz) and up to 2 kW power was used to activate the catalyst and perform the reaction studies.

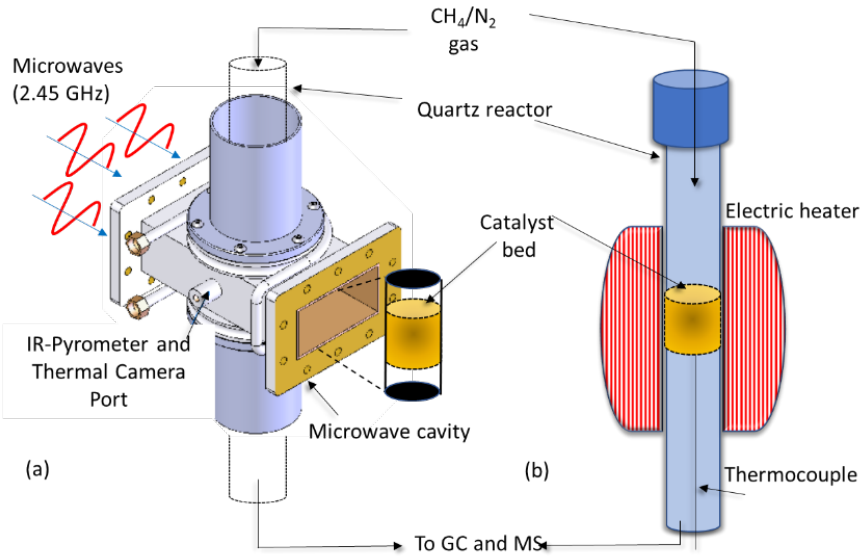

Figure 1. Experimental setup for (a) microwave reactor and (b) conventional thermal fixed bed reactor used in methane dehydroaromatization reactions.

Catalyst bed temperature was measured using different techniques such as contactless IR pyrometer and thermal camera to measure the surface temperature of the catalyst. Also, a fiber optics probe was used to check the catalyst core temperature. Different characterization tools were used to study the crystalline and microporous structures, carbon formation and surface acidity of fresh and reacted catalysts such as BET, TPO, XANES, TGA, NH_3-TPD and XRD techniques.

RESULTS AND CONCLUSIONS

In this work, we found that the CO-activated Mo/ZSM-5 catalyst has a higher activity and less carbon/coke formation compared to methane-activated catalysts under both microwave and thermal heating. Using microwaves for catalyst activation results in a rapid activation time and a lower activation temperature compared to that under conventional thermal activation. Catalyst temperature measurements during microwave irradiation continues to represent a challenge due to its dynamic changes in dielectric properties, temperature and formation of carbon/tar deposits. This could result in uneven temperature distribution throughout the bed and the formation of hotspots. The dielectric properties of the zeolite are very sensitive to the surface functionality and microwave frequency as shown in Fig. 2 where the higher the Bronsted acid sites (Al-OH) in zeolite the higher it will be selective to heat and couple under the microwaves. Zeolite with silica-to-alumina ratio of 23 has a higher tangent loss and thus was selected to support Mo catalyst for this reaction.

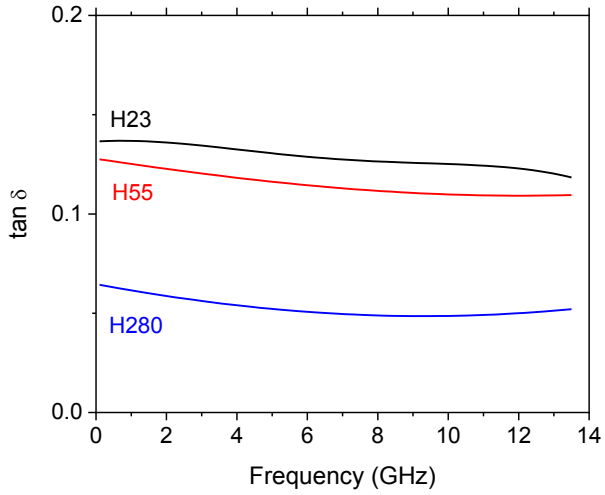

Figure 2. The tangent loss of zeolites with different surface acidity as a function of microwave frequency.

Our results also shows that the aromatic and hydrogen yields during methane dehydroaromatization are sensitive to microwave powers used during the reaction. The microwave reaction was found to be more selective to olefin formation at lower powers and to higher hydrogen and carbon yields at higher microwave powers. DFT and COMSOL calculations were also presented to help understand the catalyst activation and coupling under microwaves.

Solid-State Microwave Power Combining Techniques

Zoya Popović

Department of Electrical, Computer and Energy Engineering, University of Colorado, Boulder, CO, USA

Keywords: efficiency, power combining, solid-state microwave power amplifiers

INTRODUCTION

This paper presents an overview of power combining techniques for solid-state microwave sources. Obtaining high output power levels in the kW range from solid-state devices at microwave frequencies has been a topic of research for a few decades, e.g., [1]. A single transistor is limited in output power and gain, due to the inherent losses and field breakdown in semiconductors, and the output power is approximately inversely related to the square of the frequency of operation. Solid-state devices are nevertheless attractive because of relatively low supply voltages that are needed, long lifetimes, small size, amenability to monolithic integration and versatility in terms of circuit design.

OVERVIEW

Power combining of solid-state power amplifiers enables increased power levels, with limitations dictated by the power combining structures, implemented with waveguides, coaxial or printed transmission lines, which have inherent loss. High power combining efficiency is a function of this loss, as well as failure of one or more devices in the combiner, e.g., [2]. Approaches include corporate combiners, radial combiners and spatial combiners. Corporate combiners are limited by loss to combining up to 16 devices, while radial combiners with 32 or more devices are more common. Spatial combining, where each of many solid-state amplifiers (or oscillators) radiates through an antenna and combines power upon radiation, in theory has loss that does not increase with number of devices above a certain aperture size [3, 4]. This paper will present an overview of the results obtained from different power combining methods and conclude with outlooks for obtaining kW levels from solid-state devices at microwave frequencies.

REFERENCES

[1] N. Deo, "Microwave and millimeter wave solid state power amplifiers for future space-based communications and radars," *2018 IEEE Aerospace Conf.* pp. 1-7.

[2] N. Picard, J.M. Denoual, D. Bourreau, and A. Peden, "Analysis of failure impact on microwave power combining," *2009 European Microwave Conference,* pp. 898-901.

[3] J. Harvey, E.R. Brown, D.B. Rutledge and R.A. York, "Spatial power combining for high-power transmitters," *IEEE Microwave Magazine*, vol. 1, no. 4, pp. 48-59, Dec. 2000.

[4] R.A. York and Z. Popovic, Eds., *Active and Quasi-Optical Arrays for Solid-State Power Combining*, John Wiley and Sons, 1997.

Modular and Scalable Solid-state Architectures for Frequency-Dependent Microwave Processes

Marco Fiore, Nicola Di Modugno, Tommaso De Nicolo, and Cristian Bruno

LEANFA Srl, Ruvo di Puglia, Italy

Keywords: adaptive, frequency, modular, phase, scalable, solid-state

INTRODUCTION

Dielectric heating by means of microwave irradiation has already many remarkable applications in the Industrial and Scientific fields since it typically brings processing speed, energy efficiency and clean operating environment.

Recent advances of solid-state microwave technology have allowed innovative processes, but solid-state technology is currently far from completely replacing the good old microwave technology, still capable of providing cost-effective solutions, especially with power-hungry applications.

Noteworthy advantages of solid-state microwave technology occur whenever accurate real-time control of radiation parameters brings valuable results [1] in terms of process duration, high-quality manufacturing and especially in terms of capability of complex thermal profile engineering. Indeed, many top-grade applications like nanomaterials development, pharmaceutical chemistry, medical hyperthermia and advanced food processing require highly reliable microwave generators allowing deep and rapid interaction between the radiating devices and the processed materials.

EXPERIMENTAL EQUIPMENT

As a counterpart to magnetron-based simple open-loop microwave generators, innovative modular and scalable solid-state architectures have been conceived by means of intimate interaction between hardware and software elements, born after a careful hardware-software co-design phase started by LEANFA's R&D team at the beginning of year 2015. The main milestones of this R&D effort were, from the very beginning of the design process:

- high compactness
- instant digital control of power, frequency and phase
- allowance of 100% reflected power
- real-time assessment of forward and reflected power levels
- flexible network configuration of multi-source schemes

Figure 1. Photo of the 2,450MHz module, elementary item for scalable architectures.

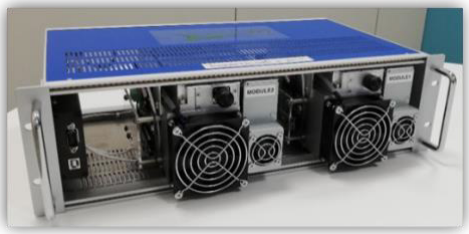

Figure 2. Laboratory kit for multi-feed experimental developments.

- capability to implement custom radiation patterns
- implementation of user-enabled fully adaptive workflows
- 15+ years of product lifespan

New compact microwave generators have been designed by a unique combination of finely tuned PCBs, precision mechanical fittings, LDMOS power devices, high-speed digital microcontrollers and thousands of lines of firmware and software code with a great focus on the simplest end user's experience. Moreover, a flexible embedded digital communication interface allows a very efficient modular approach that easily bridges the gap between experimental prototypes and subsequent scale-up phases.

RESULTS

After plenty of experimental approaches with worldwide Companies and research centers, very soon it became evident that the major applications benefiting from the new generators are the ones that show strong dependence on the radiation frequency and, when applicable, on the phase shifting capability of a number of generators managed as a frequency-synchronized array [2], [3]. Typical examples are food processing [4] in multilayer batch ovens, plasma generation for innovative materials processing and controlled heating of fluids for medical applications.

A laboratory kit has been developed for advanced testing with selected materials in order to experimentally assess the capability of frequency sweeping and phase sweeping (also with smart combination of both) "recipes" to implement highly controlled thermal profiles using static multimode applicators with multiple WR340 feeding guides.

Figure 3. A screenshot from the LeanOn software platform.

DISCUSSION

In order to allow a correct and reproduceable experimental approach, the kit has been accompanied by LeanOn, an advanced software platform for Windows OS. The software platform easily allows complete management of the overall radiating parameters, also enabling automatic reduction of reflected microwave power and providing user-friendly graphical monitoring functions and detailed output database storage for comfortable project reporting and fully documented development flow.

The laboratory kit has demonstrated to be a very flexible tool for the development of innovative processing applicators, aiming at accurate thermal profile shaping for modern industrial, scientific and medical applications.

CONCLUSION

Integration of innovative solid-state generators into new products for Industrial, Scientific and Medical (ISM) applications require careful experimental approach to firmly validate the advantages of replacing the legacy magnetron technology. The developed laboratory kit is a cutting-edge hardware-software tool that allows precise assessment of advanced microwave processes built using modular multi-feed architectures, tailored for applications requiring calibrated frequency and phase shaping.

REFERENCES

[1] S. Zuber, M. Joss, S. Tresch, and M. Kleingries, “Dynamic optimization of the transmission efficiency between the solid state microwave sources and the microwave applicator,” *IDS’2018 – 21st Intern. Drying Symp.* pp. 291-298.

[2] A. Więckowski, P. Korpas, M. Krysicki, F. Dughiero, M. Bullo, F. Bressan, and C. Fager, “Efficiency optimization for phase controlled multi-source microwave oven,” *Intern. J. of Applied Electromagnetics and Mechanics*, vol. 44, no. 2, pp. 235-241, 2014.

[3] P. Korpas, M. Krysicki, and A. Więckowski, “Phase-shift-based efficiency optimization in microwave processing of materials with solid-state sources,” *16th Seminar “Computer Modeling in Microwave Power Engineering*, *Karlsruhe, Germany, 2014*, pp. 68-71.

[4] G.B. Awuah, H.S. Ramaswamy, and J. Tang, Eds., *Radio-Frequency Heating in Food Processing*, Taylor & Francis, 2014.

Solid-State Technologies LDMOS and GaN Compared

Patrick Valk and Coen Centen

Ampleon, Nijmegen, Netherlands

Keywords: GaN, LDMOS, RF power, semiconductors, solid state

INTRODUCTION

This paper discusses the differences between RF Power transistors based on LDMOS and GaN semiconductor technologies. The pros and cons of each technology will be discussed as well as application-related benefits. The focus will be on performance, thermal resistance, and operating lifetime.

This summary is based on the Ampleon devices for ISM applications at 2.45 GHz. These devices are available in 32V LDMOS and 50V 0.45um GaN technologies. The differences in power dissipation and thermal impact of these RF power FET's is demonstrated.

METHODOLOGY

In this summary, we compare two products that may be used for similar applications, with very similar specifications. The LDMOS device is the BLC2425M10LS250, a 10th generation LDMOS FET that has an output power of 260 W with 68.5% efficiency when used for CW operation at 2.45 GHz. The GaN device is the CLF2425H4LS300P, a 4th generation 0.45 um GaN FET that can output 300 W with an efficiency of 72% when used in CW operation at 2.45 GHz.

Both devices have the exact same package size, but the LDMOS device is internally matched at input and output and uses a single lead for gate and drain, while the GaN device is matched only at the input and has 2 gate and 2 drain leads.

Testing of thermal resistance (Rth) is performed on a RF test setup, where the test circuit is placed on a watercooled plate. A thermocouple in the test circuit, right below the center of the device measures the case temperature, while an infrared camera with special lenses captures the temperature on the semiconductor surface.

The operating lifetime of devices is determined by a TFAT test, which comprises thermal cycling the device under stringent DC power conditions in an oven that can accurately control temperature and swing the temperature over a large range.

Figure 1. The BLC2425M10LS250 is a 260W LDMOS based RF power transistor for 2.45 GHz applications in an air cavity plastic package

Figure 2. The CLF2425H4LS300P is a 300W GaN based RF power transistor for 2.45 GHz applications in a ceramic package.

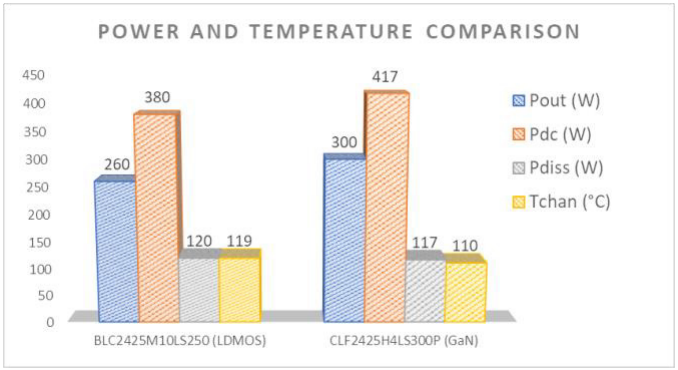

Figure 3. DC Power (Pdc), output power (Pout), dissipated power (Pdiss) and channel temperature (Tchan) of the LDMOS and GaN device compared.

RESULTS

Thermal resistance is defined as the thermal resistance between the active drain-source channel and the bottom of the package flange during operation. For the LDMOS device operating at 260 W of output power, the thermal resistance is measured 0.33 K/W, while the GaN device has a thermal resistance of 0.26 K/W. Based on the output power (Pout) and efficiency, we can calculate the DC power (Pdc), dissipated power (Pdiss) and the drain-source channel temperature (Tchan) in the active area of the semiconductors. The baseplate temperature is 80°C in the example in Figure 2.

In summary, the results show that we obtain higher power density with GaN-based devices, meaning that we can make more power per square mm semiconductor, due to the high current density in AIN interlayer [1].

The total dissipated power for the two devices is very similar, but the LDMOS device has a larger total silicon surface, thus a lower power dissipation per mm^2 compared to the GaN device. The GaN device has a higher thermal conductivity per mm^2, due to its SiC substrate, as described in [1]. This means that there is more temperature difference, concentrated in a smaller area, causing a lot more stress on the interface between the GaN dies and the package heat sink. And hence, the die attach process is more challenging to meet the required lifetime specifications.

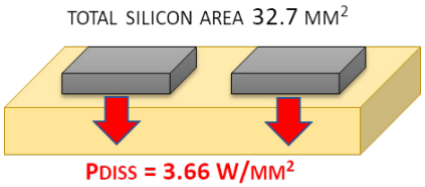

Figure 4. The LDMOS device has a power dissipation of 3.66 W per mm^2 semiconductor surface.

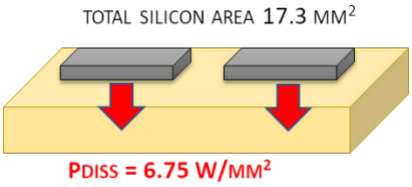

Figure 5. The GaN device has a power dissipation of 6.75 W per mm^2 semiconductor surface.

The total dissipated power for the two devices is very similar, but the LDMOS device has a larger total silicon surface, thus a lower power dissipation per mm^2 compared to the GaN device. The GaN device has a higher thermal conductivity per mm^2, due to its SiC substrate, as described in [1]. This means that there is more temperature difference, concentrated in a smaller area, causing a lot more stress on the interface between the GaN dies and the package heathsink. And hence, the die attach process is more challenging to meet the required lifetime specifications.

DISCUSSION

In pulsed applications like military, the choice for a GaN technology nowadays is rather obvious. Due to the improved power density, more power can be made with a small amplifier, and due to pulsed nature of the signals, there is not much dissipated power. For ISM applications, where size may not be critical, but temperature management and application lifetime are, LDMOS could still be the best choice today.

CONCLUSION

The main conclusion is that LDMOS has been around for 20 years and with its 10th generation is well matured and has been proven to be very reliable. GaN is a more recent technology, within Ampleon we are currently working on the 4th generation. The performance improvements with GaN are quite spectacular, we can achieve roughly 5x more power from the same active semiconductor area, with lower loss and lower parasitics such as output capacitance. This lifts the efficiency from 68% to 72% at 2.45 GHz today, but in the future, a 75-80% efficiency is on the horizon. The main challenge is to manage the flow of power dissipation from the smaller semiconductors to the heatsink.

The performance promise of GaN is not fully utilized yet, but in the next coming years the higher power density and increased frequency response, will lead to newer PA concepts such as switch mode power amplifiers. This will enable higher efficiencies at ISM frequencies.

REFERENCES

[1] R.S. Pengelly, S.M. Wood, J.W. Milligan, S.T. Sheppard, and W.L. Pribble, “A review of GaN on SiC high electron-mobility power transistors and MMICs,” *IEEE Trans. on Microwave Theory and Techniques,* vol. 60, no 6, pp. 1764-1783, 2012.

MML, Solid State Oven Interoperability and The Meta Verse

Steven Drucker

Droaster Laboratories LLC, Greer, SC, USA

Keywords: meta verse, MML, microwave markup language, solid state microwave ovens

ABSTRACT

The origins, development and beta state of solid state oven open source "MML", Microwave Markup Language is presented. The smart kitchen value proposition lags even while smart home consumer buying motivation evolves from sideline curiosity to move-up necessity. Inside the smart kitchen, Push Button Get Food oriented appliance sales lead all categories. Lowest common denominator generic microwave oven pricing persists as an insurmountable solid state oven barrier to adoption. The come-hither promise of the Meta Verse opens the door to a Consumer Packaged Goods ("CPG") cornucopia of brand opportunities. CPG brands populate Meta Verse larders, their avatar and Non Fungible Token ("NFT") values shared in meta-valuations, propelled by untold varieties of multi—dimensional animation engagement and bleeding over into Push Button Get Food Meta Verse perfected outcomes. While in the real world smart kitchen unit sales continue to lag, populated as they are by walled gardens such as Bixby, Zigbee, Alexa, Siri and so forth—until their gatekeepers broaden selling propositions with interoperability, i.e., a data standard to enable functionality among heretofore manufacturer constrained smart kitchen devices. The first such "co-opetition" based alliance was announced during CES in January 2022. As for solid state oven barriers to adoption: who could have foreseen that their barriers to adoption may well be prone to crumble as a result of from within the Meta Verse having substantiated the context and realized the *perception* of Push Button Get Food perfectly?

Microwave-Assisted Additive Manufacturing of Continuous Fiber Reinforced Thermoplastic Composites: Challenges and Opportunities

Nanya Li, Guido Link, and John Jelonnek

Institute for Pulsed Power and Microwave Technology, Karlsruhe Institute of Technology, Eggenstein-Leopoldshafen, Germany

Keywords: additive manufacturing, continuous FRP, microwave heating, solid-sate microwave generator

INTRODUCTION

Today, carbon fiber reinforced thermoplastic composites are widely used in automotive and aircraft industries, because of their higher strength to weight ratio and longer service periods compared to structures made of metal. Additive manufacturing, know as 3D printing based on fused filament fabrication (FFF) is an emerging method for manufacturing thermoplastic composites. The printing of fiber reinforced thermoplastic composite components is not subject to the limitations of traditional forming tools and complicated multi-stage manufacturing. Additionally, it eliminates the need for intense manual labor, expensive equipment and material waste in the manufacturing process.

The combination of FFF printing technology with continuous carbon fiber reinforcements instead of pure thermoplastic materials or short carbon fiber reinforced thermoplastics offers significantly higher performance and strength-to-weight ratios of the printed composite parts. However, the state-of-the-art printing methods for continuous carbon fiber reinforced thermoplastic (CCFRP) composites are limited to slow printing speed (< 10 mm/s) layer-by-layer printing, and limited mechanical properties.

In this paper, the microwave heating method is introduced which enables a rapid, large-scale printing of CCFRP because of instantaneous volumetric and selective heating. An optimized printer head was developed based on a coaxial resonator concept [1]. This paper discusses the opportunities and challenges of microwave assisted 3D printing of CCFRP.

FILAMENTS AND SYSTEM DESIGN

A first prototype of a microwave assisted additive manufacturing system named SERPENS (Super-Efficient and Rapid Printing by Electromagnetic Heating Necessitated System) for printing of CCFRP filaments has been developed at the Karlsruhe Institute of Technology since 2020. SERPENS is equipped with a small-size coaxial microwave resonator as shown

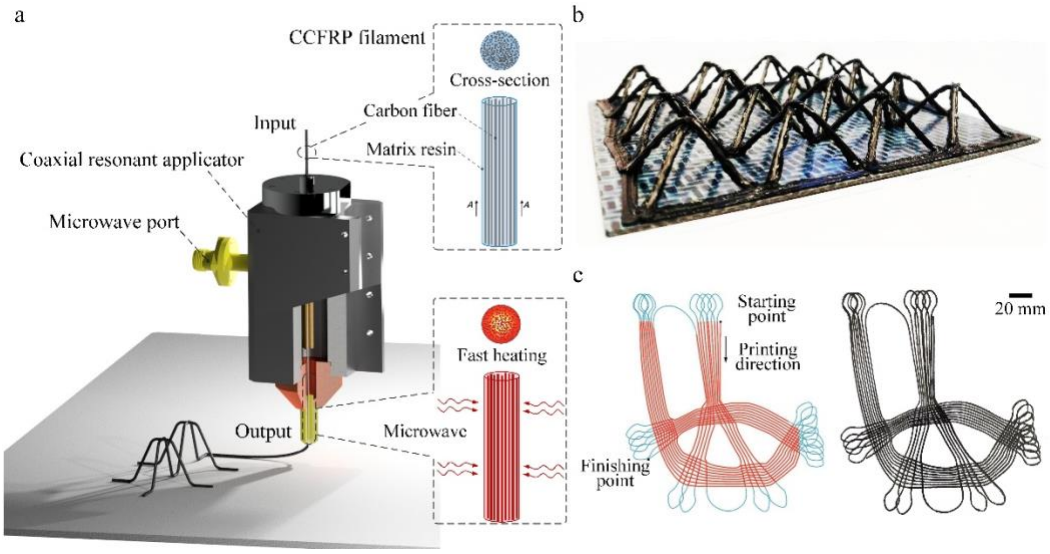

Figure 1. Schematic diagram of microwave heating assisted additive manufacturing of CCFRP (a); 3D free-hanging CCFRP printed by SERPENS (b); 2D bionic CCFRP structure (c).

in Fig. 1(a) [2]. The prepared filaments are guided through the applicator and heated inside by microwaves without contact. The applicator was integrated in an upgraded three-axis numerical control machine and fed with a commercial 300 W solid-state microwave generator from HBH Microwaves GmbH, Germany. This generator is operating in the 2.4 to 2.5 GHz ISM band, which allows fast and precise power and frequency control. At this frequency band an efficient heating of CCFRP filaments with sufficient penetration depth can be achieved. By using this novel system, the fabrication of 2D bionic structures and free-hanging 3D lattice trusses with carbon fibers oriented along load transmission paths has been successfully demonstrated (see Fig. 1(b) and (c)).

For this purpose and due to limited availability on the market, filaments of polyamide (PA), polylactic acid (PLA) and polyether ether ketone (PEEK) reinforced by continuous carbon fibers were initially produced using an impregnation system developed in-house. This system was used to produce filaments with diameters of 0.35 mm, 0.65 mm and 1.05 mm with fiber volume contents of 40%, 24% and 27%, respectively.

CHALLENGES AND OPPORTUNITIES

One major drawback of existing 3D printing FFF technology is the heating method to melt the polymer filaments in the printing head. The heat is generated in a resistive heated block and transferred to the filament, which is limited by the contact area and the typically low thermal conductivity of polymer filaments. Thus, in case of high printing speed, there is a non-uniform temperature distribution in the cross section of the filament with a hot surface, and a cold core. In addition, increasing the filament diameter aggravates this problem and leads to reduced mechanical performance. This is because the non-melted polymer in the core area may generate voids and defects during the printing process.

Microwave heating in combination with an appropriate applicator design provides the opportunity to achieve a uniform temperature distribution even with large diameter filaments. Different to state-of-the art FFF technology, where the printing speeds is limited by the heat transfer, with microwave heating the limit is given by the installed microwave power only. An increase in printing speed by a factor of 10 and more can therefore be easily achieved. Nevertheless, due to the strong correlation between the microwave power and printing speed advanced and challenging control methods are required to reach a constant printing temperature of the filament with changing printing speed [1]. As measured in an experiment with SERPENS and using PA based CCFRP filament with a diameter of 0.45 mm, when the printing speed is changed from 0 to 100 mm/s at a printing temperature of 210 °C, the power required changes from 10.5 to 65 W, accordingly.

Comparative investigation revealed even higher strength when parts were printed at 50 mm/s with microwave heating as compared to those produced at 5 mm/s by conventional printing [3]. The reason for that was revealed by microstructure analysis, which showed a larger number of voids between layers in case of conventionally printed CCFRP filaments, obviously due to a non-uniform heating.

Another novel approach using SERPENS with CCFRP filaments is the opportunity to overcome the conventional layer-by-layer process and also print into the third dimension. This offers possibilities to print along load transmission paths in three-dimensional space enabling more complex 3D structures like shown in Fig. 1(b) and (c) or advanced bionic 3D structures. The challenge along that way, however, is the need for novel printing path design methods including, digital twins for collision detection and smart sensors for printing path control.

CONCLUSION

A novel approach of microwave-assisted FFF based additive manufacturing has been introduced and the benefits and challenges with printing CCFRP filaments have been discussed. The microwave specific feature of volumetric heating allows a significant increase in printing speed compared to conventional methods. The use CCFRP filaments opens up a completely new field of design opportunities where reinforcing fibers can be printed along load transmission paths in 3-dimensional space. The challenges involved will require highly multidisciplinary future research.

REFERENCES

[1] N. Li, G. Link, and J. Jelonnek, “3D microwave printing temperature control of continuous carbon fiber reinforced composites,” *Composites Science and Technology*, 2020.

[2] N. Li, G. Link, and J. Jelonnek, “Rapid 3D microwave printing of continuous carbon fiber reinforced plastics,” *CIRP Annals*, vol. 69, no 1, pp. 221-224. 2020.

[3] N. Li, G. Link, J. Jelonnek, M.V. Morais, F. Henning, “Microwave additive manufacturing of continuous carbon fibers reinforced thermoplastic composites: Characterization, analysis, and properties,“ *Additive Manufacturing*, vol. 44, 102035, 2021.

SiC_f/SiC Ceramic Matrix Composites Using Microwave Enhanced Chemical Vapor Infiltration

Matt T. Porter[1], Andrea D'Angio[1], Jon Binner[1], Vadim V. Yakovlev[2], and Michael K. Cinibulk[3]

[1] School of Metallurgy and Materials, University of Birmingham, Edgbaston, Birmingham, UK
[2] Department of Mathematical Sciences, Worcester Polytechnic Institute, Worcester, MA, USA
[3] Materials and Manufacturing Directorate, Air Force Research Laboratory, Wright-Patterson Air Force Base, OH, USA

Keywords: ceramic matrix composites, characterization, microwaves

INTRODUCTION

To deliver the next generation of turbofan engines, modifications to the materials systems used in the hot gas path are required. Ceramic fiber reinforced ceramic matrix composites (CMCs) have been identified as candidates to operate in these hostile aero-thermo-chemical environments. Of the advanced methods capable of producing these materials is chemical vapor infiltration (CVI), which involves the thermal decomposition of gaseous precursors to deposit a solid matrix, in this case, SiC. This fills the porosity in a heated porous SiC fiber body by gradually increasing the effective diameter of the fibers to create a dense composite. CVI is not without its challenges, and subsequently use of microwave energy (ME-CVI) has been proposed as a potential method to heat the SiC fibers and initiate the decomposition to shorten the processing time. It produces a favorable inverse temperature profile, created by the volumetric heating of the fibers coupled with surface heat losses [1]. The deposition of SiC starts and proceeds fastest at the center of the sample where temperature is hottest, thus avoiding surface porosity closure, enabling gaseous reactants to continue penetrating the porous body. It is expected that the use of ME-CVI processing routes could yield near fully dense products in the order of weeks rather than months [2, 3].

This paper presents the key results associated with densifying these composites using microwave energy. It outlines the processing parameters used and describes the interplay between kinetics and microstructures of the ceramic produced, more details of which can be found in [4].

METHODOLOGY

Woven SiC fabric sheets (Tyranno ZMI, UBE Industries) were cut into 20x53 mm discs using a wad punch and laid up one disc on top of another and stitched together. A multimodal, 2.45 GHz, 3 kW magnetron generator (SAIREM Labotron HTE M30KB CL

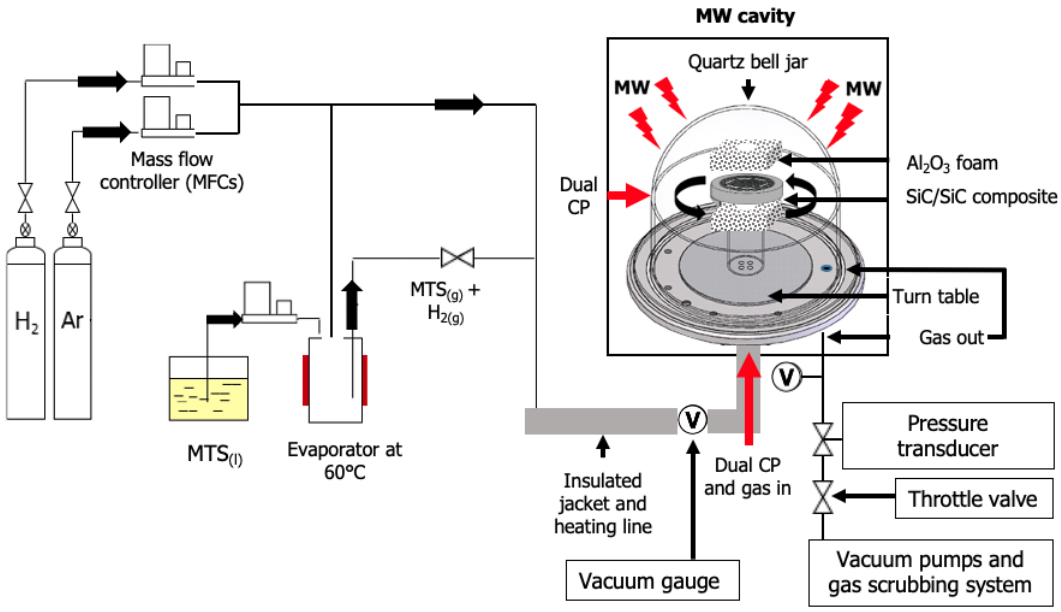

Figure 1. Schematic illustration of the ME-CVI equipment set up showing the various components that delivery the reactant to the microwave chamber, heat the sample and remove the waste by-products.

PRO, France) was connected to an automated reactant gas delivery and vacuum system (Archer Technicoat Limited, UK) which was used to produce the necessary environment for CVI (Fig. 1). Two dual-colour pyrometers (Micro-epsilon, UK) were used to measure the temperature of the SiC and control the power output of the MW. Fabric stacks were infiltrated for 8 hours at a time. Samples were infiltrated at three different temperatures and four different pressures, at a constant reactant ratio of 1:10 ($MTS:H_2$). The respective flow rates were 0.2 g min^{-1}, and 300 cm^3 min^{-1}.

RESULTS

Experiments were carried out to observe the effect of temperature and pressure on the kinetics and densification profile of SiC deposited via ME-CVI. The study found the deposition of SiC showed an Arrhenius relationship between 900-1000°C, as temperature and pressure increased the absolute deposition rate increased, see Fig. 2 (a). The increase in deposition rate with increasing pressure is due to the deposition process being surface reaction-limited. This is favorable in CVI processes as it encourages reactant diffusion into porosity at the lower temperatures and pressures used, but a transition to a mass transfer regime was seen at the higher pressures and temperatures [5]. However, both factors impacted the reproducibility of the process, see [6] for details.

Inverse temperature gradients observed using a thermal imaging camera have translated to inverse densification profiles, as seen in Fig. 2(b), particularly at lower pressures and temperatures. No gradient in deposition thickness was seen with the higher temperatures and pressures tested, this is suspected to be due to the higher temperatures creating a more isothermal preform attributed to SiC high thermal conductivity and higher pressure favoring a mass transfer mechanism of deposition.

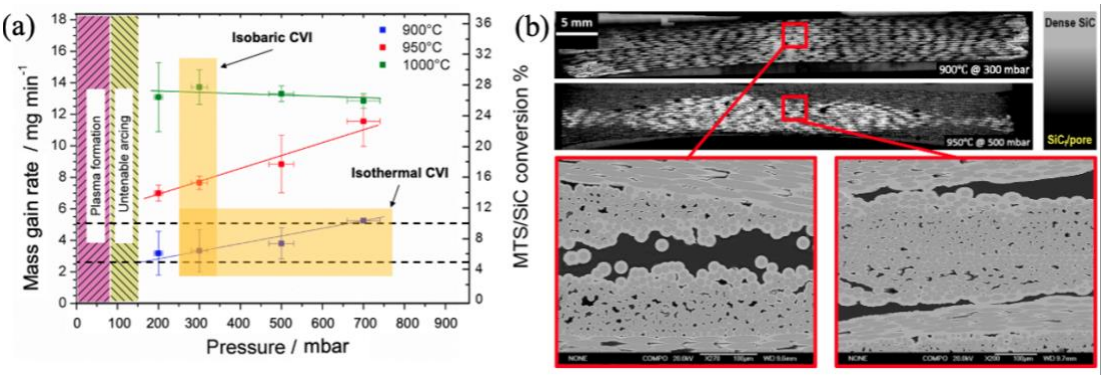

Figure 2. A graph showing the effect of temperature and pressure on the deposition rate of SiC (a), Two optical microscope images showing inverse densification profiles of two SiC_f/SiC composites after 8 h of ME-CVI (b). Two micrographs at the bottom of (b) are magnified images of the centers of the composite and show nearly 5 μm of SiC deposit encasing the fibers [4].

DISCUSSION AND CONCLUSION

With a lack of control over frequency output from the magnetron, achieving repeatability of the process was difficult. This was most noticeably at the higher temperatures and pressure tested and was later identified to be because of the dielectric properties of the material, the size MW cavity and coupling of sample [6].

The use of microwave energy to heat SiC fabric preforms and initiate the deposition of a SiC matrix to increase the density of SiC_f/SiC composites has been demonstrated. Results have shown that there are upper and lower bounds for both temperature and pressure to obtain suitable deposition profiles and rates. It is predicted that a processing temperature of approximately 950°C with an increasing processing pressure, starting at 300 mbar and increasing relative to the progress of densification should be used to obtain a suitable densification profile in the least amount of time.

REFERENCES

[1] J. Binner, M. Porter, B. Baker, J.J. Zou, V. Venkatachalam, V.R. Diaz, A. D'Angio, P. Ramanujam, T. Zhang, and T.S.R.C. Murthy, Selection, processing, properties and applications of ultra-high temperature ceramic matrix composites, UHTCMCs – a review, *Int. Mater. Rev.*, vol. 65, no 7, pp. 389-444, 2020.

[2] D. Jaglin, J. Binner, B. Vaidhyanathan, C. Prentice, B. Shatwell, and D. Grant, Microwave heated chemical vapor infiltration: Densification mechanism of SiCf/SiC composites, *J. Am. Ceram. Soc.*, vol. 89, no 9, pp. 2710–2717, 2006.

[3] L.A. Timms, W. Westby, C. Prentice, D. Jaglin, R.A. Shatwell, and J. Binner, Reducing chemical vapour infiltration time for ceramic matrix composites, *J. Microsc.*, vol. 201, no 2, pp. 316-323, 2001.

[4] M. Porter, *High-Temperature Ceramic Matrix Composites Prepared via Microwave Energy Enhanced Chemical Vapour Infiltration*, Ph.D. Thesis, University of Birmingham, 2020.

[5] R. Naslain, F. Langlais, and R. Fedou, The CVI-Processing of Ceramic Matrix Composites, *Journal de Physique Colloques*, vol. 50, no C5, pp.191-207, 1989.

[6] M. Porter, J. Binner, P. Kumi, K. Stern, and V.V. Yakovlev, Computational characterization of microwave-enhanced CVI production of SiC_f/SiC composites, *Proc. 18th AMPERE Conference on Microwave and High Frequency Heating (Virtual, September 2021)*, pp. 48-55, 10.5281/zenodo.5716071.

NETL's Microwave-Material Interaction Studies

Christina Wildfire[1], Dushyant Shekhawat [1], Candice Ellison [2] , Pranjali Muley [2], Biswanath Dutta [2]

[1]National Energy Technology Laboratory, DOE, Morgantown, WV
[2]NETL Research Support Contractor, Morgantown, WV

Keywords: catalyst design, microwave catalysis, microwave scaling

INTRODUCTION

The addition of microwaves to various chemical and material processes has recently received an increasing amount of interest in energy-related applications, including enhanced catalytic conversion of hydrocarbon resources. It is well known that variables such as frequency, power, and catalyst composition have significant effects on microwave chemistry [1-3]. What is less known are the nuances of the material properties and their interactions with the microwave field. Due to the complex nature of catalyst systems, an in-depth study is needed on the various interactions these materials have with a microwave field. Researchers at NETL are pursuing several parallel lines of study to characterize and measure these microwave-material interactions as well as looking ahead to the scaling of these chemical processes more fully.

METHODOLOGY

NETL is using catalysis to determine how particle geometry and spacing of the microwave-active materials affect dielectric properties, heating rates, and plasma generation on both a micro- and macro-scale. These studies are also looking at how the surface oxidation state and absorbed chemical species of the material changes its ability to react with the microwave field. The lab is developing a one-of-a kind characterization facility to study these surface effects in-situ so that modeling of the materials can be improved and used in material and microwave cavity designs. The new facilities will include high temperature dielectric testing, MW-Coupled FTIR and Raman.

DISCUSSION

Through NETL's catalysis work, we have seen the importance of designing catalyst specifically for their interaction with a microwave field. Scaling of the catalyst beyond benchtop, testing is also important when considering whether to pelletize, coat, or support your catalyst. This industrialization of the catalyst must also coincide with the reactor design. When developing research projects, NETL now works parallel paths of designing the materials and anticipating scale-up using COMSOL to look at particle and microwave

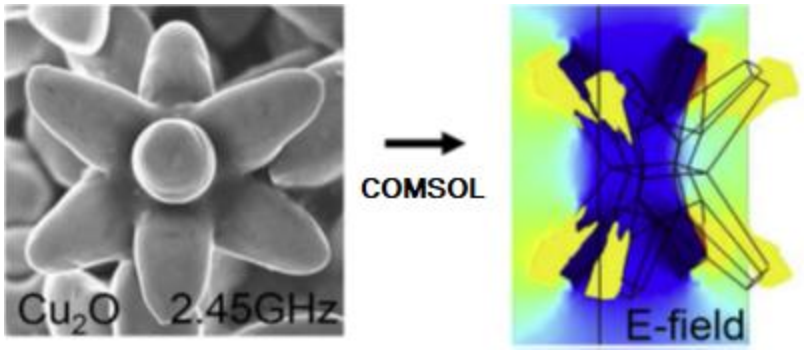

(a) (b)

Figure 1. Study of active particle geometry on microwave absorption: synthesized Cu_2O particle (a) and particle in electric field modeled in COMSOL [4] (b).

cavity designs. For scale-up to happen, the fundamentals and kinetics of the reactions must be known. This is an area in microwave catalysis that is lacking in literature due to the absence of characterization equipment paired with electromagnetic fields. NETL is focused on building out these characterization needs so that the advantages of using microwaves in chemical reactions can be better understood and used for the development of catalysts and microwave systems.

CONCLUSION

This work will be important for future understanding of the performance mechanisms of our microwave-active catalysts and will also provide additional insight about the phenomenon observed with catalyst in a microwave field. This growing body of knowledge on the microwave-material interactions will be used to optimize both the materials and chemical process for future catalyst design and development.

REFERENCES

[1] C. Wildfire, V. Abdelsayed, D. Shekhawat, and M.J. Spencer, "Ambient pressure synthesis of ammonia using a microwave reactor," *Catalysis Communications*, vol. 115, pp. 64-67, 2018.

[2] Y. Wang, C. Wildfire, T.S. Khan, D. Shekhawat, J. Hu, P. Tavadze, R. Quiñones-Fernández, and S. Moreno, "Effects of support and promoter on Ru catalyst activity in microwave-assisted ammonia synthesis," *Chemical Engineering Journal*, vol. 425, 130546, 2021.

[3] J. Hu, C. Wildfire, A. Stiegman, R. Daglec, D. Shekhawat, V. Abdelsayed, X. Bai, H. Tian, M. B. Bogle, C. Hsu, Y. Luo, S.D. Davidson, and Y. Wang, "Microwave-driven heterogeneous catalysis for activation of dinitrogen to ammonia under atmospheric pressure," *Chemical Engineering Journal,* vol. 397, 125388, 2020.

[4] T.D. Musho, C. Wildfire, N. M. Houlihan, E.M. Sabolsky, and D. Shekhawat, "Study of Cu_2O particle morphology on microwave field enhancement," *Materials Chemistry and Physics*, vol. 216, pp. 278-284, 2018.

Multiphysics Simulation of Flash Microwave Heating and Sintering

Charles Maniere[1], Geuntak Lee[2,3], Shirley Chan[2], Elisa Torresant[2], Vadim V. Yakovlev[4], John F. Gerling[5], Eugene A. Olevsky[2,3], Guillaume Riquet[1], and Sylvain Marine[1]

[1]CRISMAT, CNRS, ENSICAEN, UNICAEN, Normandie Univ, Caen, France
[2]Powder Technology Laboratory, Department of Mechanical Engineering, San Diego State University, San Diego, CA, USA
[3]Department of NanoEngineering, University of California, San Diego, La Jolla, CA, USA
[4]Department of Mathematical Sciences, Worcester Polytechnic Institute, Worcester, MA, USA
[5]Gerling Consulting, Inc., Modesto, CA, USA

Keywords: flash sintering, heating, microwave sintering, multiphysics simulations

ABSTRACT

Microwave flash sintering requires ultra-rapid heating of a ceramic powder involving heating rate near 1000 K/min and reaching sintering temperatures of about 1500°C. Controlling such process requires addressing an electromagnetic-thermal (EMT) problem where the microwave cavity resonance profile need to be adapted to the dielectric evolution of all heated parts and to the thermal runaway profile of zirconia (having a Negative Temperature Coefficient (NTC) electrical resistivity) [1]. The Multiphysics numerical tool is of particular interest to detect the inherent cavity resonance profile, determine the heat transfers by conduction/convection/radiation at the interfaces [2] and to simulate the heating stability of hybrid heating configurations in flash heating conditions [3]. The paper presents the construction of the model and then a different case study of flash microwave sintering from direct heating [1] to complex hybrid heating configurations using multiple-material susceptors obtained by 3D printing.

REFERENCES

[1] C. Manière, G. Lee, E. Torresani, J.F. Gerling, V.V. Yakovlev, D. Martin, and E.A. Olevsky, "Flash microwave pressing of zirconia," *J. Am. Ceram. Soc*., vol. 103, pp. 4110–4121, 2020.
[2] C. Manière, F. Borie, and S. Marinel, "Impact of convection and radiation on direct/hybrid heating stability of field assisted sintering," *J. Manuf. Process*., vol. 56, pp. 147–157, 2020.
[3] S. Marinel, C. Manière, A. Bilot, C. B"ilot, C. Harnois, G. Riquet, F. Valdivieso, C. Meunier, C. Coureau, and F. Barthélemy, "Microwave sintering of alumina at 915 MHz: modeling, process control, and microstructure distribution," *Materials,* vol. 12, 2544, 2019.

FDTD Modeling of Industrial Microwave Power Applicators

Bartlomiej W. Salski[1] and Marzena Olszewska-Placha[2]

[1]Warsaw University of Technology, Warsaw, Poland
[2]QWED Sp. z o.o., Warsaw, Poland

Keywords: asphalt, electromagnetic modeling, FDTD method, recycling, thermodynamic, waste tire

ABSTRACT

Practical aspects of computer modeling of microwave power applicators operating at 2450 MHz with the aid of a finite-difference time-domain (FDTD) [1] is addressed. Two particular systems dedicated to microwave treatment of asphalt pavements [2] and to the recycling of waste tire [3], designed with the *QuickWave* software [4], are discussed. It is shown that a typical design of a microwave high-power applicator consists of two major steps related to microwave heating of a load and to impedance matching of a source. Regarding the first step, it is often recommended to undertake a coupled electromagnetic-thermodynamic simulation to make sure that the geometry of the applicator allows efficiently deliver and evenly distribute electromagnetic (EM) energy in the load. In case of impedance matching, it can be undertaken using EM modeling only, usually of a waveguide section where appropriate stub tuners are in the vicinity of each microwave power source.

The applicator for on-site microwave treatment of asphalt pavements has been designed as a semi-open system, which can deliver EM energy directly to the pavement, while slowly moving along a technological longitudinal joint to be bonded (see Fig. 1). Consequently, the whole system must be supplied with a dedicated choke preventing hazardous leakage of microwave radiation beyond an exposure area and a microwave radiation control unit that turns off the system whenever exposure limits imposed by international regulations related to nonionizing radiation are exceeded. It is shown that a complete design cycle of the mobile microwave applicator, accounting for power budget analysis, coupled EM-thermodynamic modeling, microwave characterization of selected bituminous mixtures, control of the exposure to microwave radiation, and heating rates measurements, allows reaching optimum in microwave heating efficiency. Fig. 2 shows the distribution of temperature in a bituminous surface calculated with *QuickWave-BHM*, accounting for both heat dissipation and conduction during 15 min of heating with a 1 kW source. It can be observed that the microwave power is mostly dissipated in a few top centimeters of the pavement. More details can be found in [2].

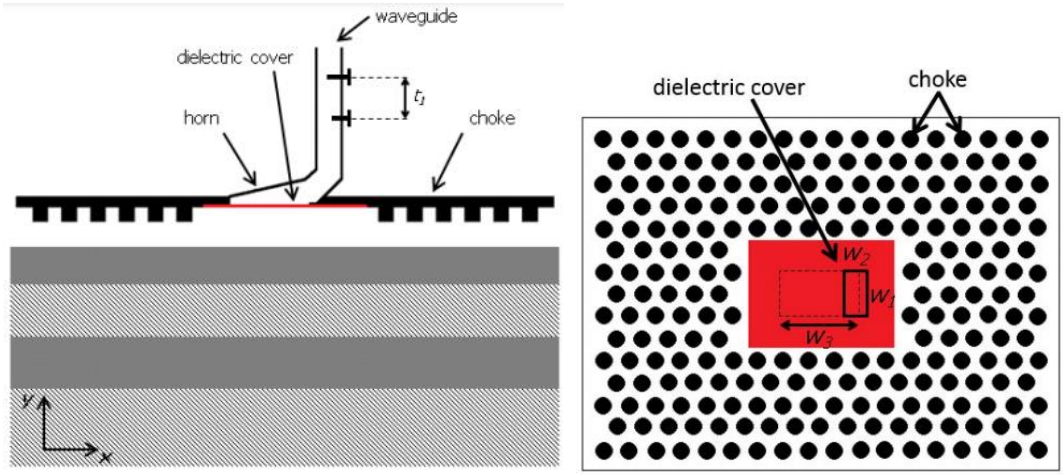

(a) (b)

Figure 1. Side (a) and bottom views (b) of a microwave applicator for thermal treatment of asphalt pavements (after [2]).

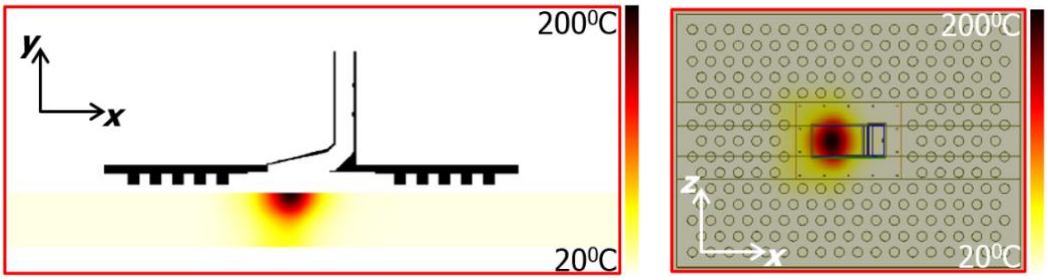

(a) (b)

Figure 2. Distribution of temperature in the pavement computed with *QuickWave-BHM* after 15 min of heating with the source having 1 kW of the mean available power shown in horizontal (a) and vertical cross sections (b) (after [2]).

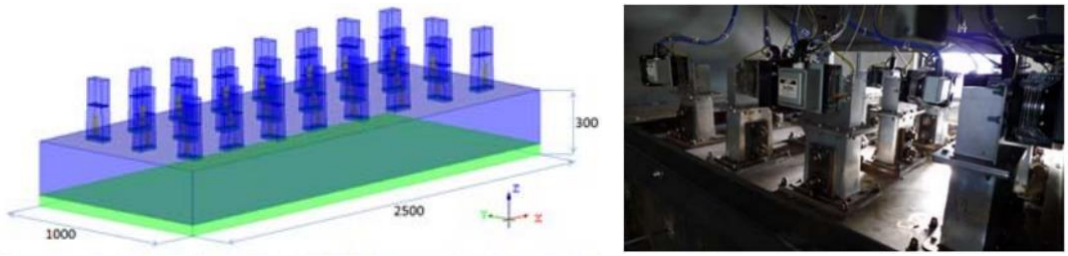

(a) (b)

Figure 3. An electromagnetic model of a single section of a microwave applicator (a) and the photo of a microwave feeding system (b) (after [3]).

Figure 4. Rectangular resonator with an asphalt sample completely filling the cavity (after [2]).

A different approach has been applied in the system for microwave recycling of waste tires, where a microwave power level had to reach 50 kW to reach 200 kg per hour of a load throughput (see Fig. 3). For that reason, a semi-closed continuous conveyor has been exploited with a power feeding system composed into a pattern of 45 magnetrons distributed along the conveyor. It is shown that in such a system much more attention must be paid to impedance matching and to the unwanted coupling between magnetrons, which may damage sources. For that purpose, at a final stage of impedance matching, a dedicated computation regime for calculating reflection coefficients at all sources operating simultaneously, shall be used.

It is essential to notice that accurate computer modeling of high-power applicators requires acquiring knowledge on dielectric properties of major components of a load to be heated. For that reason, resonant methods applicable to the complex permittivity measurement were applied, like the one shown in Fig. 4. According to [2], dielectric constant of typical asphalt samples is ca. 6-7, whereas the loss tangent can vary from $5x10^{-3}$ up to $5x10^{-2}$ depending mostly on the type of stones applied in the mixture.

REFERENCES

[1] A. Taflove and S. Hagness, *Computational Electromagnetics: The Finite Difference Time-Domain Method,* 3rd Edition, Artech House, 2005.

[2] B. Salski, M. Olszewska-Placha, T. Karpisz, J. Rudnicki, W. Gwarek, M. Maliszewski, A. Zofka, and J. Skulski, "Microwave applicator for thermal treatment of bituminous surfaces," *IEEE Trans. on Microwave Theory and Tech.*, vol. 65, no. 9, pp. 3419-3427, 2017.

[3] B. Salski and M. Przygodzki, "A low-cost high-power applicator for microwave recycling of waste tires," *2013 IEEE MTT-S Intern. Symp.,* Seattle, WA, June 2013.

[4] *QuickWave*, QWED Sp. z o. o., 1998-2021, www.qwed.eu.

Experimental and Computational Study of Microwave Heating in Single-Stream Waste Processing

Megan C. Robinson[1], Vadim V. Yakovlev[2], and Zoya Popović[1]

[1] Department of Electrical, Computer and Energy Engineering, University of Colorado, Boulder, CO, USA

[2]Department of Mathematical Sciences, Worcester Polytechnic Institute, Worcester, MA, USA

Keywords: power combining, solid-state power amplifiers, temperature, waste breakdown

INTRODUCTION

Microwave heating of waste results in breakdown that can lead to conversion of waste to fuel [1]. Heating waste mixtures with microwave energy rather than incineration results in faster breakdown and can therefore be more efficient [2]. In this paper, we compare experimental and modeling results obtained for the heating rates of microwave processing of waste within a 1.4 L metal cavity. Three common waste materials with widely differing temperature-dependent electromagnetic and thermal material parameters are considered. As uniform heating is desired for chemical processing, spatial power combining is analyzed by comparing single and double solid-state excitation. We show that the heating efficacy is improved by volumetric combining inside the waste loading.

METHODOLOGY

The key goal of this work is to evaluate to what extent simulation tools with material properties found in the open literature can be used to model and predict heating and improve reactor design. We present a loaded cavity heating comparison of two circuit-combined and spatially combined 2.45-GHz 70-W efficient GaN solid-state power amplifiers (SSPAs) with controlled relative phase. EM and thermal parameters of several common materials are summarized in [3] and relevant properties given in Table 1.

The set up for both measurement and simulation is described in Fig. 1, with single port and two port excitations shown. The cavity size is chosen so that two 70-W sources at 2.45-GHz can deposit power throughout the volume for all three loadings. *QuickWave* [4] was used to simulate the microwave heating in the cavity filled with the three loadings characterized by temperature dependent material parameters.

RESULTS

The single-port excitation results are shown in Fig. 2. All loadings show higher simulated heating than measured. The hot spots are predicted in the simulation and line up with measurements for the higher permittivity materials. Since the reflection coefficient at the excitation ports changes with heating, the delivered power is kept constant in both simulations and measurements.

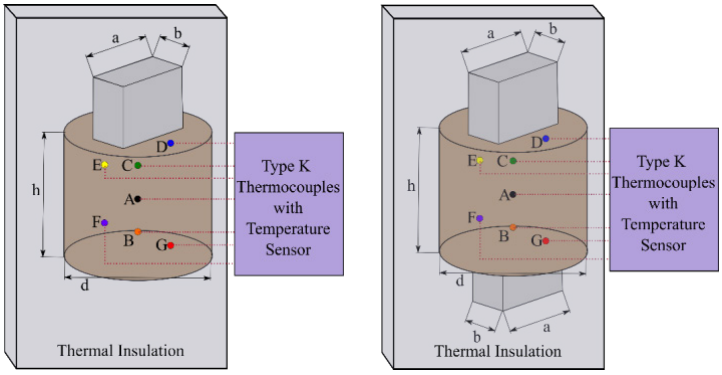

Figure 1. Geometry of the S-band waveguide probes and loaded cavity, with d = 12.5cm, h = 11.2cm, a = 7.2cm, b = 3.6cm. Seven temperature sensors are at fixed positions A through G for all experiments. Single waveguide excitation (a); two waveguide probes used to excite electromagnetic fields in the cavity (b).

Table 1. Range of Material Parameters for the Three Investigated Materials

Material	ε_r	σ (S/m)	c (J/g °C)	ρ (g/mL)	K (mW/cm°C)
Paper (25-90° C)	2.3-2.7	0.025-.033	1.36	0.105	0.51-0.57
Bread (25-85° C)	3.1-4.1	0.05-0.1	2.47	0.19	0.95-2.8
Meat (15-65° C)	48.5-51.7	2.1-2.4	3.32	1.0	3.9-5.7

Fig. 3 shows the simulated and measured results for the dual excitation case. Heating appears more linear in simulation than measurement for the bread loading indicating some temperature effect is not being modeled realistically. This is potentially related to the PA circuit heating, or additional changes in impedance match. Asymmetry in the measured temperatures at points B and C indicate that probe placement and power at the two probes may be different.

DISCUSSION

Simulations adequately predict trends in temperature distribution; however, the delivered power and reflection coefficient differs in experiments. Lack of available data for material parameters depending on temperature is reflected in Table 1. This limits the simulation accuracy since the temperature-dependent properties are required at all points. The hottest regions contribute to the disagreement between simulated and measured heating duration.

CONCLUSION

Multiphysics simulations are in general agreement with experiments for single and dual port heating of single-stream waste in a solid-state excited microwave cavity. Notable disagreement of simulated and measured temperatures is explained by inadequacy of the literature data on the material parameters to the substances in the experiment. Measurement of the properties of the material in the experiment is preferable. The next step is an investigation of effects of material parameter variations.

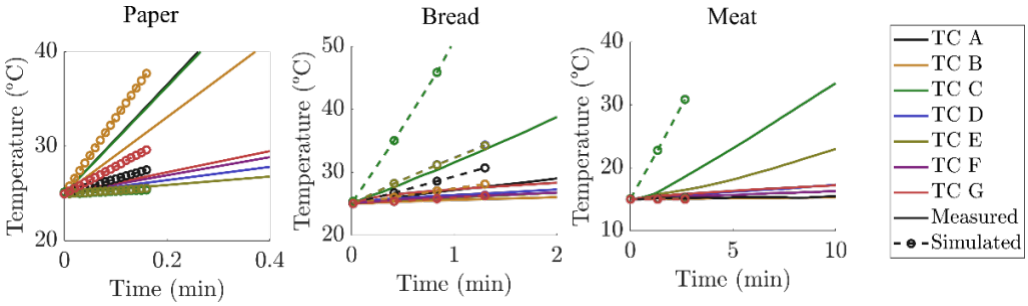

Figure 2. Measured and simulated temperature increase at seven temperature sensor locations (A to G); paper, bread, and meat loadings of the cavity with a single feed for 70 W of delivered power; the symbols show results from multiphysics simulations of heating rates at the thermocouple locations; right to left: paper, bread, and meat (hotdog) loadings.

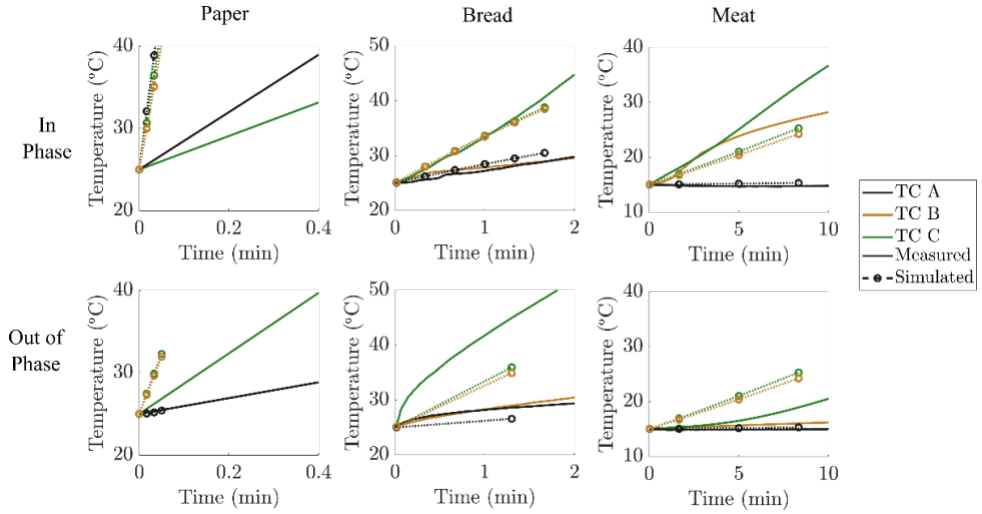

Figure 3. Measured and simulated temperature increase at three temperature sensor locations (A, B, & C) for paper, bread, and meat loadings of the cavity with two feeds for 70 W of delivered power; the symbols show results from multi-physics simulations of heating rates at the thermocouple locations; right to left: paper, bread, and meat (hotdog) loadings.

REFERENCES

[1] A. Sarkar and R. Chowdhury, "Co-pyrolysis of paper waste and mustard press cake in a semi-batch pyrolyzer optimization and bio-oil characterization," *Intern. Journal Green Energy*, vol. 13, no. 4, p. 373–382, 2014.

[2] Y. Fernandez, A. Arenillas, and J. Angel, "Microwave heating applied to pyrolysis," In: *Advances in Induction and Microwave Heating of Mineral and Organic Materials*, IntechOpen, London, U.K., 2011, doi: 10.5772/562.

[3] M.C. Robinson, V.V. Yakovlev, and Z. Popovic, "Circuit and spatial solid-state power combining for microwave waste mixture breakdown," *IEEE Microwave Theory and Tech.*, submitted.

[4] *QuickWave*, QWED Sp. z o. o., 1998-2022, http://www.qwed.eu.

Field Studies in Microwave Cavities: Magnetron vs. Solid-State RF Generator

Xu Zhou and Juming Tang

Washington State University, Pullman, WA, USA

Keywords: frequency spectrum, heating pattern, resonant cavity, simulations

INTRODUCTION

The first microwave oven was invented in 1945 and now microwave ovens are popular worldwide [1]. But a major drawback of magnetron-based microwaves is random and unpredicted frequency shift of magnetrons. Even a small frequency shift may lead to a totally different resonant mode. Therefore, magnetron-based microwaves oven are generally multi-mode cavities [1]. Semiconductor-based RF generators have been increasingly used in microwave ovens. Solid-state RF generators can provide microwaves with more accurate control in the power, frequency, phase. However, few studies paid attention to the filed distribution and energy coupling of the domestic microwave oven affected by frequency or frequency shifting.

Therefore, the objectives of this study were to (1) compare frequency spectrums of magnetron-based and solid-state RF-based microwave ovens, and to (2) study the effect of frequency on filed patterns and energy coupling of both magnetron- and solid-state RF-based microwave oven.

METHODOLOGY

The dual-frequency microwave oven consists of a heating cavity, two microwave sources and a control system (Fig. 1). A 2.45 GHz magnetron was initially mounted underneath the bottom cavity wall. A GaN amplifier based 5.8 GHz solid-state microwave generator (RIU58800-20, RFHIC Co., Anyang, South Korea) was connected to the cavity on the left side through a WR 159 rectangular waveguide. A portable frequency spectrum analyzer (SPA-6G) and an antenna (Nagoya NA773) were used to capture real frequency spectrum of leakage microwaves.

A model food made of whey protein gel (WPG) was used to obtain the heating pattern. The model food was packaged into a standard 10.5 oz tray (171 mm × 129 mm × 25.7 mm). After 2 min microwave heating, the model food was taken out of the oven and a thermal camera was used to get the temperature profiles of the model food.

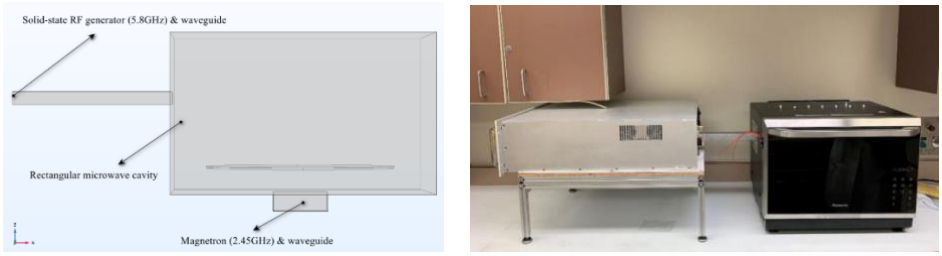

Figure 1. A dual-frequency domestic microwave oven

RESULTS AND DISCUSSION

Three loads with different dielectric properties were placed in the center of the microwave oven to determine the effects of loads on frequency spectrums. The results show that the frequency spectrum of magnetron-based microwave oven changed with the load, whereas the frequency spectrum of the solid-state based oven did not change with the loads (Fig. 2). Table 1 show the possible modes for an empty microwave cavity when the frequency range is around 2.45 GHz. Due to the frequency shift of the magnetron (Fig. 2), a magnetron-based microwave cavity would have several different modes. In contrast, the solid-state RF based microwave cavity operates at a very narrow frequency bandwidth, as shown in Fig. 2. For example, 99% of power was in the frequency range of 5.798~5.801 GHz for a water load. As a result, there is only one TE mode in the solid-state driven microwave oven. It is interesting to note that with the solid-state generator, domestic microwave oven could be a single mode cavity.

Fig. 3 shows the thermal images of model foods after they were heated for 2 min in a solid-state based microwave oven. As compared to 5800 MHz, microwaves at 5850 MHz led to more hot spot spots (more red areas) and less cold spot spots. In other words, at 5800 MHz, food absorbed less microwave energy. It maybe because 5800 MHz was farther away from the resonant frequency than 5850 MHz. It can be concluded that if the solid-state RF generator is not operating at exactly (or close to) resonant frequency of loaded cavity, there would be a energy mis-matching issue. In addition, at either of two fixed frequencies, the heating uniformity was not satisfactory. But by applying manual frequency sweeping (that is ~ use different frequencies (5800, 5825, 5850, 5875 MHz) at different time periods), the heating uniformity was greatly improved (Fig. 3). It was because frequency sweeping can generate several modes (or electric fields) inside the cavity. Such mode variations can lead to the shift of cold and hot spots in foods and avoid thermal runaway.

CONCLUSION

A magnetron-based microwave cavity can have multiple resonant modes due to the relatively wider frequency range of magnetrons. And the frequency spectrum of magnetrons is sensitive to loads. In contrast, the solid-state RF generator has a very narrow operating frequency bandwidth, and it did not change with loads. In such narrow frequency

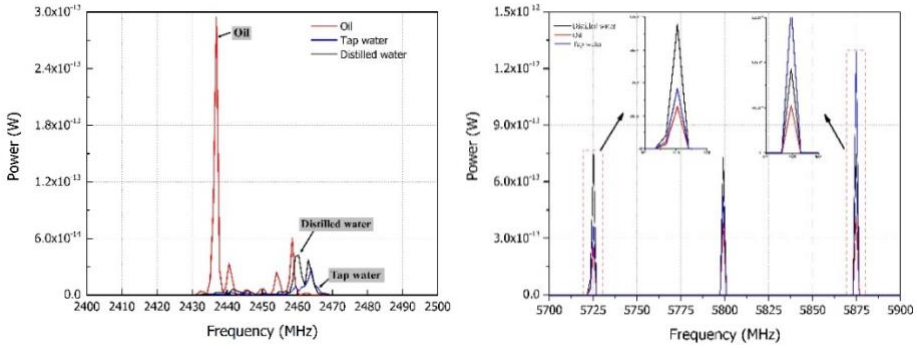

(a) (b)

Figure 2. Frequency spectrums of the magnetron-based (a) and solid-state RF based cavity (b) with different loads (1-L oil, distilled water and tap water at the same location).

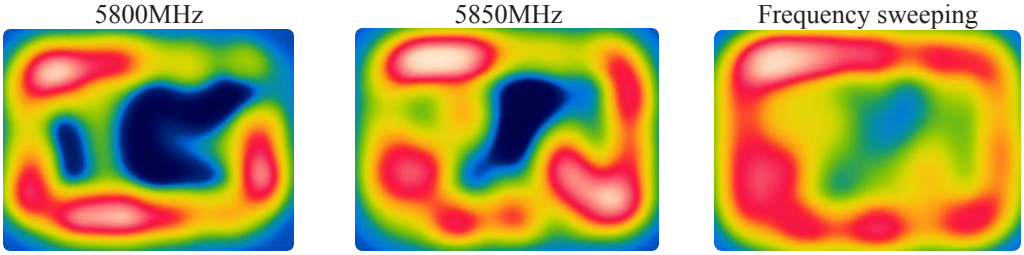

Fig. 3 Thermal images of model foods at different microwave frequencies.

Table1. Possible modes for an empty microwave cavity (*f*~[2.4GHz-2.5GHz])

m	*n*	*p*	*f*_cal (GHz)
2	3	3	2.3969
0	5	1	2.4177
1	0	4	2.4261
0	1	4	2.4437
1	5	1	2.4452
4	4	1	2.4513
6	2	1	2.4595
1	1	4	2.4709
3	4	2	2.4803

range, there may be only one mode in an empty cavity. Therefore, the solid-state RF based microwave cavity can be a single mode cavity and thus have a stable standing wave pattern. However, single-mode solid-state RF based domestic oven could have issues of mis-matching and non-uniform heating.

REFERENCES

[1] J. M. Tang, "Unlocking potentials of microwaves for food safety and quality," *Journal of Food Science,* vol. 80, no. 8, pp. E1776-E1793, 2015.

On the Multiphysics Modelling of Chemical Processes with Solid-State Driven Microwave Systems

Pablo Santón[1], Elías De los Reyes[1], Ruth De los Reyes[2], J. Vicente Balbastre[1], and José Vicente Ros[3]

[1]Institute of Information and Communication Technologies (ITACA) - UPV, Valencia, Spain
[2]Microbiotech S.L., Vilamarxant, Spain
[3]Department of Inorganic Chemistry - UV, Valencia, Spain

Keywords: calcination, chemical reactions, microwave oven, multiphysics modelling, synthesis

INTRODUCTION

There is a broad interest in synthesising mesoporous materials, i.e., inert materials with medium size porous [1, 2]. It is useful, for instance, in absorption processes, catalysis, photocatalysis, ionic exchange, petrochemistry, or gasses absorption. After the synthesis process, these materials need to be calcinated to remove the templating agent used for the porous creation and other organic materials that might be absorbed in the solid surface during the process. In the Valencian university environment, the three groups signing this abstract have been working collaboratively, developing different solutions to speed up chemical processes, such as the mentioned, with the help of microwave technology [3]. Recent developments in solid-state transistors, including cost reduction, have arisen the interest of this field of expertise. Fine frequency tuning with a high-quality spectrum, variable output power with constant values, electronic phase control, low voltages and expanded lifetime are some of the advantages of this technology. Using solid-state microwave generators is critical to lab chemical research, where precise control is mandatory.

METHODOLOGY

Given that the dried powder material doesn't absorb microwave until it has been calcinated, a new procedure based on the microwave heating of a multi-layer set of ceramic materials has been developed (see Fig. 1(b)). Each layer has a specific purpose being the most interesting, the susceptor one, made of a new material called MBT01 [4]. The modelling of these processes provides both the microwave device manufacturer and the chemical researchers the opportunity to design, test, and improve the system's specs without needing to build it only based on theoretical calculations. It also allows uniting both fields of expertise into the same language that ensures a good agreement between the original design

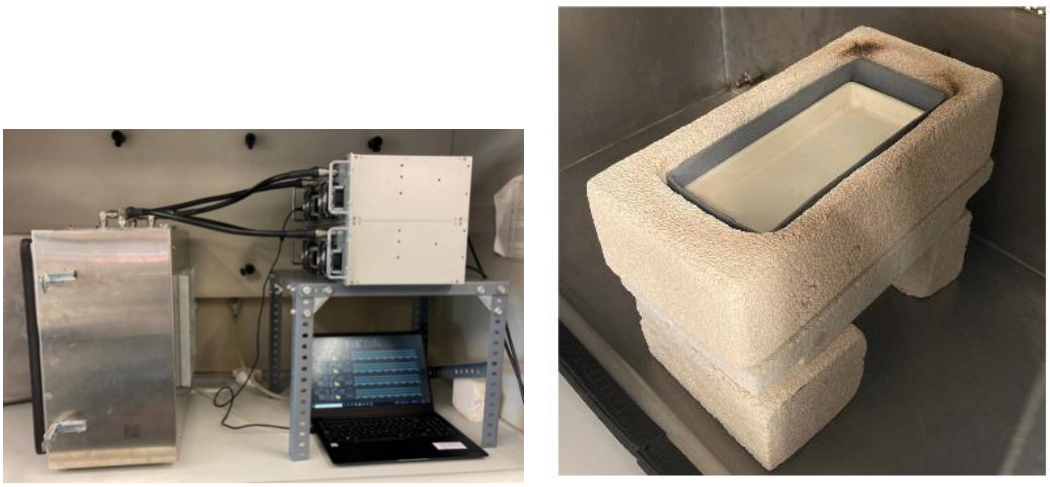

(a) (b)

Figure 1. Lateral view of the solid-state driven microwave system developed by Microbiotech S.L. [3] (a) and multilayer ceramic system for microwave-assisted calcination [3] (b).

and the implementation. Although mixing two or more physics might be complicated from a theoretical point of view, multiphysics software lightens this work.

This work has been done using COMSOL Multiphysics with two physics involved: (1) Electromagnetic Waves, Frequency Domain and (2) Heat Transfer in Solids; and the multiphysics interface is Microwave Heating. The study has been performed with a single step Frequency Transient where, for each time step, the electromagnetic waves are recalculated according to the temperature evolution. It is, therefore, a two-way multiphysics modelling.

The calcination procedure is usually done at 550º C in a muffle furnace for 5 h. With this technology, the process used to be done at night to ensure smooth heating/cooling rates. To speed up this process, solid-state microwave ovens can be an excellent solution to it. COMSOL Multiphysics modelling software has been used to optimize each final system component (Fig. 1(a)) and define the best power and operating time (see Fig. 1(b)).

RESULTS

Due to the small quantity of material, and its properties, a small amount of power is needed to obtain good results, in this case, 200 W. It is essential to state that using microwaves for this application wouldn't be an option if there weren't solid-state devices available to have fine control (manual or automatic) over the power, given that magnetrons usually give nominal power or non. Moreover, these devices allow changing the phase and the frequency too.

In Fig. 3(a) can be seen an example of the modeled thermal distribution in the MBT01-made recipient.

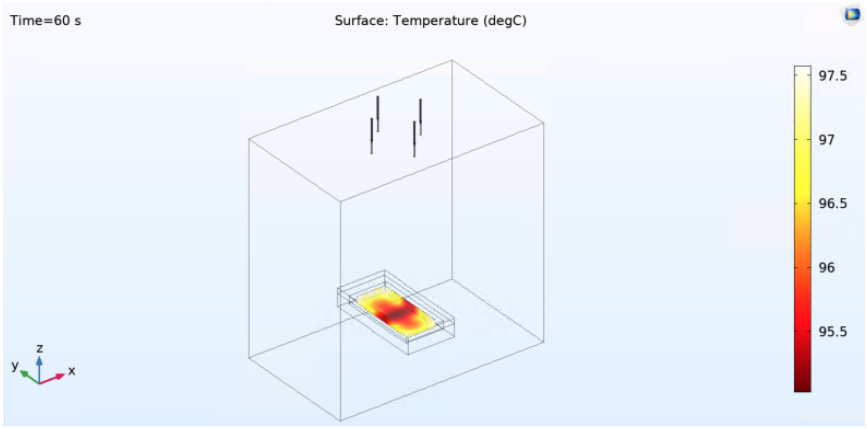

Figure 2. COMSOL Multiphysics modelling of the calcination structure in a multi-source solid-state driven microwave oven.

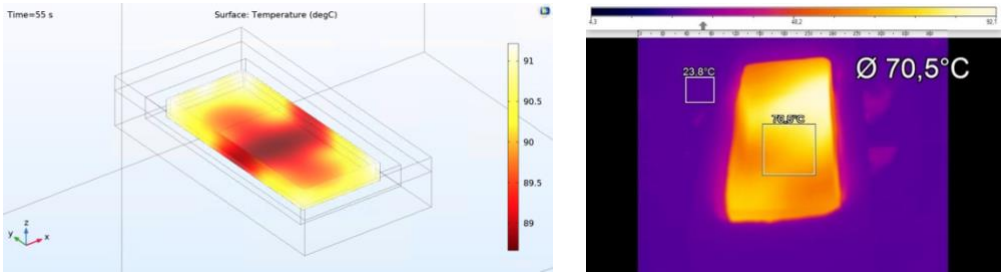

(a) (b)

Figure 3. Details of the heat pattern in the porcelain recipient after 55 s (a) and radiation pattern captured with an infrared camera after 1 min (b).

CONCLUSION

The modelling results showed a good agreement between the maximum temperatures reached (around 92 ºC). Uniformity aspects and heat patterns can be adjusted by using the frequency and phase change; the same is done in the system installed at the chemical labs (Fig. 3(b)). This is important and useful to improve the procedure by obtaining a faster but high-quality calcination method.

REFERENCES

[1] S. Cabrera, J. El Haskouri, C. Guillem, J. Latorre, A. Beltran-Porter, D. Beltran-Porter, M.D. Marcos, and P. Amoros, "Generalised syntheses of ordered mesoporous oxides: the atrane route," *Solid State Sci*., vol. 2, no. 4, pp. 405–420, 2000.

[2] J. El Haskouri J. El Haskouri, D.O. de Zárate, C. Guillem, J. Latorre, M. Caldés, A. Beltrán, D. Beltrán, A.B. Descalzo, G. Rodríguez-López, R. Martínez-Máñez, M. Dolores Marcos, and P. Amorós, "Silica-based powders and monoliths with bimodal pore systems," *Chem. Commun*., vol. 2, no. 4, pp. 330–331, 2002.

[3] L. Montes, "Resultados – ValoraSiO," January 2022, www.valorasio.blogs.uv.es.

[4] J. F. Fernandez, E. De los Reyes, R. De los Reyes, J. García, E. Vela, and A. Jara, "Célula calefactora," 2014.

AI-based Prediction of Microwave Effects on Ore Preconditioning and Breakage

Khashayar Teimoori[1,2], Brent Hilscher[1], Candice Ellison[3,4], and Dushyant Shekhawat[3]

[1]ABH Engineering Inc., Surrey, BC, Canada
[2]Department of Mining and Materials Engineering, McGill University, Montreal, QC, Canada
[3]National Energy Technology Laboratory, Morgantown, WV, USA
[4]NETL Research Support Contractor, Morgantown, WV, USA

Keywords: AI in mining, energy efficiency, microwave heating, numerical modeling, ore-microwave interaction

INTRODUCTION

To advance global leadership in mining, the industry needs to develop continuous, automated, efficient, and environmentally friendly techniques for mineral extraction and processing. One of the potential technologies that can make the downstream processes (i.e., comminution, milling, crushing, etc.) faster and automated is microwave-assisted ore preconditioning and breakage [1, 2]. With this technology, microwaves precondition ore minerals based on selective heating and as a result, energy is not wasted. The application of microwaves on preconditioning and breakage of ore minerals and the influences of microwaves with different operating parameters (e.g., power level, frequency, and exposure time) on various rock types and minerals has been investigated by numerous experimental studies. Computer simulations assist researchers with the prediction of microwave effects on ores by utilizing the numerical modelling approach, which advances the technology one step closer to real practical implementations. This study employs machine learning algorithms to predict the effects of microwave ports' variations (i.e. number and location of ports) on absorbed microwave energy by ore minerals based on the numerical model data. Artificial Intelligence technology in the form of machine learning (ML) has become more prevalent and impactful in the rapidly changing commercial fields like mineral processing and has demonstrated use in microwave applications [3]. Therefore, it is anticipated that the coupling of the numerical modeling approach and ML algorithms will improve prediction of microwave effects for an efficient and energy-saving microwave cavity design in practical applications. The present study opens a new horizon in the field of microwave-assisted ore preconditioning and breakage by employing Artificial Intelligence for the first time.

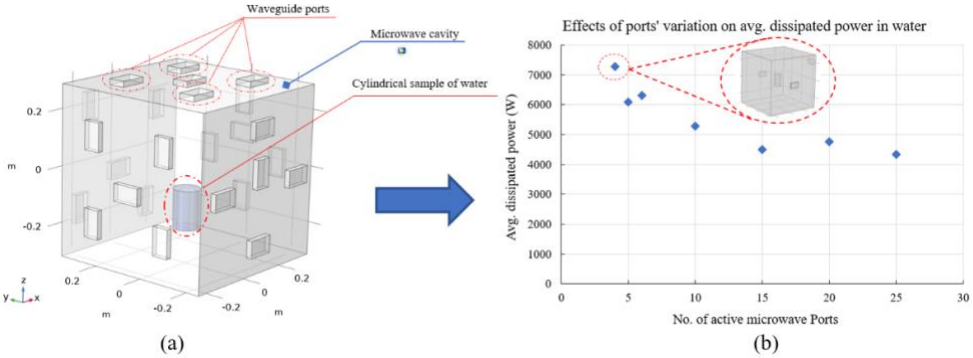

Figure 1. Schematic of the 3D numerical model of a multi-mode microwave cavity with several waveguide ports and a cylindrical sample (a), and the effects of variation in number of ports on average dissipated power in water after 0.5 s treatment at 10 kW overall power (b).

METHODOLOGY

A 3D model of an applicator for microwave-assisted ore preconditioning and breakage was numerically modeled using COMSOL Multiphysics software. The microwave model's size and shape follow the specification of a real lab-scale microwave system (Fig. 1(a)), which was validated experimentally with water [4]. The number and positioning of waveguide ports were varied and the absorbed power in a water sample was evaluated. The overall microwave power level was kept constant at 10 kW for all the models and the average dissipated power in water (after treatment for 0.5 s) was considered and compared to identify the optimum number of ports. As seen in Fig. 1(b), the most efficient irradiation of water was with 3 ports with each providing 1/3 of the overall power level. The optimum number of ports for max efficiency of the microwave cavity was identified based on the number of ports with max average absorbed power. The effect of port position on microwave power absorption was modeled using 2D and 3D geometries. Basalt rock (instead of water) was considered as the sample and the material properties given in [2] were assigned in the models. About 40 simulations were run with different port positions. The simulated change in temperature was recorded, along with port positions and entered into a .csv file that could be accessed. The numerical model results were used as training data for a machine learning algorithm. 2D simulations in COMSOL were run to assess the feasibility of using AI methods to predict sample temperature before upscaling to 3D simulations (see Fig. 2). Then, 3D simulations were used to develop a machine learning algorithm to predict the temperature in a modeled rock sample based on the location of the waveguide ports on the cavity walls. A deep learning neural network was created using Python with Tensorflow and Keras ML libraries to make temperature predictions for the positions of the ports on the walls of the microwave cavity. The data was cloned and a small random value (< 1%) was added to the temperature value in order to help with the neural network training. A 5-layer, dense, sequential deep neural network was created, and trained on the simulated data points. The AI was then used to make a prediction of the expected temperature of a port configuration that was not simulated.

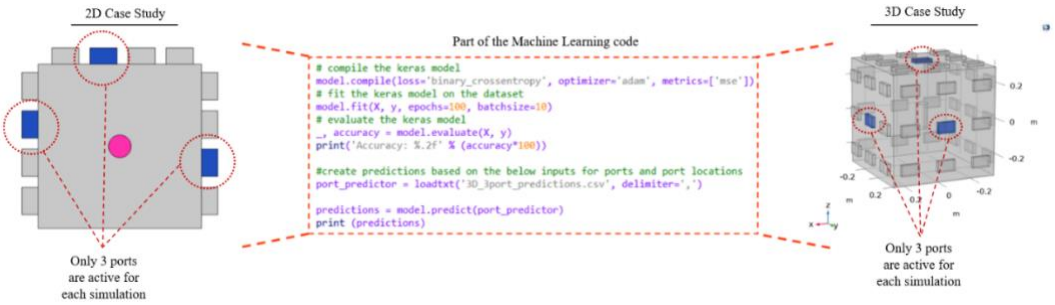

Figure 2. Schematic overview of the 2D Case Study (left) and 3D Case Study (right) for an AI-based prediction using a machine learning algorithm (middle)

RESULTS & DISCUSSION

For the 2D model, 20 unique datapoints were used for training the ML algorithm. While the 2D model does not represent a realistic situation, the results provided insight into the feasibility of using machine learning to predict power absorption in a rock sample. The temperature change predicted by the ML algorithm was compared to the temperature change determined by numerical simulation. The temperature was predicted with about 11% accuracy. Thus, the AI could pick up on the subtle relationships between different port positions. For the 3D model, about 60 simulations were run with different combinations of port positions and the neural network was modified to make predictions in the 3D case study by addition of 2 more layers and addition of neuron to the existing layers. The AI was trained on the 3D simulated data and the prediction on a non-simulated port configuration was found to predict the temperature with accuracy of 4-6%. The results of the predictions by the developed ML algorithms looked promising and the accuracy can be significantly improved by increasing the amount of training data. The model could be further improved by optimizing the number of neurons, number of layers, and the respective activation functions of each layer.

CONCLUSION

The number and the positioning of the waveguide ports in multimode microwave cavities are the determining factors in energy-saving and efficient cavity designs for microwave-assisted ore breakage and mineral processing applications. As rocks are comprised of various ore minerals with complex microwave absorption characteristics, ML can be a useful tool for microwave cavity design for rock preconditioning and breakage. By coupling numerical modeling with ML, the effects of microwaves on rock preconditioning and breakage can be accurately predicted and analyzed.

REFERENCES

[1] K. Teimoori and F. Hassani, "Twenty years of experimental and numerical studies on microwave-assisted breakage of rocks and minerals-a review," *arXiv:2011.*14624, 2020.
[2] K. Teimoori and R. Cooper, "Multiphysics study of microwave irradiation effects on rock breakage system," *IJRMMS*, vol. 140, pp. 1-16, 2021.
[3] C. Ellison, R. Tempke, S. Pandya, and D. Shekhawat, "Prediction of material dielectric permittivity by machine learning," *IMPI's 55th Microwave Power Symp.*, Virtual, June 2021.
[4] K. Teimoori, *Multiphysics Study of Microwave Irradiation for Rock Pre-conditioning and Breakage*, Doctoral dissertation, McGill University, 2021.

Use of Dielectric Properties Measurement for Monitoring Water Activity Changes in Almonds

Samir Trabelsi

Quality and Safety Assessment Research Unit, U.S. National Poultry Research Center, USDA-ARS, Athens, GA, USA

Keywords: dielectric properties, microwaves, moisture content, water activity

INTRODUCTION

Water activity of water-containing materials including foods, agricultural products, and pharmaceuticals is a critical parameter often used to determine their shelf life and conditions for their safe storage. Conventional methods for water activity measurement are tedious and time consuming [1]. In this paper, water activity changes were tracked in real time for almonds through measurement of their dielectric properties at a single microwave frequency. Samples of relatively dry almond kernels were placed in a chamber where humidity was kept very high. As the almond kernels absorbed water, their water activity and moisture content changed. These changes were monitored every few hours by measuring the dielectric properties of the almond kernels by using a free-space transmission technique [2]. These measurements revealed the dielectric constant, dielectric loss factor, and loss tangent were highly correlated to water activity. For this abstract and because of length considerations only the loss tangent is shown. Analytical expression of water activity in terms of dielectric properties was established. This expression can be used to predict water activity from measurement of the dielectric properties at a single microwave frequency. Results are shown for measurements at 10 GHz at room temperature (22-23 ºC).

METHODOLOGY

Samples of almond kernels were place in a tray with perforated metallic bottom as shown in Fig. 1. The perforated bottom allowed the humid air to circulate freely through the almond kernels. The tray was place inside a chamber where the humidity was kept very high. Fig. 2 shows almond kernels moisture content as a function of the number of days in the chamber. Starting with a sample of 4.6% moisture content, after 13.5 days inside the chamber, the sample moisture content increased to 10.3%.

To track water activity changes dielectric properties of the sample were measured every few hours over the 13.5 days span. Each time the sample was taken out of the chamber and loaded into a Styrofoam sample holder which was placed between two horn-lens antennas

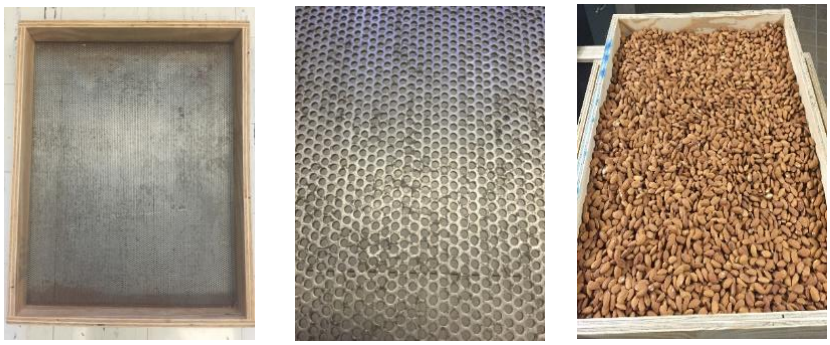

Figure 1. Tray with perforated bottom to allow almond kernels to absorb humidity from surrounding air.

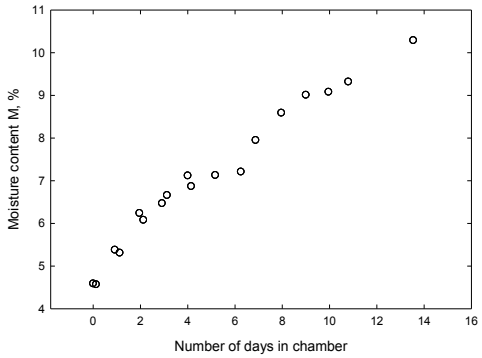

Figure 2. Almond kernels moisture content as a function of days in the chamber.

Figure 3. Free-space measurement arrangement.

(Fig. 3). The dielectric properties were determined from measurement of the attenuation and phase with a vector network analyzer [2]. Once the dielectric measurements were performed a few almonds were collected for moisture content and water activity determination.

RESULTS AND DISCUSSION

Fig. 4 shows variation of the loss tangent with water activity. The loss tangent was used because it is less influenced by bulk density changes and involves both the dielectric loss

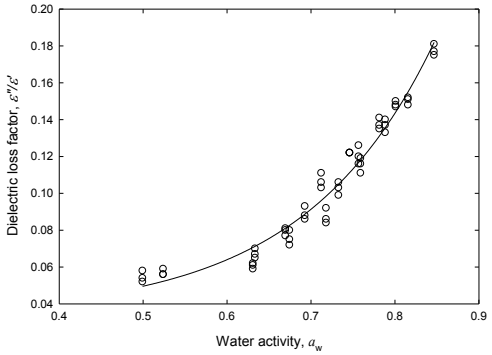

Figure 4. Variation of the loss tangent measured at 10 GHz with water activity of almond kernels.

factor and dielectric constant. The loss tangent increased exponentially with water activity. A regression fitting provided the correlation between the loss tangent and water activity:

$$\frac{\varepsilon''}{\varepsilon'} = 0.034 + 0.0006e^{6.436\,aw} \quad (1)$$

Solving Eq. (1) for *a*w, an equation in terms of the dielectric properties is obtained:

$$aw = \frac{1}{6.436} ln\left[\frac{\frac{\varepsilon''}{\varepsilon'} - 0.034}{0.0006}\right] \quad (2)$$

Eq. (2) is water activity calibration equation for water activity determination from measurement of the dielectric properties at a single microwave frequency. Eq. (2) provided water activity with a standard error of calibration, SEC, of 0.02.

CONCLUSION

Dielectric-based sensing can be used for real-time and nondestructive determination of water activity of water-containing materials. The measurement principle presented here for tracking changes in water activity of almond kernels while absorbing water from surrounding air can be extended to other commodities and foods. The method can be used for static and dynamic situations for in-process measurement of water activity.

ACKNOWLEDGEMENT

The author is grateful to former student worker, Laine Ellington, UGA, for taking the measurements.

REFERENCES

[1] B.A. Prior, "Measurement of water activity in foods: A review," *J. of Food Protection*, vol. 42, pp. 668-674, 1979.

[2] S. Trabelsi and S.O. Nelson, "Free-space measurement of dielectric properties of cereal grain and oilseed at microwave frequencies," *Measurement Science and Technology,* vol. 14, pp. 589-600, 2003.

[3] S. Trabelsi and S.O. Nelson, "Density-independent functions for on-line microwave moisture meters: a general discussion," *Measurement Science and Technology,* vol. 9, no. 4, pp. 570-578, 1998.

The Effect of Different Microwave Powers and Frequencies in the Reduction of Magnetite to Iron

Morgan Chen[1], Shuyan Zhang[1], Victor Abdelsayed[2], Daniel Haynes[2], and B. Reeja Jayan[1]

[1]Carnegie Mellon University, Pittsburgh, PA, USA
[2]National Energy Technology Lab, Morgantown, WV, USA

Keywords: magnetite, microwave heating, pair distribution function analysis, variable frequencies

INTRODUCTION

The application of microwaves in processing materials has demonstrated considerable reductions in observed reaction temperatures and accelerated reaction kinetics [1]. Specifically, microwave-assisted reduction of magnetite to iron has significant energy-saving implications in the steel-making industries to energy applications such as methane decomposition for hydrogen [2]. We present experimental results in the microwave-assisted reduction of magnetite to iron at various microwave powers and frequencies. The latter datasets are novel as most studies with commercial microwave applicators are conducted at 2.45 GHz. Additionally, we couple classical X-ray diffraction (XRD) methods with X-ray pair distribution function (PDF) analysis to probe the local atomic structure.

EXPERIMENTAL APPARATUS AND PROCEDURE

As-received magnetite, Fe_3O_4, powder from Sigma-Aldrich was loaded into a quartz reactor tube centered inside the cavity of a variable frequency microwave reactor as shown in Fig. 1. A frequency scan was conducted over 3 bands (2-4 GHz, 4-6 GHz, and 6-8 GHz) to determine the optimal frequency with the highest microwave absorption (impedance matching) within each band. The powder was reduced under a microwave frequency of 4.6 GHz with powers set at 30, 60, 100, 150, and 300 W. The experimental data presented here further explores the powder samples irradiated with 100 W of microwave power at frequencies of 3.4, 4.6, and 6.8 GHz. A quartz transparent infrared (IR) pyrometer was used to measure the surface temperature of the material bed and was positioned in the lower portion to accommodate volume change of the sample during reduction. For comparison, the magnetite powder was also reduced under conventional thermal processing in a fixed bed at temperatures comparable to those observed under microwave – 550 ºC and 900 ºC.

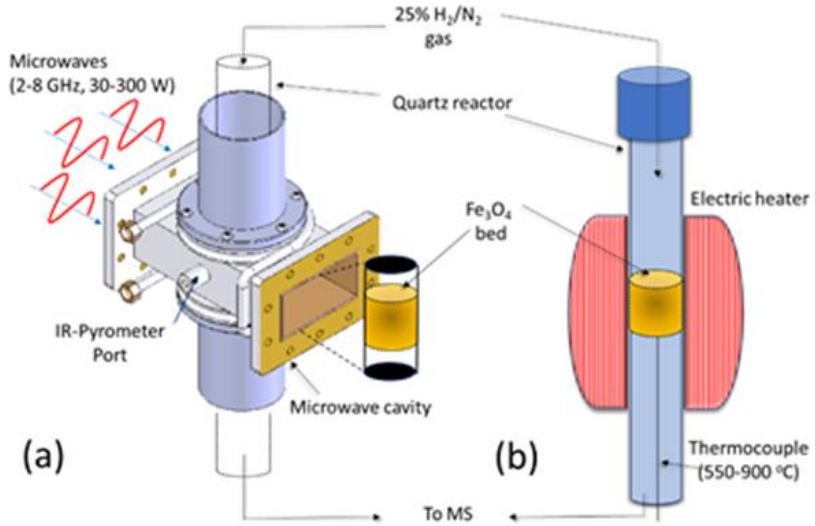

Figure 1. Schematic diagram of the systems used for magnetite reduction: experimental microwave setup (a) and conventional thermal system (b).

RESULTS AND DISCUSSION

We couple classical XRD methods with X-ray PDF analysis to probe the local atomic structure. While XRD analysis can identify well-ordered iron oxide phases and long-range crystallinity, it is ill-equipped for distinguishing local changes in the atomic environment. Incorporating PDF analysis via PDF refinements can provide enhanced insights into nearest interatomic iron/oxygen distances, lattice constants, and atomic displacement parameters. This can be achieved by allowing such parameters of input structural models to change as the model PDF is refined to match that of the experimental data. Therefore, the combination of XRD and PDF methods allow for more comprehensive analysis of subtle changes in phase composition, amorphous-crystalline boundaries, and other atomic structural nuances as a result of varying microwave processing parameters like power and frequency.

We observe that certain processing powers and frequencies result in greater crystallinity of the iron structure. Within the samples irradiated with 4.6 GHz microwaves at various applied power levels, a power of 100 W seemed to result in the greatest amount of iron reduced from magnetite powder. Within the samples exposed to 100 W of microwave power at various frequencies, a frequency of 4.6 GHz resulted in the greatest amount of iron reduced from magnetite powder. The results are summarized in Fig. 2.

CONCLUSION

Microwave power and frequencies are tunable parameters that can affect the reduction behavior of magnetite. All frequencies were able to reduce iron, but to different extents. The 4.6 GHz frequency demonstrated a reduction to iron metal at lower observed bulk temperatures (ca. 550 ºC) at all powers, with the extent of reduction decreasing with power due to more reflected power.

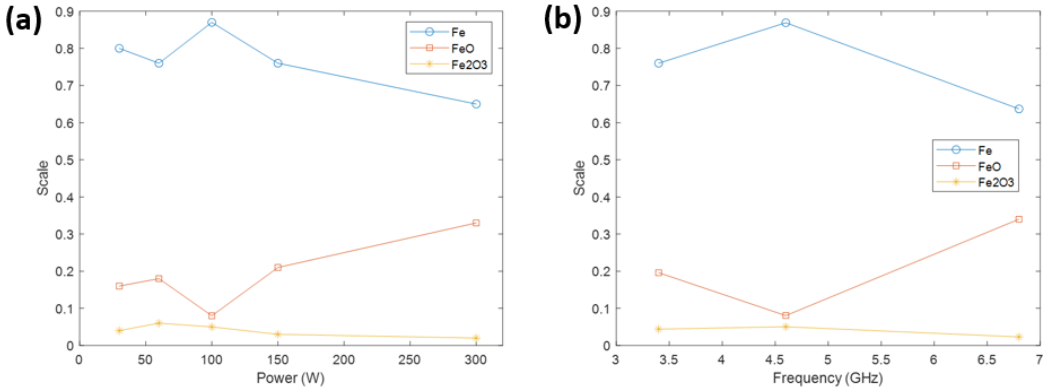

Figure 2. The refined scale parameter values of the various microwave processing conditions.

REFERENCES

[1] K. Ishizaki, M. Stir, F. Gozzo, J.M. Catala-Civera, S. Vaucher, and R. Nicula, "Magnetic microwave heating of magnetite carbon black mixtures," *Materials Chemistry and Physics*, vol. 134, no. 2-3, pp. 1007-1012, 2012.

[2] M. Stir, K. Ishizaki, S. Vaucher, and R. Nicula, "Mechanism and kinetics of the reduction of magnetite to iron during heating in a microwave E-field maximum," *J. of Applied Physics*, vol. 105, no. 12, 124901, 2009.

New World of Internet-Of-Energy with Wireless Power Transfer via Microwaves

Naoki Shinohara

Kyoto University, Kyoto, Japan

Keywords: internet-of-energy, internet-of-things, microwave power, wireless power transfer

SUMMARY

People use microwaves as heat energy for a microwave oven and microwave chemistry. But one can also use the microwaves as electricity as a wireless power transfer. We call it “Wireless Power Transfer" (WPT) or "Microwave Power Transmission" (MPT). Merit of the WPT/MPT is to realize unconscious wireless charging of electrical equipment and battery-free devises. The WPT/MPT is suitable for IoT (Internet-Of-Things) society and the so-called IoE (Internet-Of-Energy) society with the WPT/MPT. In everywhere, every time, we can use electricity like an air, which is most important, but is not usually recognized, with the WPT/MPT technology. Some of WPT technologies are common to the microwave heating technology.

The new WPT market is growing in the world. Some start-up companies in the US develop wireless powered sensors. Xiaomi, Chinese smartphone company, published technology of the wireless charger of smart phones with phased array antenna in millimeter waves in January 2021. Japanese government establishes new radio regulation for the WPT in microwave frequency in March 2022. These WPT technologies are supported by scientific academic communities all over the world. For example, IEEE MTT-S conducts every year special international conference of the WPT named “IEEE Wireless Power Week”. The IEEE MTT-S also establishes “WPT initiative” to promote the WPT/MPT technologies. This talk introduces recent developments in the WPT/MPT technology and WPT market in the world.

Microwave Drying of Lithium Oxide for Battery Manufacturing

Kenneth Kaplan

Cellencor, Inc., Ankeny, IA, USA

Keywords: lithium battery, lithium magnesium oxide, lithium nickel cobalt manganese oxide, lithium oxides, microwave mixer

INTRODUCTION

Rapidly growing applications for electric vehicles and power storage for solar and wind energy sources is driving enormous demand for lithium batteries. Many new manufacturing plants are under construction or planned by battery and automobile manufacturers. Optimization of manufacturing processes are essential to future battery cost reduction. This paper describes a novel method of utilizing microwave heating in preparation of Lithium Nickel Cobalt Manganese Oxide (LiNCM) cathode material.

METHODOLOGY

LiNCM is the cathode material most used in cylindrical lithium battery cells. It is used to coat a metal foil substrate, which is then layered with insulation, followed by another layer of metal foil coated with anode material. The layers are wound together and inserted in the battery body. The stability and cycle life of the battery can be improved by coating the LiNCM particles with tungsten trioxide and other additives [1]. They are combined with a solvent solution to produce a slurry which is mixed in a high-shear mixer. After coating, the solvent musts be removed to a very low concentration.

The applicator used was a 10 ft^3 (0.28 m^3) horizontal paddle mixer manufactured by Eirich Machines, Inc. The mixer was fitted with a WR-975 waveguide feed on its roof, and RTD and IR temperature sensors. The mixer is fabricated from stainless steel and is sealed to prevent microwave and vapor leakage. A low-volume exhaust system extracted and condensed vapors. Microwave power was supplied by a Crescend Technologies 50kW 902-928 MHz solid-state microwave generator.

There are many species of lithium oxides with varying properties. Generally, they are electrically conductive with a relatively low dielectric constant [2]. LiNCM is quite heavy, with a density of about 2.5 kg/l. A slurry was prepared consisting of 225 kg (~500 lbs.) of LiNCM, a small amount of coating material, and 12 kg of a 50% methanol/50% water solution. The starting liquid content was 5% liquid w/w, and the objective was to dry to less than 1% w/w. The material filled the mixer a little more than halfway. The applied microwave power averaged 12 kilowatts; higher power caused minor arcing within the material.

(a) (b)

Figure 1. Views of the overall test setup (a) and the horizontal mixer (b).

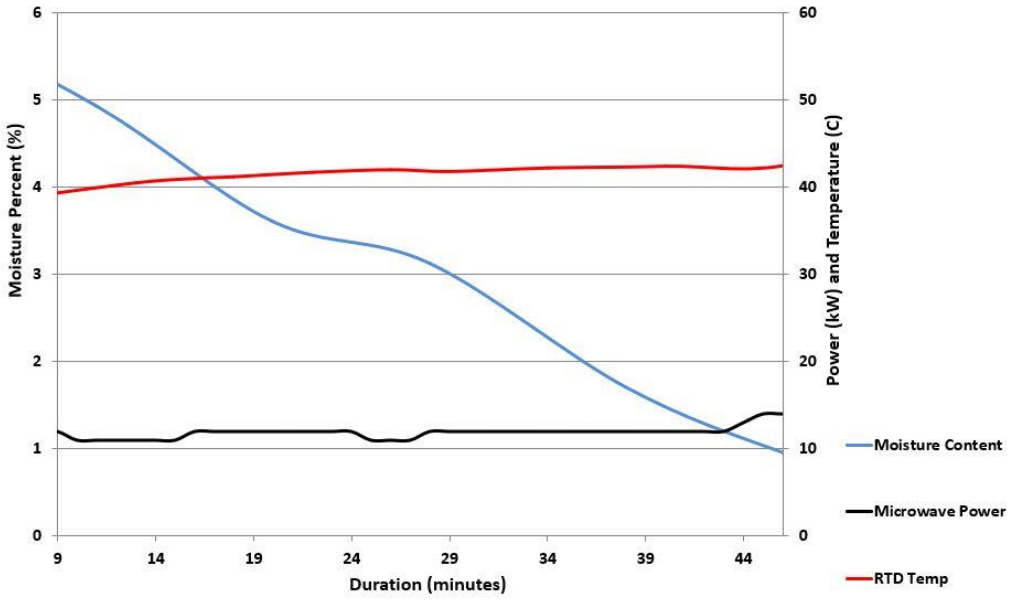

Figure 2. The drying curve of an example test run with LiNCM.

RESULTS

The liquid content decreased from 5% to less than 1% in about 45 minutes (Fig. 2). The equivalent process typically takes about 6 hours with a conventional convection dryer. Similar results were obtained in tests with Lithium Magnesium Oxide (LiMnO), another commonly used cathode material. The calculated drying rate was 2,987 kJ per kg of vaporized liquid. There was significant heat loss through the mixer's metal shell. The drying rate can be significantly improved by adding insulation to the mixer's exterior.

DISCUSSION

The LiMnO slurry dried efficiently and rapidly. It is interesting to note that the product temperature remained low at about 43° C throughout the duration of the drying process. This indicates that most of the energy was absorbed by the polar solvent molecules and not the LiMnO itself. This results in very efficient drying and is important because some of the slurry ingredients such as coatings and binders are temperature sensitive. The key benefits of lithium oxide drying using a microwave mixer applicator are:

Energy efficiency: Drying rates of about 2,500 kJ/kg versus 5,000 kJ or more in a conventional convection dryer. This may vary depending on the solvents used.

Speed: Up to 10 times faster than convection drying.

Exhaust: Solvent vapor must be captured and condensed for recycling. A microwave mixer exhaust airflow is a small fraction of a convection dryer, making the condensing system smaller and more efficient.

Product quality: The mixing action during drying produces a highly uniform product, which is critical in this application.

Environmental: There is no CO_2-producing combustion, and the equipment can be powered from renewable energy sources.

CONCLUSION

These tests demonstrated that microwaves can effectively and efficiently dry lithium oxide slurries. In addition to pre-treatment of slurries, the results suggest that microwave drying may also be an effective method for drying cathode and anode coatings on foil substates in the main battery manufacturing process.

REFERENCES

[1] F. Reissig, M.A. Lange, L Haneke, T. Placke, W. Zeier, M. Winter, R Schmuch, and A Gomez-Martin, "Synergistic effects of surface coating and bulk doping in Ni-rich lithium metal cobalt manganese oxide cathode material for high-energy lithium-ion batteries," *ChemSusChem*, vol. 14, pp. 1-12, 2021.

[2] N. Murali and V. Veeraiah, "Preparation dielectric and conductivity studies of LiNiMgO cathode material for lithium-ion batteries," *Processing and Application of Ceramics*, vol. 11, no. 4, pp. 258-264, 2017.

Control of Phase Offset Between Coherent Microwave Sources for Industrial Applications

John F. Gerling

Gerling Consulting, Inc., Gilroy, CA, USA

Keywords: coherent, microwave heating, phase offset, solid state RF

INTRODUCTION

The benefits of solid-state microwave and RF (hereinafter referred to collectively as "RF") energy sources for industrial microwave heating are increasingly apparent as more applications adopt this technology. A key benefit is the ability to control output frequency as a means of impedance matching and improving process stability. When multiple solid state RF sources delivery power to a single cavity, the need for coherent operation depends largely on the cavity type and characteristics of the application. In some applications where coherence is required, this alone may not be sufficient to achieve stable performance. Phase control may be equally as important as frequency control and coherence, particularly the relative phase, or phase offset, between sources.

COHERENCE AND PHASE

Two (or more) RF sources are often described as operating coherently when their waves have identical frequency and waveform [1]. Coherence is required when combining two or more RF sources to operate as a single source, whether in a transmission line or waveguide using combiners [2] or in a resonant cavity applicator within which the excitation mode must be well defined and controlled [3]. In both cases, precise control of relative phase between each RF source is also required for optimal and stable operation.

When coherent RF sources are combined in a resonant cavity, their waves cause both constructive and destructive interference, often referred to as standing waves or "hot" and "cold" spots, at specific locations within the volume of the cavity. The distribution pattern of interference depends on the geometry of the cavity and its contents relative to wavelength. When the relative phase between the sources is constant, the patterns of interference remain constant. Some applications require a static interference pattern while others benefit from controlled variation of the pattern.

Fig. 1 illustrates a simplified standing wave pattern (the "sum") in a cavity excited by two RF sources. The standing wave pattern remains static as long as the operating frequency of both sources are the same and the relative phase between them remains constant. A shift in relative phase between the two sources will shift the standing wave pattern one direction

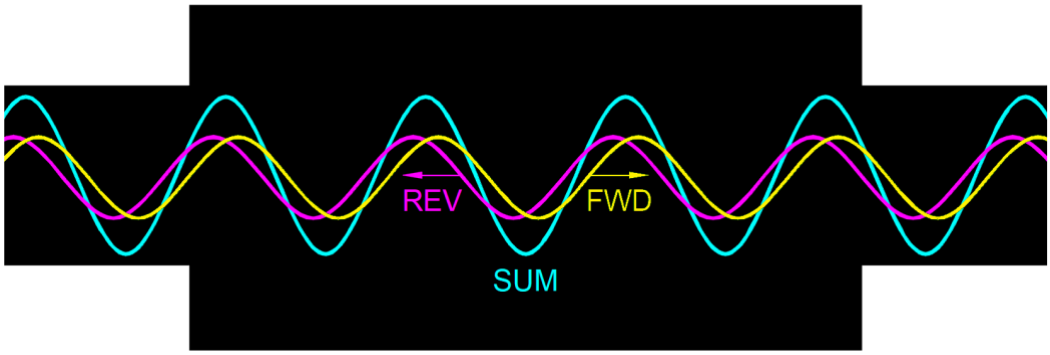

Figure 1. Standing wave pattern ("SUM") due to constructive and destructive interference from two coherent waves propagating in opposite directions.

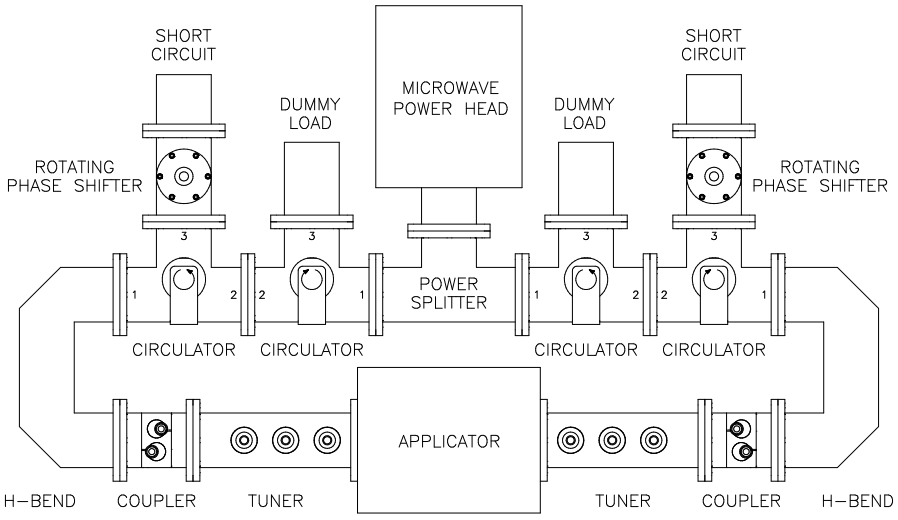

Figure 2. Waveguide configuration for controlling phase offset between two coherent waves generated by a single magnetron-based source [3].

or the other, while a gradual drift in the phase of either source (or both) will put the standing wave pattern into constant motion.

PHASE CONTROL USING MAGNETRON-BASED SOURCES

When using multiple magnetron-based RF sources, control of the output frequency and phase to achieve coherent operation is difficult [4] and often not practical for industrial applications. Fig. 2 is a system configuration for controlled movement of a standing wave pattern utilizing a single magnetron-based source. Two coherent RF signals are generated by splitting the output of a magnetron. The phases of both signals are then varied synchronously to control the movement of a standing wave pattern inside the applicator. In this case the phase offset between the two coherent signals remains constant.

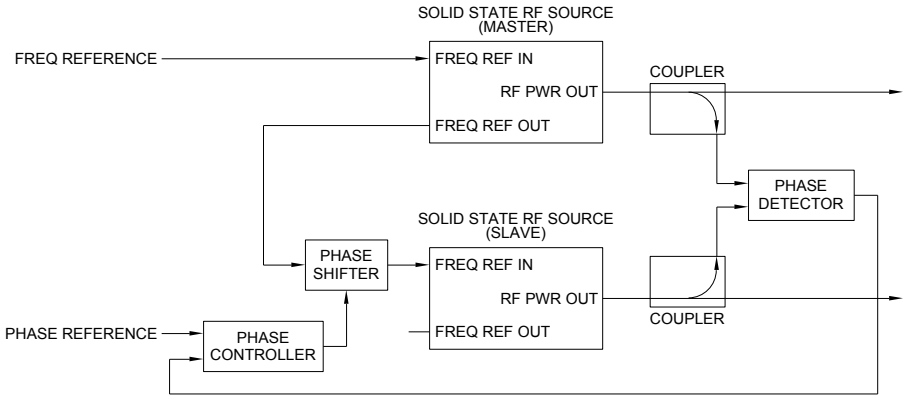

Figure 3. Schematic diagram for precise control of phase offset between solid state RF sources.

PHASE CONTROL USING SOLID STATE RF SOURCES

The output frequency and phase of solid-state RF sources can be precisely controlled to achieve coherent operation between multiple sources. Commercially available products commonly utilize a master-slave architecture to operate multiple sources at the same frequency. Independent control of output phase from each source is also a commonly available feature, although it can be subject to uncontrolled drift due to both internal and external effects such as temperature. Consequently, phase offset between each source can be unstable.

A scheme to precisely control phase offset is illustrated in Fig. 3. This scheme compensates for uncontrolled phase drift of the source output by detecting phase within the transmission line.

CONCLUSION

Utilizing multiple RF sources for industrial applications may require coherent operation between the sources to achieve stable process performance. Methods for precise control of output phase can be employed for both solid state and magnetron-based sources.

REFERENCES

[1] ”Coherence (Physics),” en.wikipedia.org/wiki/Coherence_(physics).
[2] ”Power Combining,” www.microwaves101.com/encyclopedias/power-combining.
[3] J. M. Pinneo, “Apparatus and method for controlling plasma size and position in plasma-activated chemical vapor deposition processes,” US Patent 5,449,412, Sept 1995.
[4] P. Yuan, Y. Zhang, W. Ye, H. Zhu, K. Huang, and Y. Yang, “Power-combining based on master slave injection-locking magnetron,” *Chinese Physics B*, vol. 25, no. 7, pp. 542-545, 2016.

Improved Manufacturing through Continuous High Temperature Microwave Process: The Destiny Project

Koen Van Reusel[13], Dimitrios Giannopoulos[1], Luis Guaita[2], Angel Lopez[3], Paolo Chiariotti[4], Beatriz Garcia[5], Ana Felis[6], Oscar Centelles[7], Kersten Marx[8], Lukas Schmidt[9], Kerstin Walter[10], Ana Santos[11], Marco M. Colella[12], and Jose F. Pereira[14]

[1]National Technical University of Athens, Greece
[2]Keraben Grupo SA, Spain
[3]Innceinnmat SL, Spain
[4]Universita Politecnica delle Marche, Italy
[5]Universitat Politecnica de Valencia, Spain
[6]Al-Farben S.A, Spain
[7]Chumillas Technology, Spain
[8]VDEh-Betriebsforschungsinstitut GmbH, Germany
[9]K1-MET GmbH, Austria
[10]DK Recycling und Roheisen GmbH, Germany
[11]Cemex Research Group AG, Switzerland
[12]Ciaotech Srl, Italy
[13]Belgisch Laboratorium van de Elektriciteitsindustrie – Laborelec, Belgium
[14]Instituto Superior Tecnico, Portugal

Keywords: container size microwave plant, continuous process, energy intensive industrial sectors, production flexibility, reduction of emissions

INTRODUCTION

The DESTINY project aims to realize a functional, green and energy saving, scalable and replicable solution, employing microwave energy for continuous material processing in energy intensive industries. The target is to develop and demonstrate a new concept of firing for granular feedstock to realize material transformation using full microwave heating as alternative energy source and complement to the existing conventional production in the cement, ceramics, and steel industry. Fig 1. the goals, key innovations and concerned industrial sectors.

The DESTINY system is conceived as cellular kilns in a mobile modular plant (Fig. 2).

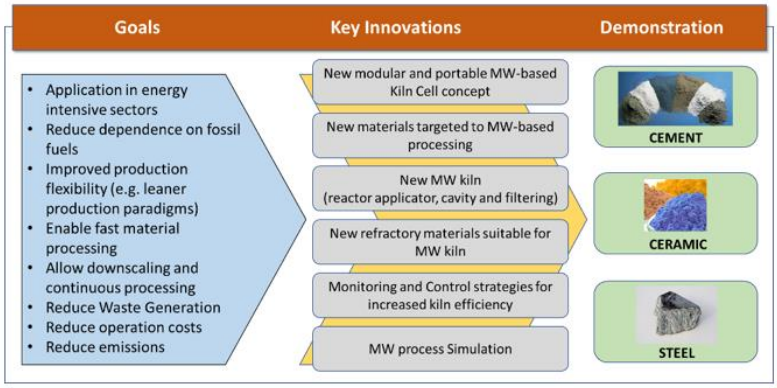

Figure 1: Goals, key innovations and industrial sectors.

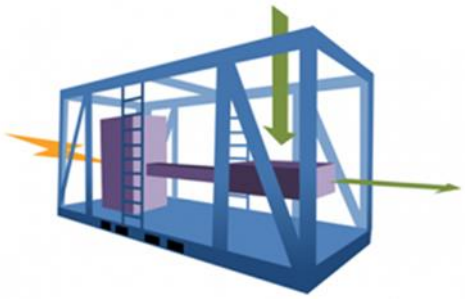

Figure 2: Cellular kilns in a mobile modular plant.

The microwave power can (depending on the charge) amount to 54 kW at a (slightly adjustable) frequency of 915 MHz.

The industrialization and sustainability of DESTINY high temperature microwave technology will be assessed through the evaluation of relevant key performance indicators (KPI)s with life cycle methodologies.

OBJECTIVES

The DESTINY project aspires to introduce a "first-of-a-kind" high temperature microwave processing system at industrial level offering a variety of vital benefits to energy intensive sectors: reduced energy consumption, lower lifetime operating costs and enhanced sustainability profile.

EXPECTED IMPACTS

The DESTINY concept is a paradigm change: it enables new small low-cost solutions for new processes or to retrofit existing plants. The system is designed as a modular unit to create any production capacity required by clients on-site. Due to a reduced size, it offers a production on demand, delocalized and with high flexibility of production and portability,

it gives the chance to develop new business strategies and allowing increased flexibility of the energy input. Thus, the DESTINY concept perfectly fits to energy efficiency policies for the performance of the next generation renewable based electricity grids.

RESULTS

The specific results expected in the project are:

- A portable ”ready-to-use” container size microwave pilot plant (prototype) with a production capacity higher than 20 kg/h by a single cell kiln, and able to reach working temperatures over 1000 °C
- With a minimum of 30% of energy savings on the process (due to the use of microwave technology and the use of advanced control strategies)
- Reducing operation costs between 15-30%
- A minimum of 10 times faster heating up of the production process
- Reducing SOx, NOx, CO_2 and CO emission in 40% (minimum) by avoiding combustion (also via targeted new emission monitoring and control strategies, with high reduction of particle matter).

The DESTINY concept will be proved in two demo sites located in Spain and Germany covering high energy demanding sectors of strategic interest as Ceramic (Pigments), Cement (Calcined clay) and Steel (Sinter, iron pellets/sponge iron (DRI), ZnO) to validate the critical parameters of the developed technology in relevant environment. It will be implemented as two feeding modules per demo site and one mobile microwave kiln module and product treatment.

ACKNOWLEDGMENT

The authors wish to acknowledge that project DESTINY has received funding from the European Union’s Horizon 2020 research and innovation program (H2020-NMBP-SPIRE-2018) under Grant Agreement No. 820783.

REFERENCES

[1] A. Olympios, D. Katsourinis, D. Giannopoulos, and M. Founti, “Process Simulation and Life Cycle Assessment of Ceramic Pigment Production: A Case Study of Green Cr_2O_3,” *Processes*, vol. 9, no. 10, p. 1731, 2021.

A Dry, Flexible, Modular and Digital Microwave System for Pasteurization at Atmospheric Pressure

Klaus M. Baumgaertner, Markus Dingeldein, Guido Kassel, Tom Georgi, Markus Reichmann, Daniel Baars, Parth Patel, Moritz Gorath, and Robert Mueller

Muegge GmbH, Reichelsheim (Odenwald), Germany

Keywords: atmospheric pressure, digital cooking, dry process environment, industrial microwave heating, microwave pasteurization, modular setup

INTRODUCTION

Combining ready-to-eat food products and high quality nutrition still is and will increasingly be a challenge for food industry. One of the major issues of this challenge is to find the best balance in food preservation and conservation of food quality. Pasteurization instead of sterilization is a promising option.

Traditional pasteurization, such as the retort process, is generally carried out by drastic heat treatments, resulting in a loss of product quality. Microwave pasteurization offers the potential of shorter process times and improved quality. Therefore, pasteurization in food industry is increasingly performed by microwave heating.

SPECIFICATIONS FOR PASTEURIZATION BY MICROWAVE HEATING

Regarding preservation of food products, microwaves can be applied in different ways. Shelf life of food can be extended by microwave assisted brine injection, applied on meat and fish in particular, in a dehydration process or by "ordinary" heat sterilization or pasteurization by means of microwaves. Short process times and relatively homogeneous tempering and heating of the bulk and not only of the surface are major advantages of microwave technology in food sterilization and pasteurization.

Nowadays and most probably in future, too, preservation of nutrients seems to be more important compared to extension of shelf life for consumers worldwide. This will lead to an increasing change from sterilization processes towards pasteurization. In conjunction with this change, there will be new challenges for microwave technology. Reducing the temperature of the process to a minimum of 70°C and a maximum of 95°C, pasteurization processes require a more precise dosing of the microwave energy compared to sterilization processes. Focusing on ready-to-eat products consisting of various kinds of food material, the dielectric constant ε' and the dielectric loss factor ε'' of the different food components determine their ability to store electric energy and the conversion of microwave energy into

thermal energy, respectively [1]. In extreme cases, the temperature of one food component can already be close to decomposition of its nutrients while the temperature of another food component is still below the threshold necessary for pasteurization after microwave heating. For avoidance, anisotropic launching of the microwave and controlled variation of the microwave frequency within the limits assigned by the local authorities can be envisaged. This will require new microwave antenna concepts and application of solid state technology for microwave generation. Simulation and measuring techniques for cold spot detection, performed by thermal imaging for example, will support the targeted design and application of these new launcher concepts and solid state microwave components.

DRY, FLEXIBLE, MODULAR AND DIGITAL MICROWAVE-BASED PASTEURIZATION AT ATMOSPHERIC PRESSURE: METHODS AND APPLICATIONS

Common industrial microwave heating systems require excess pressure and rely on microwave coupling into the processing chamber by horn antennas. In contrast to existing microwave pasteurization systems designed for applications in food industry, the novel microwave pasteurization system developed by MUEGGE works at ambient pressure and is based on a novel microwave launching system for targeted deposition of microwave energy. Thus, the distance of this tailored microwave launching system to the food products to be pasteurized is much shorter, and less microwave energy is required. In addition, microwave injection via the novel microwave launching system of MUEGGE can be specifically adapted to various kinds of food components to be processed at the same time, having different dielectric constants ε' and dielectric loss factors ε''. Consequently, the exposure time can be significantly reduced, which helps maintaining the nutritional value of the food products in particular.

The novel microwave pasteurization system operating at the microwave frequency of 2.45 GHz combines several advantages. It works at ambient pressure, i.e. no excess pressure is required. In combination with in-situ temperature monitoring by thermal imaging, the individually controllable microwave antennas and the microwave generators featuring response times in the range of milliseconds offer temporarily and spatially targeted deposition of the microwave energy. As a result, heterogeneous food products with extremely different dielectric properties – which is characteristic for a large variety of ready meals – can be selectively heated. The resulting uniformity of this heating process allows for both fast and mild pasteurization without local overheating. Each modular unit of the novel microwave pasteurization system can provide at least 60 kW of microwave power. The modular setup facilitates cascading according to the individual requirements of the particular food products to be pasteurized.

The dry process environment of the novel pasteurization system from MUEGGE offers another advantage: ready meals in sustainable packaging materials at least partly made of cardboard or paper (i.e. up to 80% less plastic materials in the packaging) can be efficiently pasteurized, which is not possible in the presence of water or steam.

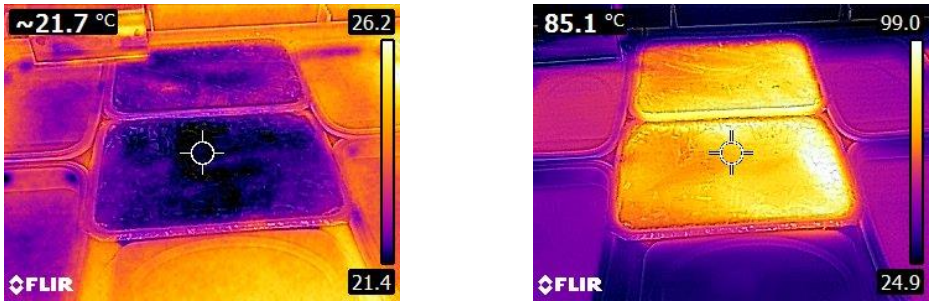

(a) (b)

Figure 1. Lasagna in sealed trays before (a) and just after pasteurization (b) in the novel microwave pasteurization system from MUEGGE; the images recorded with a FLIR®-E63900 infrared camera.

Various microwave pasteurization experiments with the novel microwave pasteurization system from MUEGGE have been performed on packaged ready meals composed of different main and side dishes in trays of customized design (see Fig. 1 showing pasteurization of lasagna in sealed trays as an example). Despite even extremely diverging dielectric properties of the different food components in the ready meals tested, results proved homogeneous tempering of all edibles in the same tray within an extremely narrow temperature zone between 90°C and 93°C, being prerequisite for maintaining nutrient content. These experiments not only focused on proving homogeneity of the microwave heating process, but also showed unchanged taste, flavor, texture and appearance of the food products by tasting.

CONCLUSION

Industrial systems for microwave pasteurization of packed ready-to-eat food products in particular can provide for both acceptable shelf life and high-quality nutrition. MUEGGE's novel microwave driven industrial pasteurization system is based on new developments in microwave launchers and microwave components based on solid state technology. Due to its modular setup and individually controllable microwave antennas, the microwave pasteurization system is suited for pasteurization of different kinds of food products, e.g. bread, meat, nuts, dates, tea, spices and even packaged ready meals. The combination of in-situ temperature monitoring, microwave generators showing response times in the range of milliseconds, adaptable microwave antennas and a smart control system provides for "digital cooking", resulting in homogeneous and uniform heating of different food products at atmospheric pressure without local overheating.

REFERENCES

[1] J. Tang, "Unlocking potentials of microwaves for food safety and quality," *J. of Food Science*, vol. 80, no 8, pp. E1776-E1793, 2015.

Development of Solid-State Microwave Defrosting Strategies with Adaptive Power and Shifting Frequency

Ran Yang and Jiajia Chen

Department of Food Science, University of Tennessee, Knoxville, TN, USA

Keywords: adaptive power, Microwave defrosting, shifting frequency, solid-state

INTRODUCTION

Microwave ovens have been used to thaw frozen foods and showed high defrosting efficiency due to the volumetric heating characteristic. However, the standing wave pattern in the microwave ovens leads to non-uniform defrosting results. Furthermore, the thermal-runaway phenomenon worsens the non-uniform thawing and leads to an increased temperature difference between the cold and hot spots, which influences the quality of the thawed products. Given the advantage of flexible control over power and frequency, the solid-state microwave system can address the standing wave pattern and thermal run-away problems and improve the microwave defrosting performance. Previous studies demonstrated that shifting frequency during heating could generate different heating patterns that could complement each other to improve the heating uniformity [1, 2]. However, previous research only focused on heating from refrigerated temperature and did not include the rotation of turntable in the solid-state microwave process. Since frozen food products have different power absorption characteristics from refrigerated foods, the microwave power may need to be dynamically adapted to ensure energy efficiency. Hence, this study aimed to develop and experimentally test novel solid-state microwave control methods that combined shifting frequency and adaptive power for the defrosting purpose. The necessity of the rotatory turntable in the solid-state microwave defrosting process was also evaluated.

METHODOLOGY

A solid-state microwave system comprised of a generator (PA-2400-2500MHz-200W-4, Junze Technology) and a domestic microwave oven cavity (Panasonic Model NN-SN936W) were used in this study (Fig. 1(A)). The microwave frequency ranged from 2.40 GHz to 2.50 GHz and the power output was up to 200 W. The mashed potato samples of 150 g each was prepared in a round-shaped plastic tray (Fig. 1(B)) and stored at -18 °C overnight before use. Several solid-state defrosting modes were compared to the one by the commercial microwave oven with a same oven cavity. Since the solid-state generator has a maximum power of 200 W, the power level 1 of the commercial microwave oven was used to deliver equivalent microwave power to the food products.

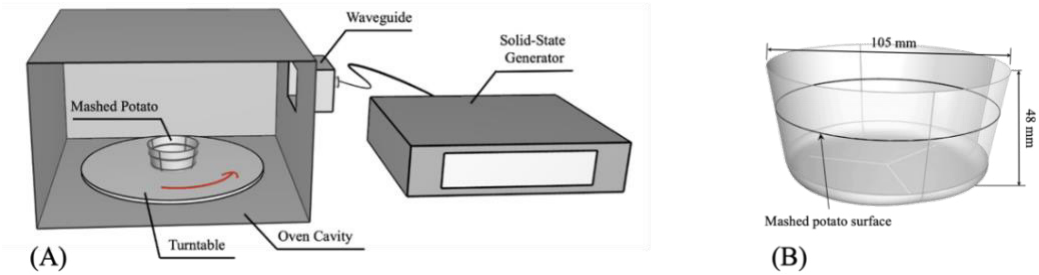

Figure 1. Schematic diagram of (A) the solid-state microwave system, (B) sample diameter

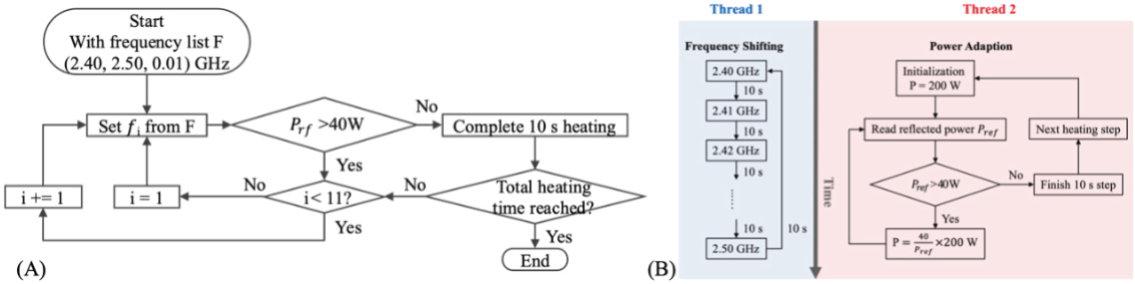

Figure 2. Algorithms of the solid-state dynamic heating. (A) Selective-frequency shifting, (B) Adaptive-power control.

The solid-state defrosting modes tested in this study included: 1) constant frequency at 2.45 GHz with rotation, as a mimic of the defrosting in the domestic microwave oven; 2) selective-frequency shifting that only orderly shifted high-power efficiency (< 20% reflection) frequencies (Fig. 2(A)); 3) adaptive-power control that shifted all frequencies orderly and adjusted the power level to ensure low power reflection (< 40 W) (Fig. 2(B)). Both the selective-frequency shifting and adaptive-power control modes were evaluated under stationary and rotatory conditions. The total heating time was 8 min for each scenario, which was preliminarily determined to ensure the samples were nearly thawed at the center. After the defrosting process, both top and middle layers' thermal results were captured with a thermal camera (FLIR C3, Boston, MA) and quantified for analysis by software FLIR Tools (2020 © FLIR® Systems, Inc.). The microwave defrosting experiments were conducted in triplicate for each mode. The results comparison was conducted using one-way ANOVA to detect differences in the performances by all the defrosting modes, where p-values < 0.05 were considered statistically significant.

RESULTS

Among all the tested methods, the adaptive-power control with rotation method (Fig. 2(B)) showed significantly lower hot spot temperature (Fig. 3(A)) and the difference between cold and hot spots (Fig. 3(C)), for both top and middle layers. And the assessment based on the combined top and middle layers showed consistent results, where the hot spot temperature and temperature gap were significantly reduced by using adaptive power (Figs. 4 (A) & 4(C)), which are desired results in a defrosting process. In addition, in terms of the necessity of turntable, the results were slightly improved by including turntable in the

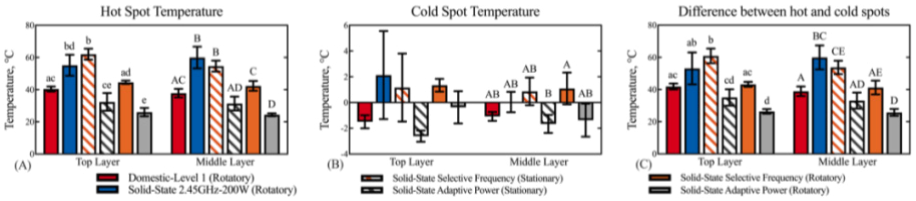

Figure 3. Thermal results of samples processed under different modes for top and middle layer results respectively: hot spot temperatures (A), cold spot temperatures (B), and the difference between the hot and cold spots (C); all experiments were conducted in triplicate and the results were expressed as mean ± standard deviation.

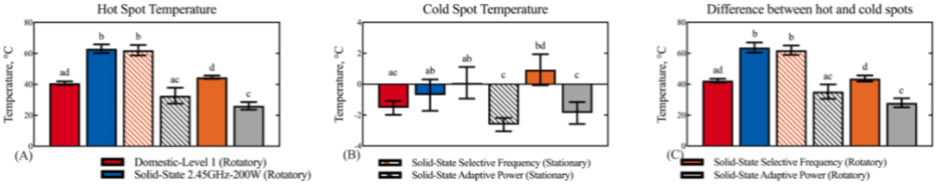

Figure 4. Thermal results of samples processed under different modes for combined thermal data from the top and middle layers: hot spot temperatures (A), cold spot temperatures (B), and the difference between the hot and cold spots (C); all experiments were conducted in triplicate and the results were expressed as mean ± standard deviation.

defrosting by using adaptive-power control but not significant, while for the selective-frequency shifting modes, the improvement by the turntable was significant (Figs. 3-4).

DISCUSSION

The adaptive-power mode yielded optimal performance compared to all others, by shifting all available frequencies non-selectively and adapting the power level continuously. The improved performance is the diverse thermal patterns created by different frequencies for shifting. Besides, scaling down the input power when the power reflection is high under some frequencies could raise the power efficiency, and alleviate the overheated hot spots. Additionally, the contribution by the rotatory turntable was not significant under this mode, implying a potential to remove turntable in future oven design, which helps better utilize the patterns variety generated by different frequencies to achieve further improvement.

CONCLUSION

The developed microwave defrosting mode with adaptive power and shifting frequency by the solid-state microwave system can significantly improve the defrosting performance.

REFERENCES

[1] Z. Tang, T. Hong, Y. Liao, F. Chen, J. Ye, H. Zhu, and K. Huang, "Frequency-selected method to improve microwave heating performance," *Appl. Therm. Eng.*, vol. 131, pp. 642–648, 2018.

[2] Z. Du, Z. Wu, W. Gan, G. Liu, X. Zhang, J. Liu, and B. Zeng, "Multiphysics modeling and process simulation for a frequency-shifted solid-state source microwave oven," *IEEE Access*, vol. 7, pp. 184726–184733, 2019.

Product-Friendly Heating and Drying of Model Food Using a Solid-State Microwave Generator

Isabel Kalinke and Ulrich Kulozik

Technical University Munich, Munich, Germany

Keywords: magnetron, microwave heating, solid-state microwave generator, uniformity

INTRODUCTION

Microwave (MW) solid-state (SS) generators based on semiconductor technology represent an emerging alternative to the conventional magnetron generator (MG) concept. They allow for the flexible adjustment of excitation frequency, phase, and power input. By a targeted setting, this should result in an increase of microwave absorption in the product or uniformity of heating [1-4]. Compared to the MG system, this allows for flexible response to the formation of an inhomogeneous temperature distribution and to changing product parameters in the running process.

The knowledge on how to exploit the possibilities of the new SS technology on uniform heating of the product is still lacking. Therefore, we investigated the effect of microwave frequency on the uniformity of heating, which is fundamental for the successful integration of SS MW technology in the food sector, i.e., to increase quality and product safety of MW heated foods. We hypothesized that a targeted selection of microwave frequency can result in a more uniform heating process compared to the MG system. Further, we hypothesize that resulting from a more uniform processing in the SS system, the additional benefit of sample rotation in the cavity could be less dominant in the SS system and therefore, possibly be omitted.

METHODOLOGY

To assess the heating uniformity, a model food system containing Maillard reactants was heated in identical microwave ovens of both generator systems (SS and MG) and the uniformity of the resulting Maillard-induced browning patterns on the sample, as exemplary depicted in Fig. 1, was evaluated. In the SS system the microwave treatment was performed either at a constant, a random or at the resonant frequency within the range of 2400-2500 MHz at 270 W input power. The uniformity of the heating process was assessed by the COV value (coefficient of variance) describing the standard deviation of total color change across the entire sample surface standardized by the mean total color change of the sample. Thus, the COV value describes the normalized inhomogeneity with respect to the varying total color change of the individual sample.

Figure 1. Maillard-induced browning pattern due to inhomogeneous heating of the sample.

RESULTS

Figs. 2(a)-(b) depict the effect of microwave treatment in the SS and MG generator system on the heating uniformity of the process for TToff and TTon, with a lower COV value describing a more uniform heating pattern. The COV level of the MG reference is given as dotted line in both graphs. It can be seen that for TToff (Fig. 2(a)), the uniformity of browning for all frequency settings in the SS system was higher compared to the MG reference. While for lower frequencies below 2440 MHz the COV value varied in relation to the frequency, for frequencies above 2440 MHz, and for random and resonant frequency, uniformity was hardly affected by the setting.

The COV values for TTon in the SS system scattered around the value of the MG reference (Fig. 2(b)). For some frequencies, namely 2410, 2430, 2480 and 2500 MHz the COV value for TTon was lower than for the reference. For 2400 MHz, COV value reached its maximum and showed therefore, the highest inhomogeneity in the SS system for both, TTon and TToff. Uniformity for random and resonant frequency was at the same level as for the MG reference. The direct comparison of TToff and TTon showed no or a beneficial effect of sample rotation on the heating uniformity.

DISCUSSION

The experiments show that by a targeted selection of the microwave frequency in the SS generator system, a higher uniformity can be achieved compared to the MG system under both, TToff and TTon, conditions. The positive effect of a treatment in the SS system on heating uniformity was more significant for TToff. Therefore, especially in systems without sample movement in the microwave field, a targeted selection of microwave frequency increases uniformity of heating.

If treated at resonant frequency, uniformity was high and the same as for random frequency. This is due to the fact that resonant frequency was for all experiments at 2450 MHz and treatment at constant frequency 2450 MHz showed a high uniformity of heating. Since most constant frequencies showed a similarly low COV value, the random selection of frequencies over the entire process resulted in a comparably high uniformity. An additional benefit of random frequency treatment on uniformity could not be observed. Even though this could have been expected, since the excitation at different frequencies should result in a better spatial distribution of absorbed energy in the sample.

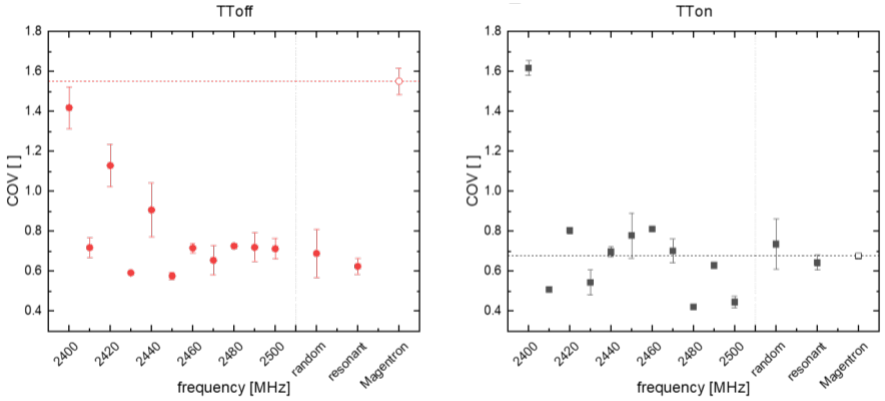

(a) (b)

Figure 2. Effect of frequency treatment on heating uniformity in the SS generator system (■●) compared to the reference MG system (□○) is given for TToff (A) and TTon (B). The dotted lines visualize the level of uniformity in the reference MG system.

CONCLUSION

Resonant and random frequency treatment resulted in a good uniformity of browning. Whether this is widely applicable for other products, should be investigated for other sample geometries and cavity loads in the future, to be able to derive universally applicable process concepts. Further, the COV value, as standardized color deviation, should be put into perspective to the extent of overall color change, since a high inhomogeneity of browning is negligible, if overall browning is low. It was shown that more uniform heating can be achieved in the SS system compared to the conventional magnetron system as hypothesized. Further, the beneficial effect of sample movement on heating uniformity was more pronounced in the SS generator system. This and further work on promising process concepts, helps to unlock the potential of SS generators for uniform and energy-efficient microwave processes and is crucial for industrial applications of microwave heating and drying processes. Promising process concepts derived from these heating experiments are therefore, being investigated in further experiments for their applicability in product-friendly microwave-assisted freeze-drying.

REFERENCES

[1] K.K. Chang, *Solid State Microwave Heating Apparatus*, US Patent 3,691,338, Sept. 12, 1972.
[2] S.T. Dinani, E. Feldmann, and U. Kulozik, "Effect of heating by solid-state microwave technology at fixed frequencies or by frequency sweep loops on heating profiles in model food samples," *Food and Bioproducts Processing,* vol. 127, pp. 328–337, 2021.
[3] J.C. Atuonwu and S.A. Tassou, "Energy issues in microwave food processing: A review of developments and the enabling potentials of solid-state power delivery," *Critical Reviews in Food Science and Nutrition,* vol. 59, pp. 1392–1407, 2018.
[4] J.C. Atuonwu and S.A. Tassou, "Quality assurance in microwave food processing and the enabling potentials of solid-state power generators: A review, *Journal of Food Engineering,* vol. 234, pp. 1–15, 2018.

Electric Heating Technologies: Ohmic and Microwave Heating, Comparison of Industrial Applications

Pablo M Coronel[1] and Josip Simunovic[2]

[1]CRB Consulting Engineers, Cary, NC, USA
[2]North Carolina State University, Raleigh, NC, USA

Keywords: aseptic packaging, ohmic food processing, microwave food processing, sterilization

INTRODUCTION

Electric heating technologies have the potential of replacing fossil fuels in thermal processing of foods. Among those technologies ohmic and continuous flow microwave heating are readily available. Aseptic processing of liquids and pumpable foods produces high quality shelf stable products, which don't require freezing or refrigeration during their storage and distribution, and therefore contributes to making food products sustainable. Combinations of these technologies, i.e., aseptic processing utilizing ohmic heating; as well as aseptic processing utilizing continuous flow microwave heating have been applied industrially in Europe and the US. These combinations are especially appropriate for processing of difficult to heat, poorly conductive, highly viscous and/or particulate food materials. In some cases, these technologies are the only viable options, enabling processing and preservation of thermo-sensitive products and ingredients which would undergo unacceptably high rates of nutritional and/or sensory degradation if processed using conventional heating technologies. Therefore, ohmic heating, continuous flow microwave heating, and their applications for preservation of homogeneous and heterogeneous (particulate) foods are often referred to as advanced aseptic processing technologies.

Both technology groups have independently received regulatory approvals, with numerous commercialized products available in consumer, food service and industrial/ingredient package formats and sizes.

Industrial acceptance and application of electric heating technologies is still limited, and still presents numerous challenges such as design, installation, safety validation, regulatory approval, operation, and sanitation. These remaining challenges provide a unique opportunity for the food process engineering community, as the industry needs guidance, and support to develop appropriate procedures and methodologies.

This presentation summarizes many years of work which have resulted in commercial installations of these technologies at large industrial scales. Review and discussion of their

validation and regulatory approval will follow an engineering overview of the challenges and hurdles which have been overcome in the past and continue to be addressed in emerging applications.

REQUIREMENTS FOR IMPLEMENTATION OF ELECTRIC PROCESSES

Industrial installations of electric heating applied to thermal processing of pumpable foods, beverages and biomaterials under continuous flow conditions have appeared over the last 20 years and require an intentional design which is significantly different from the standard (or conventional) installations in the food industry. Most of the process lines remain identical to traditional heating, with only the heating segments being replaced by the electric systems. However, many questions remain among engineers and operators regarding these implementations.

Industrial installation of continuous flow ohmic and microwave heating for aseptic processing in the food industry requires the application of multidisciplinary methods, combining electrical engineering, hygienic design, metrology, product and process development, mathematical modeling, and microbiology.

The authors have independently implemented Ohmic and Microwave heating for aseptic processing of foods, which required invention, development, and application of new paradigms in product development and scale-up, and implementation of advanced methods such as:

- Measurement of electric and thermo-physical properties of processed materials over the range of process temperatures and frequencies
- Mathematical models for feasibility, scale-up and process simulation
- Development of laboratory scale and pilot scale equipment and procedures, which are representative of industrial processes
- Development of procedures for managing ingredient variability
- Understanding of flow profiles in pilot and industrial scale, and adjustments of processing protocols to their variability
- Monitoring and control of temperature uniformity
- Advanced control systems to cope with and handle the faster response times
- Novel and advanced methods of process safety validation

These processes have received regulatory approval and have produced commercially available products.

EXAMPLES OF SUCCESSFUL OHMIC AND MICROWAVE PROCESSES

Successful applications of Ohmic and Continuous Microwave processes include a line of industrial vegetable purees, sweet potato, cauliflower, pumpkin, made by YAMCO in Snow Hill, NC, as well as many aseptic retail products made by Aseptia, in Troy, NC using microwave. While ohmic has been successfully used for a line of complex aseptic soups

sold in Europe by Unilever, and many types of industrial fruits and vegetable pieces, such as pears, peaches, tomatoes, green peas, etc.

CONCLUSION

Electric heating technologies for continuous flow processing of foods and biomaterials are a viable alternative to conventional processing and present a unique opportunity for food process engineers to guide the industry to more sustainable and flexible processing systems, and better quality, broader variety and more nutritious food product lines.

Microwave Soil Heating Promotes Strawberry Runner Production and Progeny Performance

Graham I. Brodie[1], Dylan J. McFarlane[2], Muhammed J. Khan[1], Valerie B.G. Phung[1], and Scott W. Mattner[2]

[1]James Cook University, Douglas Campus, Townsville, Australia
[2]VSICA Research and La Trobe University Vic, Australia, Melbourne, Australia

Keywords: crop growth, crop protection, fumigation, microwave disinfestation, soil disinfestation

INTRODUCTION

Soil fumigation is used in several high value agricultural industries to improve the management of pests and diseases. For several decades methyl bromide was the preferred fumigant; however, because it is an ozone depleting gas the compound was banned from use in many industries under the international agreement known as the Montreal Protocol [1]. The strawberry runner industry at Toolangi, Victoria, which grows strawberry plants for domestic and commercial fruit production, has traditionally used methyl bromide to disinfest soil but is now seeking alternative soil treatment technologies. Microwave soil heating is a technology that has been investigated for weed seed control and soil disinfestation [2]. Studies have shown that microwave soil heating can significantly reduce weed competition and pathogen pressure in cropping systems [3]. This paper presents microwave soil heating as a potential soil disinfestation option for the strawberry runner industry.

EXPERIMENTAL OUTCOMES

A series of small to moderately scaled field and pot experiments examined the potential of microwave soil heating for strawberry runner production and progeny performance.

EXPERIMENT 1

Initially, a field experiment was established in which mother plants were grown in one of two soil treatments: soil heated along narrow strips using a small microwave field system; and an untreated control. Microwave soil heating significantly reduced laboratory-prepared and natural inoculum of pathogens (*Sclerotium rolfsii*, *Fusarium oxysporum*, *Pythium* spp.) in the soil, compared with the untreated control; however, pathogen control, in microwave heated soil, decreased as soil depth increased. Strawberry runner production, from mother plants that were grown in the microwave treated strips, was 10 % higher than from the mother plants grown in the untreated soil.

EXPERIMENT 2

To explore this result further, a replicated pot experiment was conducted where strawberry plants were grown in soils that were treated with steam, fumigated with methyl bromide, or microwave heated. A set of untreated control pots was also included in the experiment. Steam treated soils and untreated soils produced similar results for stolon number (stolons are vegetative reproductive structures upon which daughter plants grow), daughter plant number, and ripe fruit weight per plant. Fumigated soil and microwave treated soils produced 83 % and 75 % more stolons, 150 % and 91 % more daughter plants, respectively.

EXPERIMENT 3

A second field experiment was established in which mother plants were grown in one of two soil treatments: soil heated in 4 m^2 plots using a small microwave field system; and untreated control plots arranged in a randomised block design. Again, microwave soil heating significantly reduced laboratory-prepared and natural inoculum of pathogens (*Sclerotium rolfsii*, *Fusarium oxysporum*, *Pythium* spp.) in the soil, compared with the untreated control. As before, pathogen control in the microwave heated soil decreased as soil depth increased, which is consistent with the microwave heating pattern in the soil. Evidence also showed that *Pythium* spp. recolonised microwave-treated soil at greater depths (10 cm). Microwave soil heating significantly reduced weed emergence (by 70 %) and increased the early growth of strawberry plants and runner yields (by 40 %), compared with the untreated soil.

EXPERIMENT 4

Daughter plants, from the two soil treatments established in Experiment 3, along with daughter plants sourced from soils that were treated with methyl bromide and chloropicrin, were grown in soils that were treated with methyl bromide and chloropicrin, steam heating, microwave heating and no treatment (control). This was a larger, replicated, two-factor, repeated measure pot experiment involving 120 pots with ten replicates per experimental combination. Plants, originally sourced from microwave heated soil, had a 21 % higher plant vigour score than plants originally grown in untreated soil, based on the number of leaves, leaf length, plant height, number of flowers, number of harvested fruits, stolon length, number of daughter plants, and weight of harvested fruits. These parameters were measured each week through the 200-day long experiment. Plants that were sourced from fumigated plots had plant vigour scores that were statistically like those sourced from the microwave-treated plots (Fig. 1 (a)). Regarding the soil treatment imposed on the pots, there was no statistical difference in plant vigour scores; however, when only production parameters (stolon length, number of daughter plants, and weight of harvested fruits) were considered, microwave soil treatment resulted in a 23 % increase in normalized production parameters compared with the control and steam soil treatments (Fig. 1 (b)). Soil fumigation resulted in a 9 % increase in normalized production parameters, compared with the control and steam soil treatments. This was statistically greater than the control and the steam treated soils; however, it was statistically less than the microwave treated soil treatment (Fig. 1 (b)).

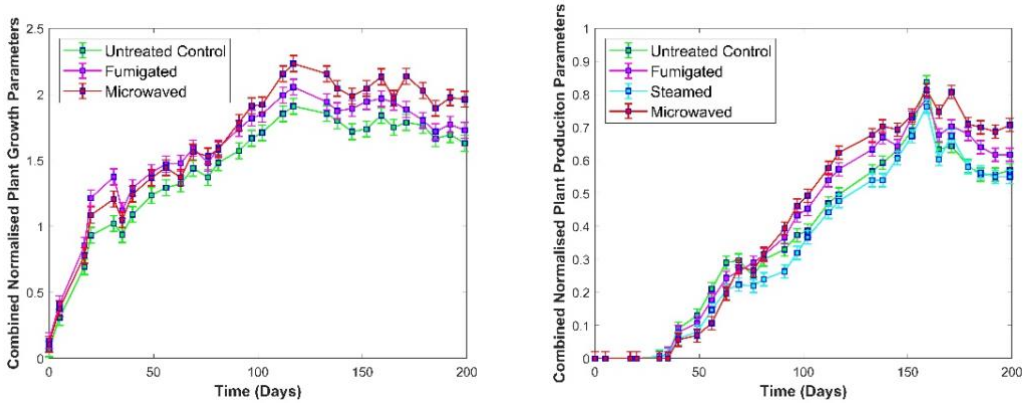

(a) (b)

Figure 1. Normalized plant vigour (based on eight growth parameters measured each week through the course of Experiment 4) of strawberry sourced from transplants grown in the nursery in soils disinfested with different treatments (a), and normalized crop production parameters (based on three production parameters measured each week through the course of Experiment 4) of strawberry grown in soils disinfested with different treatments (b). (Error bars represent the least significant differences between treatment means).

CONCLUSION

In conclusion, microwave soil treatment can reduce pathogen load and increase productivity in strawberry production systems. More research is required on improving pathogen control at greater soil depths, but microwave soil treatment has the potential to replace chemical soil fumigation in the future.

REFERENCES

[1] C.A. Carter, J.A. Chalfant, R.E. Goodhue, F.M. Han, and M. DeSantis, "The methyl bromide ban: economic impacts on the California strawberry industry," *Review of Agricultural Economics,* vol. 27, no 2, pp. 181-197, 2005.

[2] M. J. Khan and G. Brodie, "Soil modifications," In: *Agritech: Innovative Agriculture Using Microwaves and Plasmas: Thermal and Non-Thermal Processing.* Springer Singapore, 2022.

[3] G. Brodie, D. Gupta, and M.J. Khan, "Microwave treatment of soil for weed and pathogen control," *Novel Techniques in Nutrition & Food Science,* vol. 6, no 1, pp. 530-532, 2021.

Effect of Microwave Treatment of Soil in a Metal Planter on Crop Yield

Raymond L. Boxman[1,2] and Amogh Panchagatti[1]

[1]Tel Aviv University, Tel Aviv, Israel
[2]Clear Wave Ltd, Herzliya, Israel

Keywords: harvest yield, microwave soil treatment

INTRODUCTION

Brodie *et al.* showed that microwave radiation could not only kill weeds and weed seeds, but also produce greater wheat and canola harvests [1]. However, Boxman showed that microwave radiation could decrease the harvest of garden vegetables [2]. The objective of the present research was to determine the effect of microwave radiation on harvest in a set-up in which the microwave field could be well characterized, and which can be safely deployed in a home garden environment.

METHODOLOGY

Experiments were conducted in riveted Al sheet planters (Fig. 1), partitioned into 3 sections, each with W×L×D of 29.5×70×60 cm. The bottom 7 cm of each section was filled with tuff (course volcanic gravel). Potting soil was placed thereon, filling each section up to 15 cm of the top. A drip irrigator with 10 outlet holes was placed on the surface of the soil, but was removed during VNA characterization and microwave treatment. Prior to sowing, the soil was saturated with water, characterized, and microwave treated.

An Al plate flange with a protruding λ/4 monopole antenna was positioned above each section to characterize it with a nanoVNA V2 vector network analyzer or treat it using a 2M248H magnetron. The nanoVNA was operated using NanoVNA-App v1.1.206 software by OneOfEleven. After characterization, two of the three sections of the planter were irradiated with 2.46 GHz microwaves for time periods in the range of 0.75-1.25 hr, in order to heat the soil at a depth of 8 cm to 60-80 C. One section of each planter was not treated, and served as a control.

The soil in the planter was left to cool overnight, before sowing. Each section of planters 1, 2 and 3 was sowed with either 9 or 10 seeds of soybeans, bush string beans, or Chinese cabbage, respectively. The seeds were planted near the end of the dry Israeli summer. The drip irrigator was operated automatically twice daily. In addition, until the first true leaves emerged, each section was lightly sprayed manually, to keep moist the soil adjacent to the seeds. Safran, baited grains against *Spodoptera littoralis* caterpillars, was applied when some holes in the leaves were noted. The string beans and soybeans were harvested and weighed when market ready.

Figure 1. Left: Schematic diagram of experimental setup, illustrating one planter section. During characterization or heating, the flange was mounted directly on the top surface of the planter, and removed during plant growth. Right: Photograph of string beans growing in a planter.

RESULTS

The back-scattering parameter $|S_{11}|$ over the frequency range 2.4-2.5 GHz of a planter section filled with moist soil is shown in Fig. 2(a). $|S_{11}|$ had a single sharp minimum of approximately zero, at 2.43 GHz. At the nominal magnetron frequency, 2.46 GHz, $|S_{11}|$ was 0.41.

Fig. 2(b) shows a graph of the bean harvest, as a function of the soil temperature after microwave heating at a depth of 8 cm. The smooth curves are 2nd order polynomial fits. The largest string bean harvest was obtained from the soil which was heated to 65 C the day before planting, more than twice that of the control sample. In contrast, the best soybean harvest, at 62 C, was only 3% more than the control. For both bean types, higher temperatures (71 and 78 C) produced smaller harvests. The polynomial fit suggests that a larger harvest might be obtained at a lower treatment temperature, i.e., at 45-55 C.

DISCUSSION

The simple scattering spectrum from the soil-filled planter shown in Figs. 1-2(a), in contrast to the complicated spectrum from an empty planter, suggest that multiple cavity modes are excited in the empty planter. However, the soil effectively damps these modes in the filled planter, and the resulting $|S_{11}|$ spectrum is mainly shaped by the resonance of the $\lambda/4$ antenna.

Previous experiments by Brodie et al. [1] found that microwave heating of the soil prior to sowing had a decisively positive influence on yield, even for a 2nd planting, while Boxman's previous experiments in an open garden plot mainly showed a negative

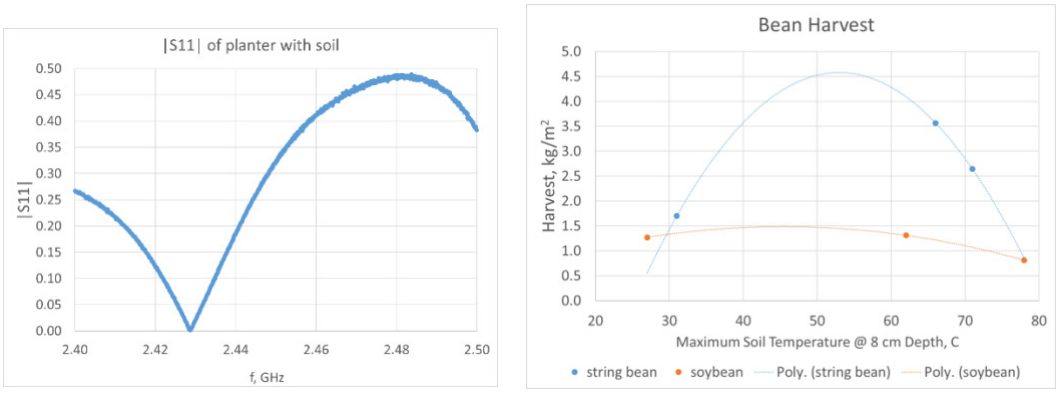

(a) (b)

Figure 2. $|S_{11}|$ measured by nanoVNA (a) and string bean and soybean harvest, as a function of soil tretment temperature at depth = 8 cm (b).

influence [2]. The current experiment likewise shows mixed results, i.e., a dramatic increase in string bean yield, and only negligible influence on the soybean yield.

Possible mechanisms for positive influence include preventing weed seed germination and hence subsequent weed competition, killing harmful organisms (fungi, bacteria, insects, worms, etc.), and decomposing organic compounds to nutrient forms which the plants can more readily absorb. Possible mechanisms for negative influence include killing useful organisms (e.g. bacteria that produce plant nutrients, earthworms, etc.). Using virgin potting soil in planters eliminated weeds and large (i.e. visible) organisms as potential causes. The mixed results in the present experiment, as well as the contradictory previous results, suggest that the effect of microwave heating of the soil prior to sowing depends on the particulars of treatment temperature, crop, soil, etc., and that further work is required to establish under what conditions microwave treatment is beneficial and optimum treatment conditions.

CONCLUSIONS

Microwave heating of soil prior to sowing can dramatically increase harvest yield, e.g. ×2 for string beans in the present experiment, or have negligible or negative effect. Further research is required to establish optimal conditions for positive benefit.

REFERENCES

[1] G. Brodie, N. Bootes, and G. Reid, "Plant growth and yield of wheat and canola in microwave treated soil," *Proc. 49th IMPI Microwave Power Symp.,* San Diego, CA, June 2015, pp. 40-41.

[2] R.L. Boxman, "Microwave treatment of garden soil prior to planting," *Proc. 50th IMPI Microwave Power Symp.,* Orlando FL, June 2016, pp. 82-84.

Microwaves as the Optimal Tool for Microbiological Decontamination of Air and Surfaces

Iurie A. Bosneaga

Institute of Applied Physics, Chisinau, Republic of Moldova

Keywords: Microbiological sterilization, microwaves, ozone generation, UVC and low-temperature plasma

INTRODUCTION

With the Earth's growing population, accelerated urbanization, and unprecedented mobility, the risk of the emergence and explosive spread of infections increases sharply. The economic and social impact of the *SARS-CoV-2* (*COVID-19*) coronavirus has surpassed all previous epidemics of dangerous diseases of the 21st century (*SARS, Ebola, swine and avian flu*). Data indicate that a significant number of COVID-19 infections are transmitted by air without direct contact with the source and have a long incubation period before the infection is symptomatic. As such, infected people cannot establish when or where they were infected, although they respected the rules of personal hygiene. We consider that coronavirus particles in the airborne aerosol coming from the source of infection are electrostatically attached to dust particles and other colloidal particles contained in the air and (after probable dehydration) can be transferred in such a "conserved" form for significant distances. In the case of high levels of infection, the drastic rise in the number of infected persons (reflected by the increase of the *effective reproductive number* R_t which becomes $R_t > 1$) usually means that the weight of non-contact contamination through air and surfaces increases (dominates). Considering the emergence of new epidemic threats, the *optimal microbiological decontamination* (especially of the air and surfaces) is becoming an important task, today.

OPTIMIZING MICROBIOLOGICAL DECONTAMINATION

We prove that *irreversible chemical oxidation reactions* applied to infections are the shortest and most reliable way to achieve sterility. It is established that *oxygen is optimal as an oxidant*, including ecological considerations, because all of its reactive forms harmoniously fit into natural exchange cycles. This work demonstrates that the use of low-temperature ("cold") plasma is optimal for obtaining reactive oxygen species for disinfection. Low temperature plasma provides energy-efficient generation of oxidative reactive forms including atomic oxygen (O), ozone (O_3), hydroxyl radical ($\cdot OH$), hydrogen peroxide (H_2O_2), superoxide (O_2^-), and singlet oxygen $O_2(a^1\Delta_g)$. Due to the short lifetime for most of the above forms outside the plasma applicator, objects remote

from the plasma generator should be sterilized with ozone (O_3), the minimum lifetime of which is quite long (several minutes).

The main constants of atoms (molecules) referred to for plasma forming gases are presented in Table 1.

In air gas discharge (when the ionization threshold of the electric field intensity is exceeded), collisional ionization by electron impacts occurs with the formation of molecular ions and electron multiplication:

$$O_2 + e^- \rightarrow O_2^+ + 2\,e^- ;\ N_2 + e^- \rightarrow N_2^+ + 2\,e^-. \quad (1)$$

Dynamic ionization balance is maintained by electron volume recombination, which at low temperatures occurs mainly in a dissociative way:

$$O_2^+ + e^- \rightarrow O + O ;\ N_2^+ + e^- \rightarrow N + N. \quad (2)$$

There also takes place a mechanism of dissociative attachment of electrons to oxygen molecules (electron-capture dissociation), for which there is an electron energy threshold of ~ 4 *eV* (this estimate follows from the data given in Table 1):

$$O_2 + e^- \rightarrow O^- + O. \quad (3)$$

Such a mechanism of atomic oxygen (O) and its anion formation by means of electron-capture dissociation is less frequent than dissociative recombination.

The factor of predominantly dissociative recombination is crucial for obtaining the sterilizing qualities of plasma. As a result, atomic oxygen (O) is generated, which is a highly active oxidizing agent. Atomic oxygen is generated because reactions (2 – 3) are highly active and, consequently, short-lived. Atomic oxygen (O) is of greatest interest for the implementation of disinfection. It enters a three-particle reaction with molecular oxygen to form ozone O_3:

$$O + O_2 + M \rightarrow O_3 + M^* \quad (4)$$

The reaction takes place with the obligatory participation of the third particle, which receives the relatively low binding energy of the oxygen atom in the ozone molecule (Table 1: E = 1.11 eV, or 107.0 kJ / mol). Such a low binding energy predetermines the relative instability of the ozone molecule, which grows with increasing temperature. On the other hand, this low separation energy of the O atom from the O_3 molecule, coupled with the high electron affinity for O_3 (Table 1: E = 2.26 eV, or 217.9 kJ / mol), results in the high oxidizing capacity of ozone, which is required for decontamination. Ionization and further dissociation of nitrogen molecules (N_2) conduct to formation of harmful oxides (NOx) in air gas discharge, which partly compromise ozone production.

But the above-considered plasma method of ozone generation (through dissociation of molecular oxygen (O_2) in plasma) is apparently not the single way of obtaining ozone. As seen in Table 1, *direct action of the sufficiently short UV radiation (with* λ < 242,4 nm*) can photo*-dissociate molecular oxygen, avoiding the necessity of ionization. Additionally, if the wavelength λ of the UV radiation is simultaneously large enough for non-dissociation of N_2 molecules (Table 1, non-dissociation limit for N_2: λ >126,6 nm), then the problem of nitrogen oxides (NOx) formation in air disappears. In this case, there is no need of oxygen-enriched air or pure oxygen, which is mandatory for corona and barrier discharge devices, which are widely used. The only problem is ensuring such UV radiation in a cost-effective way.

Table 1. Constants of Atoms (Molecules) for Plasma Forming Gases [1].

Molecule type	**N_2**	**Hg**	**O_2**	**O_3**	**H_2O**
Bond (dissoc.) mol. energy, *eV(kJ/mol)* &respec.rad.λ (λ_{max} dissociation limit)	9,81 (945,3) (λ_{max}= 126,6 *nm*) $N_2 + h\nu \rightarrow N + N$	N/A	5,12 (493,6) (λ_{max}= 242,4 *nm*) $O_2 + h\nu \rightarrow O + O$	1,11 (107,0) (λ_{max}=1117,3 *nm*) $O_3 + h\nu \rightarrow O_2 + O$	5,19 (498,7) (λ_{max}= 238,9*nm*) $H_2O + h\nu \rightarrow H + OH$
Electron affinity, *eV*	-0,21 (for atom N)	-0,19 (for atom Hg)	1,47 (for atom O) 0,44 (for mol.O_2)	2,26 (for mol. O_3)	0,75 (for atom H) 1,83 (for OH)
Ionization potential (for atoms, molecules), first (external) electron detachment *eV,* (λ)	14,53 (λ= 84,8*nm*) ($N + h\nu \rightarrow N^+ + e$) 15,58 (λ= 79,6*nm*) ($N_2 + h\nu \rightarrow N_2^+ + e$)	10,44 (λ= 118,8*nm*) ($Hg + h\nu \rightarrow Hg^+ + e$)	13,62 (λ=91,0*nm*) ($O + h\nu \rightarrow O^+ + e$) 12,08(λ=102,6*nm*) ($O_2 + h\nu \rightarrow O_2^+ + e$)	12,52 (λ= 99,0*nm*) ($O_3 + h\nu \rightarrow O_3^+ + e$)	12,61 (λ= 98,3*nm*) ($H_2O + h\nu \rightarrow H_2O^+ + e$)

Two options exist for energy-efficient generation of UV in the range 126,6 nm < λ < 242,4 nm: LEDs and plasma sources (quartz UV lamps). Both technologies have room for progress and improvement, but *currently microwave-generated plasma UV lamps are considered to be more beneficial*. Microwave plasma is "cold" and energy-efficient, being essentially non-equilibrium, that is, the average kinetic energy of electrons is much higher than that of gas molecules (respectively, $T_e >> T_g$). It happens due to significant difference in masses (for example, $M_{O2}/M_e \sim 5{,}8\times10^4$), respectively electrons are accelerated in the same electric field ~$5{,}8\times10^4$ times more intensely than mono-charged ions. So, microwaves optimally solve the problem of selectively transmitting kinetic energy to electrons. Among the advantages of the microwave plasma devices are the absence of wearable electrodes, practically unlimited duration of operation, and reduced warm up time. Additional arguments for the use of microwave plasma ozone generation are the widespread availability of microwave heating technology (MW ovens) in everyday life and in production. Only a relatively simple adaptation of a MW oven is required, which usually maintains the initial (basic) purpose. Also, the wide commercial availability of the quartz UV lamps is important. Performance of ozone production and UV radiation intensity can be governed by the density (number) of installed quartz UV lamps and variation of applied microwave power.

CONCLUSION

Currently the optimal way for ensuring microbiological decontamination of air and surfaces is the application of microwave resonators (microwave ovens) with inserted quartz UV lamps – for ozone and germicidal UV generation.

REFERENCES

[1] V.A. Rabinovich and Z.Ya. Khavin, *Brief Chemical Reference Book*, Chemistry Publishing House, 1977.

Multifrequency Dielectric Properties Measurement Method Based on Coplanar Waveguide

Pablo Santón[1], J. Vicente Balbastre[2], Mariano Baquero[2], Ruth De los Reyes[1], and Elías De los Reyes[2]

[1]Microbiotech S.L., Vilamarxant, Spain
[2]Polytechnic University of Valencia, Valencia, Spain

Keywords: coplanar waveguide, dielectric properties, multifrequency, TEM

INTRODUCTION

Techniques for measuring microwave dielectric properties can be classified as reflection or transmission measurements using resonant or non-resonant systems, with open or closed structures for the sensing of the properties of the material under test [1]. Recently, there has been some work on new measurement methods based on transverse electromagnetic (TEM) modes [2]. Working with TEM structures allows a single device to cover a wide bandwidth (from DC to 10 GHz). This work aims to define a new method to measure the complex permittivity of materials. To this end, a coplanar waveguide (CPW) is built and filled with a slab of the material under test. The scattering matrix is measured between two reference planes and then the real and imaginary parts of the complex dielectric constant are extracted through equations. Being able to obtain these values is the first step toward accurate modelling in the design of new high-power microwave heating devices. The present method will provide information of both permittivity and loss tangent values.

METHODOLOGY

Coplanar waveguide (CPW) transmission lines are well-known TEM structures [3]. The quasi-TEM mode of propagation on a CPW has low dispersion and hence offers the potential to construct wideband circuits and components. Furthermore, the characteristic impedance is determined by the transmission line geometry and relative sizes of the conductors. Therefore, size reduction is possible with the only penalty being higher losses. These two characteristics make this structure an ideal candidate to build an asymmetric transmission line by inserting the conductors between two slabs of different materials. It can therefore be analyzed as a lossy transmission line.

A lossy transmission line is characterized by complex characteristic impedance and propagation constant, the latter being composed of a real part (the attenuation factor α) and an imaginary part (the phase constant β). From these two parameters, the effective dielectric properties of the materials on either side of the coplanar line can be derived.

After several manipulations [4] it is possible to relate the currents and voltages on a reference plane (Fig. 1) with the scattering matrix parameters, and therefore the reflection coefficient ρ and propagation constant γ, on the same plane. The propagation constant is related to the S_{12} parameter in the form $e^{-\gamma_0' l}$. The final equations that define the dielectric properties, as a result of the scattering matrix parameters, are [4]:

$$S_{11} = \frac{\rho}{1-\rho^2 e^{-2\gamma_0' l}}(1-e^{-2\gamma_0' l}) \quad (1)$$

$$S_{12} = \frac{e^{-\gamma_0' l}}{1-\rho^2 e^{-2\gamma_0' l}}(1-\rho^2) \quad (2)$$

RESULTS

To solve these two equations, let $x = e^{-\gamma_0' l}$, and use an alternative variable, k.

$$k = \frac{S_{11}^2 - S_{12}^2 + 1}{2S_{11}} \quad (3)$$

$$\rho = k \pm \sqrt{k^2 - 1} \quad (4)$$

$$x = \frac{S_{11} + S_{12} - \rho}{1-\rho(S_{11}+S_{12})} \quad (5)$$

being S_{11} and S_{12} the scattering parameters measured on the sample plane. With these equations we obtain the propagation constant, relative effective permittivity and effective loss tangent of the line being analyzed.

The device is an embedded CPW, designed with a 50 Ω characteristic impedance and excited using a uniform TEM mode. The method to obtain the S-parameters in the reference planes, with the sample placed over the structure (Fig. 2(a)), is a TRL (Thru, Reflect, Line) calibration [5] using a metallic material with the same dimensions as the sample. This calibration method is often performed when high accuracy is required and there are no calibration standards in the same connector type as the DUT (Device under test). In our case there is no connector on the sample (DUT) planes.

DISCUSSION

This method allows us to map the effective dielectric constant to the actual dielectric constant over a wide frequency range (Fig. 2(b)). Further details on the method and more numerical results will be presented in the poster.

CONCLUSION

A new non-destructive dielectric properties measurement method has been developed to be compatible with the wide range of industrial, scientific and medical applications where the knowledge of dielectric parameters is crucial to the development of new electromagnetic processes.

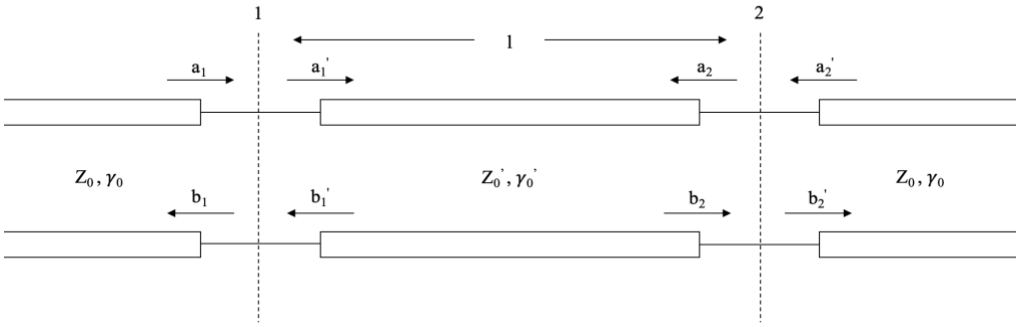

Figure 1. Schematic of a lossy transmission line.

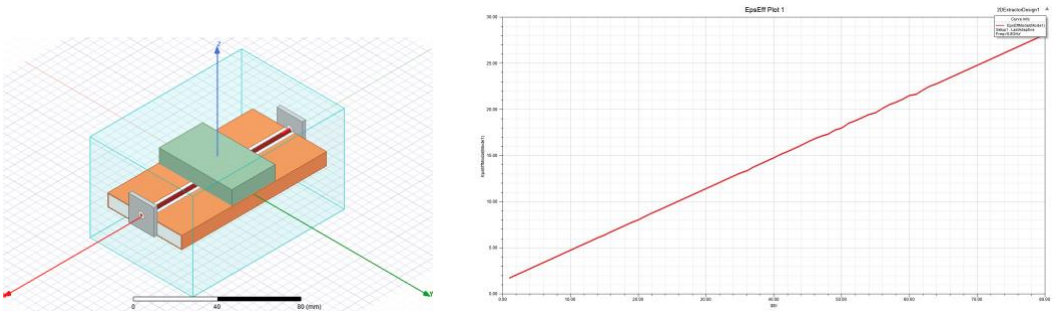

(a) (b)

Figure 2. Enclosed CPW structure modelled in finite elements electromagnetic simulation software (a) and effective relative permittivity against actual relative permittivity value (b).

REFERENCES

[1] A. Kraszewski, "Microwave aquametry — a review," *J. of Microwave Power*, vol. 15, no. 4, pp. 209–220, 1980.

[2] M.A. Saed, N. Patil, and M.J. Green, "Radio frequency dielectric characterization and processing of polymers containing nanomaterial susceptors," In *Proc. of the 2019 21st Intern. Conf. on Electromagnetics in Advanced Applications*, ICEAA, September 2019, pp. 916.

[3] R. N. Simons, "Coplanar waveguide circuits," In *Components and Systems*, Wiley & Sons, 2001.

[4] D.K. Ghodgaonkar, V.V. Varadan, and V.K. Varadan, "A free-space method for measurement of dielectric constants and loss tangents at microwave frequencies," *IEEE Trans. on Instrumentation and Measurement*, vol. 38, no. 3, pp. 789–793, 1989.

[5] Keysight Technologies, "TRL Calibration," 2002, na.support.keysight.com/vna/help/latest/S3_Cals/TRL_Calibration.htm.

Microwave-Assisted Frying and Post-Frying of French Fries

Xu Zhou, Zhongwei Tang, and Juming Tang

Washington State University, Pullman, WA, USA

Keywords: crispness, fat reduction, microwave frequency, potato

INTRODUCTION

French fries are popular items in the diets of many countries, but the relatively high fat content of French fries is a major health concern for consumers. The food service industry has been seeking new frying methods and techniques that would produce healthy and nutritious French fries but not compromise with quality. There is an ongoing effort to combine microwave heating and deep-fat frying for oil reduction in fried foods [1]. Given that most of the oil is absorbed during post-frying (cooling) [1], we hypothesize that microwave energy has the potential to reduce surface oil intake after frying and before cooling suction begins. However, there is little understanding on the mechanisms of fat reduction during microwave post-frying holding. Moreover, current microwave fryers available in the market all operate at 2.45 GHz frequency [2]. A higher frequency of 5.8 GHz may be more applicable to post-frying treatments for reduction of oil in French fries, as the microwave energy can be directed more intensely to create vapor pressure at the interface between the crust and the interior of French fries. There are no food applications with this frequency so far. The objective of this study was to determine the effectiveness of microwaves on fat reduction in French fries by using the microwave frying testing unit developed at Washington State University.

METHODOLOGY

EXPERIMENTAL APPARATUS

The microwave frying unit (Fig. 1) consists of six main components: a frying/heating cavity, an oil container made from quartz glass, a Teflon food holder with perforated walls, two microwave sources with different operating frequencies (2.45 and 5.8 GHz), a temperature measurement device with four fiber optic sensors (Model MAN-00075 R5, FISO, Quebec, Canada), and a control system. A 2.45 GHz magnetron was initially mounted underneath the bottom cavity wall. A GaN amplifier based 5.8 GHz solid-state microwave generator (RIU58800-20, RFHIC Co., Anyang, South Korea) was connected to the cavity on the left side through a WR 159 rectangular waveguide. The microwave fryer test unit could be operated at either individual frequency (2.45 or 5.85 GHz) or with a combination of the two frequencies.

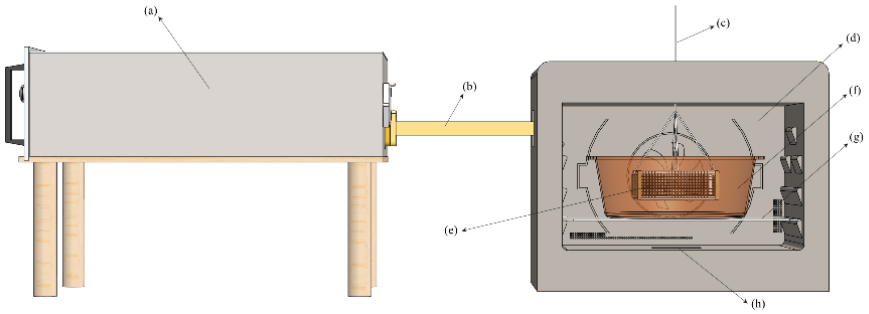

Figure 1. Schematic diagram of the microwave frying unit including (a) 5.8 GHz solid-state generator, (b) WR159, (c) nylon wire, (d) frying cavity, (f) oil container, (e) Teflon sample holder, (g) glass plate and (h) 2.45 GHz magnetron.

MATERIAL AND FRYING PROCEDURES

Fresh potatoes were washed, peeled, cut into strips and blanched in hot water. And then, the frying tests were carried out in four methods: (1) deep-fat frying, (2) 2.45 GHz microwave frying, (3) 5.85 GHz microwave frying, and (4) dual-frequency (2.45 + 5.85 GHz) microwave frying. The frying times for each frying method were 1, 3 and 5 min. Microwave post-frying (holding) refers to a heating period between frying and cooling. Potato strips were first fried in 180 °C heated oil (microwaves off) for 5 min, and secondly the sample holder was elevated above the oil. The microwave-assisted post-frying holding was then carried out in three ways: (1) no microwaves, (2) 2.45 GHz microwaves, and (3) 5.85 GHz microwaves. After holding of total 120 s, the French fries were removed from the microwave oven and cooled down.

RESULTS AND DISCUSSION

Regardless of frying methods, an approximate linear correlation was observed between moisture losses and fat intakes in Fig. 2. This relationship confirmed that the more water was lost from the fried samples, the more oil was absorbed by the samples.

The 9% and 16% of oil reductions in French fries were achieved by using 2.45 GHz and 5.85 GHz microwaves, respectively, as compared with controls at 60 s of holding (Fig. 3). The oil reduction during the microwave-assisted holding may be due to two reasons: (1) the oil on the food surface continued to be heated by microwave energy and more easily drained off from the surface due to the reduced viscosity. During the subsequent cooling, there was little or no surface oil available for fat pickup; (2) a great amount of vapor pressure was generated inside French fries because of microwave heating, which could prevent oil from migrating into the fries.

It is interesting to note that microwaves at 5.85 GHz reduced much more fat contents (16±2%) than microwaves at 2.45 GHz (9±2%). Most oil is retained in the crust region of a French fry [1]. At 5.8 GHz, the microwave energy could be directed more intensely in the crust area of French fries to create moisture vapor pressure, which could improve the pore pressure to remove the oil or prevent oil from penetrating.

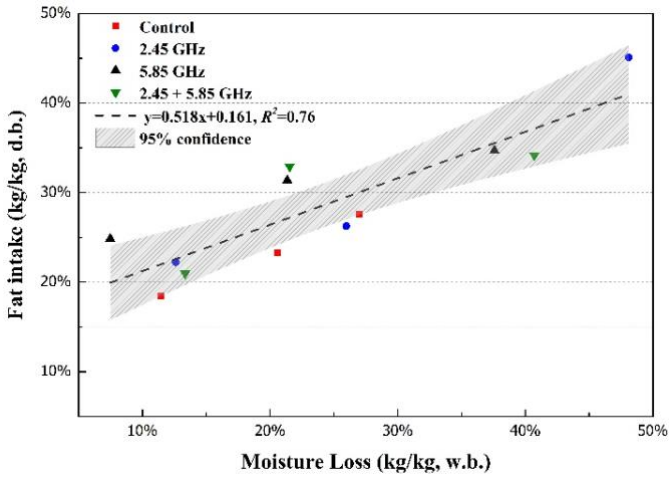

Figure 2. The relationship between water loss and fat intake of French fries during frying.

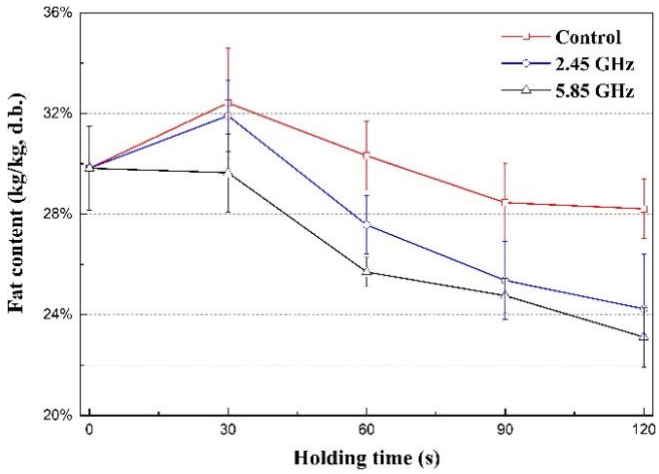

Figure 3. Fat contents of French fries during microwave post-frying holding.

CONCLUSION

The fat absorption increased with increasing water loss during frying, regardless of frying methods. It was not microwave frying but rather the microwave post-frying holding which was the key factor for fat reduction of French fries.

REFERENCES

[1] P. Bouchon, "Understanding oil absorption during deep-fat frying," In *Advances in Food and Nutrition Research,* vol. 57, Academic Press, 2009, pp. 209-234.

[2] R. Schiffmann, "Microwave-assisted frying" In *The Microwave Processing of Foods,* M. Regier, K. Knoerzer, and H. Schubert, Eds., 2nd Ed., Woodhead Publishing, 2017, pp. 142-151

Characterizing the Effect of Oven Geometry on the Modeling Accuracy of Microwave Heating

Kartik Verma[1], Hao Gan[2], and Jiajia Chen[1]

[1]Department of Food Science, The University of Tennessee, Knoxville, TN, USA
[2]Department of Biosystems Engineering and Soil Science, The University of Tennessee, Knoxville, TN, USA

Keywords: geometry, heating pattern, microwave heating, modeling

INTRODUCTION

Multiphysics modeling of microwave heating of foods has been used as a useful tool to improve the understanding of the microwave heating process and assist the food product developers in efficiently designing better microwaveable foods. Prior to the model application, these models need to be validated on their prediction accuracy. The most common validation method is to compare the thermal images of the food after heating with the simulation results and make sure the heating patterns match so that the model can accurately predict the hot and cold spots. However, there is a significant challenge to develop computer simulation models that match well with microwave heating experiments due to the complicated interactions between microwaves and food products. The model prediction accuracy can be influenced by several model parameters, including the geometry of the oven cavity, food properties, and the physics that are used in the models [1].

The dielectric and thermal properties of food products have been accurately measured; the multiphysics have been evaluated [2]. However, the effect of the geometric parameter on the model accuracy has not been systematically studied. Early-stage microwave heating models usually used simple rectangular boxes to represent the oven cavity; later models attempted to incorporate major geometric details, such as protrusions on the cavity walls, in the model with improved prediction accuracy. However, these models were still not able to accurately predict the hot and cold spots. The objective of this study is to characterize the effect of oven geometric details (major protrusion, minor curvatures, etc.) on the model prediction accuracy and propose to develop a 3-dimensional scanning method to better create the oven cavity geometry for microwave heating modeling.

METHODOLOGY

A solid-state microwave system comprised of a generator (PA-2400-2500MHz-200W-4, Junze Technology) and a domestic microwave oven cavity (Panasonic Model NN-SN936W) were used in this study. The solid-state microwave system has four ports, and

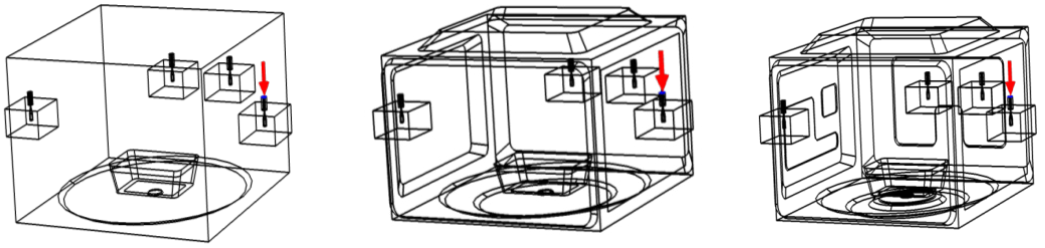

a. Simple box b. Major protrusions c. Minor curvatures

Figure 1. The geometric models with different oven details

only one port on the right side wall (200 W, 2450 MHz) was used in the heating process. Mashed potato was used as a model food and heated from about 4 °C for 6 min without rotating on the turntable. After heating, the thermal profiles at the top layer of the heated samples were captured by a thermal imaging camera (FLIR C3, Boston, MA).

The multiphysics-based computer simulation models were developed in a finite-element-method-based commercial software COMSOL Multiphysics (by COMSOL Inc.). The multiphysics of electromagnetics and heat transfer were used in the models. Three models with different geometries (simple box, major protrusions, minor curvatures) were performed, as shown in Fig. 1. The simple box geometry only included the cuboidal cavity along with waveguides (Fig. 1a); the major protrusion geometry incorporated the major protrusions on the left, right, back, front, top, and bottom walls (Fig. 1b); the minor curvature geometry incorporated the minor protrusions on the left, back, and bottom (Fig. 1c). Each model includes about 500,000 tetrahedral elements. The modeling results (locations of the hot and cold spots) were compared to the experimental results to characterize the effect of geometric details of the oven cavity on the model prediction accuracy.

RESULTS AND DISCUSSIONS

The comparison of the thermal profiles at the top surface of the food product between experiments and simulation is shown in Fig. 2. Three replications of the microwave heating experiments showed similar hot and cold spots locations with good consistency. Without rotation, the mashed potato samples were mainly heated at the edges, corners, and the right side of the samples. A cold spot was observed on the left side of the mashed potato samples. The modeling thermal profiles with different geometric details showed significantly different heating patterns. For the model with simple box geometry, the heating pattern did not match with the experimental results, where the central region of the food was not heated. After adding the major protrusions on the oven cavity walls, the heating pattern of the hot and cold spots was improved significantly and generally matched with the experimental results. The geometric details of the minor curvatures could further improve the match of hot and cold spots between the simulation and experiments. As shown in Fig. 2, the minor hot spot at the left bottom corner was observed in the minor curvature model

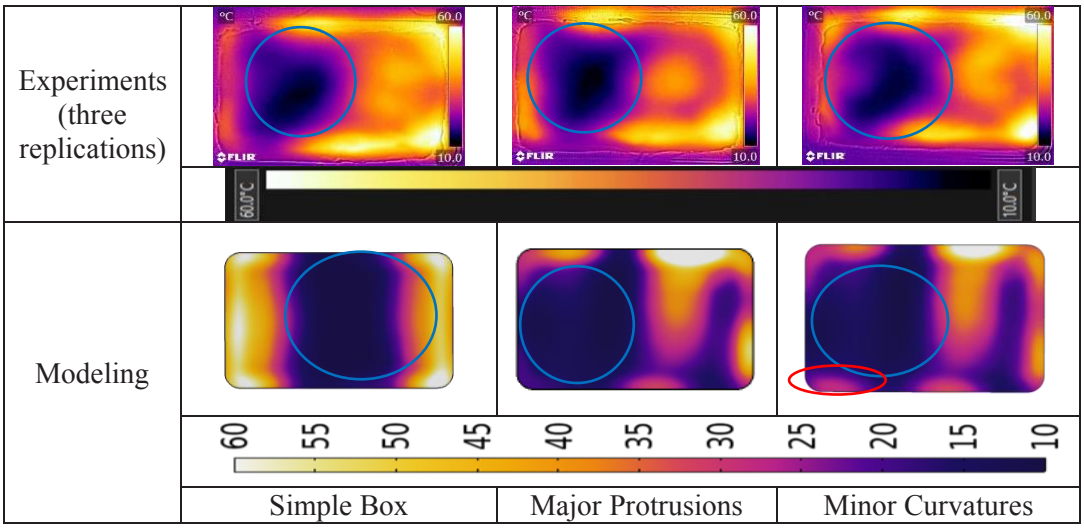

Figure 2. Experimental and simulated thermal profiles at the top layer of the heated mashed potato.

but not the major protrusion model. The geometric details are important for accurately characterizing the modeling performance.

However, the model with minor curvatures that were measured manually still did not match exactly with the experimental results. This might be because the minor details were not precisely measured. We are working on developing a three-dimensional (3-D) scanning approach using the Artec space spider 3-D scanner to better create the geometries of the oven cavity and food product for improving modeling accuracy.

CONCLUSION

Multiphysics models to simulate the microwave heating process were developed to study the effect of geometric details on the modeling accuracy. The major protrusion and minor curvatures are important for accurately characterizing the hot and cold spot locations. A more precise geometry of the oven cavity and a food product that can be measured by a 3-D scanning approach may further improve the modeling accuracy.

REFERENCES

[1] K. Pitchai, J. Chen, S. Birla, R. Gonzalez, D. Jones, and J. Subbiah, "A microwave heat transfer model for a rotating multi-component meal in a domestic oven: Development and validation," *J. Food Eng.,* vol. 128, pp. 60–71, 2014.

[2] J. Chen, K. Pitchai, S. Birla, D. Jones, M. Negahban, and J. Subbiah, "Modeling heat and mass transport during microwave heating of frozen food rotating on a turntable," *Food Bioprod. Process.*, vol. 99, pp. 116-127, 2016.

The MATS Process Validation

Moses A. Magana

915 Labs, Centennial, CO, USA

Keywords: MATS, microwave thermal process validation

INTRODUCTION

Microwave assisted thermal sterilization (MATS) is a novel process technology to deliver in-package sterilization of shelf-stable food products. The goal of MATS is to deliver rapid heating to efficiently inactivate food bacterial load and maintain product characteristics.

Shelf stable thermally processed food are FDA regulated and food manufacturers are required to obtain scientific and technical evidence that a thermal process is capable of reducing a significant hazard to an acceptable level that does not pose a public health risk under normal conditions of distribution and storage.

A validation study of the equipment and product is required by the FDA to provide evidence that a control measure is capable of controlling the identified hazard under a worst-case scenario for the process and product parameters tested. It also defines the critical parameters that must be controlled, monitored, and verified during processing

The MATS process also falls within the FDA requirements under the low-acid canned food (LACF) regulations as with other conventional thermal processing methods. The use of the microwave as a heating method to assist with the conventional heating creates a new challenge in the validation process to comply with FDA requirements when using conventional testing protocols for in-package sterilization.

The FDA regulation requires food processor using MATS technology to demonstrate consistency and uniformity in the heating process from both the microwave and the conventional heating from water immersion. This requirement was addressed in the past by the early adopters of MATS technology and academia via complex validation protocols involving microwave heating simulations, the use of whey gels to trace the microwave heating homogeneity, the use of image processing to validate the MW heating pattern uniformity, and the use of microbial validation as per convectional heating validation protocols.

The initial validation methodology for MATS creates complexity and extends validation to several months and requires training and specialized equipment and software.

VALIDATION APPROACH

To simplify the validation process, the new approach is about using microwave heating in the MATS system as an assist of the conventional thermal process. Since MATS uses water immersion in combination with microwave heating, the food packages are processed in

pressurized hot water and simultaneously heated with microwaves at a frequency of 915 MHz to rapidly achieve sterilization temperatures.

This simplified new approach uses the conventional heating time and temperature heating effect as the baseline and compares it to the curve when both conventional and microwave heating are used. The baseline temperature curve using conventional heating determines the conventional heating characteristics of the product at the coldest spot and the difference is the effect of the microwave heating on the slowest heating point which typically is the geometric center.

RESULTS AND DISCUSSION

Because microwave heating and microwave energy coupling can vary significantly by certain factors of the product recipe, such as dielectric properties, salt content, etc., the baseline demonstrates to FDA that the minimum come-up to temperature time is provided by conventional heating while the microwave serves as an auxiliary process used to shorten the total heating period. This way the product achieves the baseline process temperature via microwave heating before the actual accumulation or hold process starts conventionally. This approach removes the inherent complexity of the analysis of electric field distribution within MATS microwave heating coupling with food items as the variation is compensated by the conventional heating that provides the baseline for food safety [1]. This adjusted approach is expected to make a significant contribution to expanding the use of microwave heating for the safe sterilization of food products.

At 915 Labs, we have led the development of a more versatile and less microwave centered validation protocol always using mobile metallic temperature sensor as in previous filing process approach that tracks and accounts for microwave heating as a complementary booster heating source that would not be considered part of the critical heating to achieve thermal sterilization [2]. The approach considers the MW heating section of the MATS system an auxiliary heating source that reduces the time it takes for the product to reach processing temperature.

CONCLUSION

When MATS system is approached with a conventional validation, it reduces the validation complexity of microwave heating for regulatory authorities. To improve the consistency of the processing system, microwave heating can be accounted as a heating aid to conventional heating, for example, in systems where a fan is used to distribute the steam to get faster homogenous heating.

REFERENCES

[1] D. Luan, J. Tang, P.D. Pedrow, F. Liu, and Z. Tang, "Analysis of electric field distribution within a microwave assisted thermal sterilization (MATS) system by computer simulation," *J. Food Engineering,* vol. 188, pp. 87-97, 2016.

[2] D. Luan, J. Tang, P.D. Pedrow, F. Liu, and Z. Tang, "Using mobile metallic temperature sensors in continuous microwave assisted sterilization (MATS) systems," *J. Food Engineering,* vol. 119, no 3, pp. 552-560, 2013.